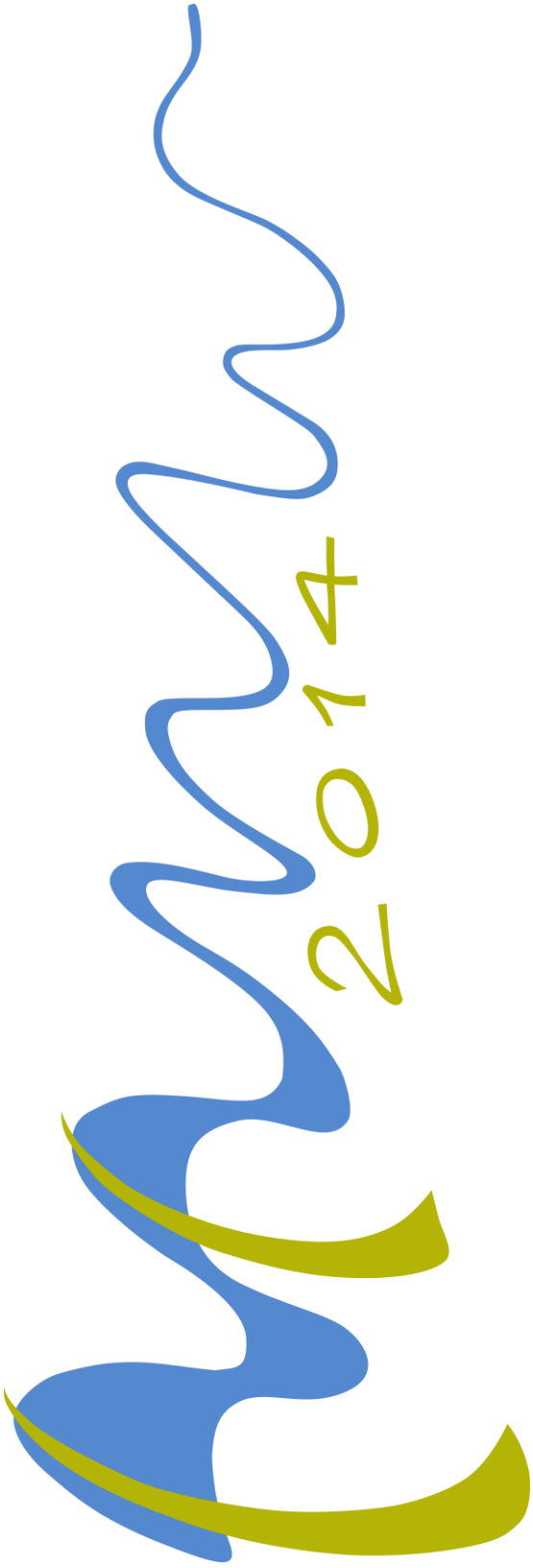


# Proceedings of the 17th International Workshop on Physical Processes in Natural Waters

## PPNW2014
## Trento (Italy)
## 1-4 July 2014

**Editors:**
**Marco Toffolon**
**Sebastiano Piccolroaz**

UNIVERSITY
OF TRENTO - Italy

# PHYSICAL PROCESSES IN NATURAL WATERS: PPNW2014

# Proceedings of the 17th International Workshop on Physical Processes in Natural Waters (PPNW2014)

## Trento (Italy), 1-4 July 2014

**Marco Toffolon**
**Sebastiano Piccolroaz**
**(Editors)**

UNIVERSITY
OF TRENTO - Italy
Department of Civil, Environmental and Mechanical Engineering

**SPONSORS**

Hortus

INSTRUMENT SERVICE
Sistemi di monitoraggio ambientale

WATEC.IT WATER TECHNOLOGY

YSI
a xylem brand

17th International Workshop on
Physical Processes in Natural Waters
PPNW2014
Trento (Italy), 1-4 July 2014

Editors: Marco Toffolon and Sebastiano Piccolroaz



Department of Civil, Environmental and Mechanical Engineering
University of Trento, Italy
Via Mesiano 77
38123 Trento
Italy

Bibliographic information:
M. Toffolon and S. Piccolroaz (Eds.), *Proceedings of the 17th International Workshop on Physical Processes in Natural Waters: PPNW2014, Trento, Italy, 1-4 July 2014*, Trento: Università degli Studi di Trento, 2014, pp. 112. - URL: http://eprints.biblio.unitn.it/4293/

ISBN: 978-88-8443-551-4
Printed version: ISBN: 978-88-8443-550-7

# Table of contents

# Preface

The 17th International Workshop on Physical Processes in Natural Waters (PPNW2014) belongs to a series of workshops that were conceived to facilitate the dialogue between physical limnologists and modellers with colleagues in other disciplines, such as biologists, chemists and engineers. With a specific focus on the physics of inland and coastal water bodies, the workshops traditionally cover a broad spectrum of scientific topics, actively seeking to expand contacts and establish interactions with neighbouring fields. The participation of a relatively small number of scientists, the organization in a single session with a comfortable time frame for presentations and discussion, and the informal atmosphere, are key elements characterizing the workshop. The goal is that of fostering the development of new collaborations and crossing the boundaries between disciplines.

The scientific interests of the two keynote speakers of this edition are a practical demonstration of the interdisciplinary traits that characterize the workshop: starting from their different backgrounds (physics and biology, respectively), Andreas Lorke and Nico Salmaso have tackled different aspects of the more general problem of water quality, recognizing the strong interactions among physical, biogeochemical and ecological processes.

This edition of the workshop was organized by the Department of Civil, Environmental and Mechanical Engineering of the University of Trento, and held in the historical building of the Department of Sociology and Social Research in the centre of the city of Trento, Italy, from 1st to 4th July 2014. During the workshop, two technical field trips were organized to visit two lakes that provide a good picture of the varied features of water bodies in a mountainous region: one of the largest lakes in Europe, Lake Garda, with a high ecological and economic value (about $11 \cdot 10^6$ visitors per year), and a much smaller montane lake, Lake Tovel, characterized by intense reddening events that occurred until the 1960s but still attracts scientific interest. Being caused by blooms of the microscopic dinoflagellate protist *Tovellia sanguinea*, sustained by nutrient inputs from the inflowing water and possibly further enhanced by transport and aggregation by an upslope breeze, the study of this singular phenomenon is another demonstration of the fruitful coupling of physical and biological investigation.

For the organization of the workshop, we gratefully acknowledge the support of the administrative offices of the University of Trento, and especially Myriam Stettermayer, and the contribution of the three sponsors (Instrument Service; Hortus; Watec-YSI). Special thanks are due to Marco Cantonati and Massimiliano Tardio (MUSE), Maurizio Siligardi, and Chiara Defrancesco (APPA Trento) for the kind support in the technical visits. Finally, I wish to thank Sebastiano Piccolroaz for his great contribution to PPNW2014.

Marco Toffolon
University of Trento

# Committees

Local Organizing Committee (*University of Trento*)

Marco Toffolon (chair), *Department of Civil, Environmental and Mechanical Engineering*

Sebastiano Piccolroaz, *Department of Civil, Environmental and Mechanical Engineering*

Myriam Stettermayer, *Communication and Events Service*

Virna Eccli, *International Activities Staff*

Contacts PPNW2014

ppnw2014@unitn.it (*scientific*)
comunicazione-collina@unitn.it (*administrative*)

International Steering Committee

Josef Ackerman, *University of Guelph, Canada*

Hrund Andradóttir, *University of Iceland, Iceland*

Lars Bengtsson, *Lund University, Sweden*

Bertram Boehrer, *Helmholtz Centre for Environmental Research (UFZ), Germany*

Xavier Castamitjana, *University of Girona, Spain*

Giuseppe Ciraolo, *University of Palermo, Italy*

Nikolai Filatov, *Karelian Research Centre of RAS, Russia*

Andrew Folkard, *Lancaster University, United Kingdom*

Georgiy Kirillin, *Institute of Freshwater Ecology, Berlin (IGB), Germany*

Charles Lemckert, *Griffith University, Australia*

Madis-Jaak Lilover, *Marine Systems Institute, Estonia*

Francisco Rueda, *University of Granada, Spain*

Geoffrey Schladow, *University of California, Davis, United States*

Adolf Stips, *European Commission, Italy*

Arkady Terzhevik, *Karelian Research Centre of RAS, Russia*

Marco Toffolon, *University of Trento, Italy*

Lars Umlauf, *Leibniz-Institute for Baltic Sea Research (IOW), Germany*

Alfred Wüest, *Eawag & EPFL, Switzerland*

Ram Yerubandi, *Canada Centre for Inland Waters, Canada*

# Keynote lectures

# Vertical transport at biogeochemical interfaces in lakes

A. Lorke[1]*, J. Kreling[1], L.N. Wickramarathna[1], C. Noss[1] and D.F. McGinnis[2]

[1*] *Institute for Environmental Sciences, University of Koblenz-Landau, Landau, Germany*
[2] *IGB – Leibniz-Institute of Freshwater Ecology and Inland Fisheries, Berlin, Germany*

**Corresponding author, e-mail lorke@uni-landau.de*

**KEYWORDS**
Lakes; diapycnal transport; dissolved oxygen; bio-mixing.

## EXTENDED ABSTRACT

### Introduction

Turbulent transport and mixing processes in stratified aquatic systems are often described in terms of vertical fluxes of density, i.e. heat and salt, because these fluxes interact directly with the turbulent flow. While the pronounced short-term dynamics of turbulent mixing in response to wind forcing and internal waves has been studied intensively, the effect of vertical mixing on metabolic rates and biogeochemical cycling in lakes was mainly studied on seasonal and climatic time scales. Dissolved oxygen can serve as a proxy for estimating biogeochemical turnover in aquatic systems and is readily accessible with fast-response sensors. Direct observations of turbulent oxygen fluxes in response to hydrodynamic forcing, however, were mainly restricted to the sediment-water interface, where in-situ flux measurements can be performed with sufficient temporal resolution using benthic lander systems. Here we compare the magnitude and hydrodynamic driving forces of oxygen fluxes measured simultaneously at the benthic and at the pelagic oxycline of a lake using the aquatic eddy-covariance method. We further analyse laboratory measurements of fluxes across density gradients and biogeochemical interfaces caused by vertically migrating zooplankton. While bioturbation and –ventilation are known to enhance vertical fluxes at the sediment-water interface, energetic arguments and numerical simulations led only recently to the hypothesis that the currents generated by swimming animals can significantly contribute to mixing in the stratified pelagic zone.

### Materials and methods

We present data from an extensive field campaign conducted at Lake Scharmützelsee, Germany. Turbulent oxygen fluxes were measured as the the eddy-covariance of velocity and oxygen concentration fluctuations by using moored instrumentation as well as a benthic lander. The flux measurements were complemented by intensive observations of current velocity, turbulence and density stratification using moored and profiling instruments as well as water samples for chemical analyses of redox-sensitive compounds (Kreling et al., 2014).

Laboratory measurements were conducted with the *Daphnia* swimming in different pattern including vertical migration in a density-stratified water column. The hydrodynamic trails of the zooplankton organisms were characterized using particle-image velocimetry (Wickramarathna et al., 2014) and mixing rates were quantified at the scale of individual organisms in terms of the dissipation rates of small-scale spatial variance of tracer concentration measured by laser-induced fluorescence (Noss and Lorke, 2014). At the bulk scale, we analysed temporal changes in the mean density stratification.

**Results and discussion**

While the vertical fluxes of dissolved oxygen (DO) were highly variable in time in both the pelagic and the benthic zone, the mean fluxes did not differ significantly at the two types of oxyclines. Short energetic periods contributed disproportionately to the overall oxygen flux at both sites. In the pelagic region, mean fluxes at the depth of the oxycline were limited to molecular diffusion and were more than three orders of magnitude smaller than fluxes measured in the stratified part of the water column above the oxycline ($5\times10^{-3}$ and 32 mmol $m^{-2}$ $d^{-1}$, respectively). A mass balance approach revealed that >99% of DO transported into the oxycline is utilized by respiration and the mineralization of organic material imported into the oxycline from the epilimnion; chemical oxygen consumption associated with the upward flux of reduced substances is negligible. Our findings indicate that under such conditions, mineralization rates within the pelagic oxycline can be of comparable magnitude as the corresponding rates occurring in the sediments of eutrophic lakes (Kreling et al. 2014).

Viscous dissipation rates of kinetic energy in the hydrodynamic trails of swimming zooplankton organisms were high compared to turbulent dissipation rates in the thermocline of lakes ($1.8\times10^{-6}$ W $kg^{-1}$ to $3.4\times10^{-6}$ W $kg^{-1}$). The size of the hydrodynamic footprint is increasing proportional to the third power of organism Reynolds number and the largest trail volume observed corresponds to about 500 times the body volume of the 3 mm sized organisms (Wickramarathna et al., 2014). Organism and bulk-scale estimates of apparent diffusion coefficients in trails of swimming individuals and organism groups, however, revealed only mean diffusivities in the order of magnitude of molecular diffusivity of dissolved substances ($0.8\text{-}5.1\times10^{-9}$ $m^2$ $s^{-1}$) (Noss and Lorke, 2014). The present results agree with scaling arguments and suggest the negligible enhancement of vertical transport under turbulent flow conditions, but potential contributions to vertical transport were turbulence is suppressed by density stratification, such as the pelagic oxycline discussed above ( Fig. 1).

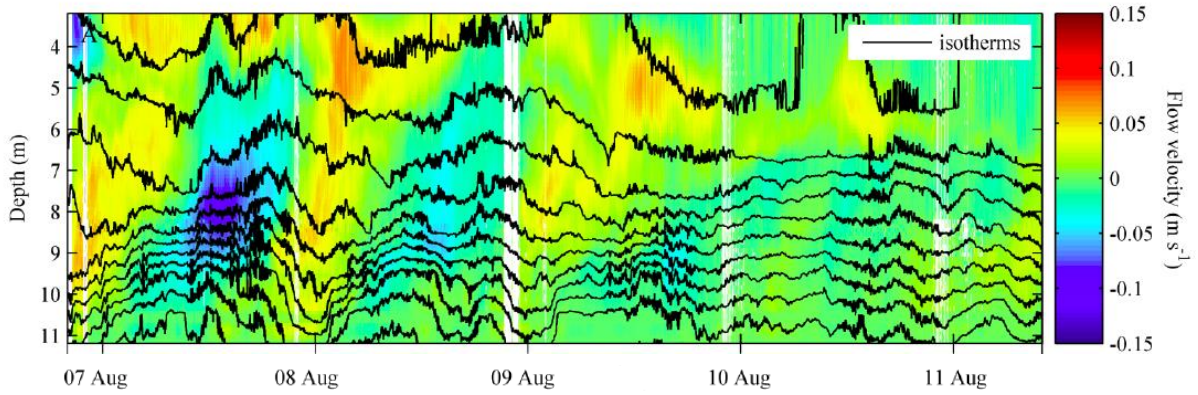


**Figure 1**. Longitudinal current velocity measured in Lake Scharmützelsee (colour scale) and overlaid isotherms (black lines: from bottom to top 11°C to 21°C with 1°C increment). Vertical fluxes of dissolved oxygen were measured at 3.5 m depth using the eddy-covariance technique. In spite of the strong temporal dynamics of current shear and isotherm displacement, turbulence was suppressed by density stratification below ~6 m depth and vertical transport was governed by molecular diffusion for most of the time.

**REFERENCES**

Kreling, J., J. Bravidor, D.F.McGinnis, M. Koschorreck, and A. Lorke (2014): Physical controls of oxygen fluxes at pelagic and benthic oxyclines in a lake. *Limnol. Oceanogr*. (under review).

Noss, C., and A. Lorke. (2014). Direct observation of biomixing by vertically migrating zooplankton. *Limnol. Oceanogr*., **59**, 724–732.

Wickramarathna, L. N., C. Noss, and A. Lorke (2014), Hydrodynamic Trails Produced by *Daphnia*: Size and Energetics. *PLoS One*, **9**: e92383.

# Scale-dependent relationships between climatic fluctuations and development of toxic cyanobacteria in large lakes

N. Salmaso

*IASMA Research and Innovation Centre, Istituto Agrario di S. Michele all'Adige - Fondazione E. Mach, Via E. Mach 1, 38010 S. Michele all'Adige (Trento), Italy.*

*e-mail nico.salmaso@fmach.it*

**KEYWORDS**
Large lakes; climatic fluctuations; teleconnection indices; toxic cyanobacteria; selective adaptation

## EXTENDED ABSTRACT

### Introduction

The effects of climatic fluctuations on aquatic communities are strongly dependent on the temporal scales and the ecological characteristics of species. Meteorological fluctuations at the weekly and monthly scales affect the short-term dynamics of living organisms. With long-term temporal scales, climate change causes alterations in the physics, chemistry and biology of lakes, affecting ecological processes and life cycles, with the potential of causing the disappearance of autochthonous species and the introduction of alien organisms. Further, the effects are strongly dependent on the physiographic characteristics of water bodies. The complexity of interactions and the implications of climate change and physiographic features on the lake functioning mechanisms are not always simple to recognise, requiring a wide approach, able to overcome the classical disciplinary academic barriers. In this review, we will report a few examples highlighting the strict coupling between the physical environment (climate and morphometric features) and the development of cyanobacteria (both at the population and genotypic level) in deep and large lakes. Examples will include the effects of the winter climate on the development of summer cyanobacteria in Lake Garda, and the selection of specific strains adapted to lakes of different depth (i.e. with gas-vesicles of different strength). Both processes are mediated by fluctuations in the deep mixing regimes.

### Materials and methods

The experimental setup has been described in D'Alelio et al. (2011) and Salmaso et al. (2014). In the southern subalpine and Mediterranean regions the winter climate can be effectively summarized by the East Atlantic pattern measured between December and February ($EA_{DJF}$) (Salmaso et al., 2014). Positive values of the index are associated with warm winters, and vice versa. In this contribution, the relationships have been updated to the period from 1993/1995 to 2013. To avoid spurious correlations originating from the presence of temporal trends, before regressions the variables were linearly de-trended.

### Results and discussion

The $EA_{DJF}$ showed a strong influence on the winter climate, with significant effects on the spring lake temperatures (Fig. 1a; $r^2$=0.56, $p$<0.01). In turn, the extent of the winter cooling triggered a long chain of events which included the impact of spring water temperatures on the extent of vertical mixing ($r^2$=0.55, $p$<0.01), the impact of vertical mixing on the spring epilimnetic concentrations of total phosphorus ($TP_{epiS}$, $r^2$=0.79, $p$<0.01), and the effects of fertilization ($TP_{epiS}$) on the biovolumes of cyanobacteria in summer and autumn

($r^2$=0.34, p<0.01). The key role of EA in the control and origin of the chain of causal events was exemplified by the significant relationship between $EA_{DJF}$ and the biovolume of cyanobacteria in summer and autumn (Fig. 1b, $r^2$=0.29, p<0.05). Nevertheless, the effects on cyanobacteria were mediated by the autoecology of the impacted species. Whereas an increase in the early-spring replenishment of nutrients after harsh winters favoured a stronger development of summer metalimnetic Oscillatoriales (*Planktothrix rubescens*, the dominant species), the formation of summer surface blooms of a different minor group (*Dolichospermum lemmermannii*, Nostocales) was relatively unaffected by the availability of nutrients, and more strictly linked to local, weekly meteorological conditions.

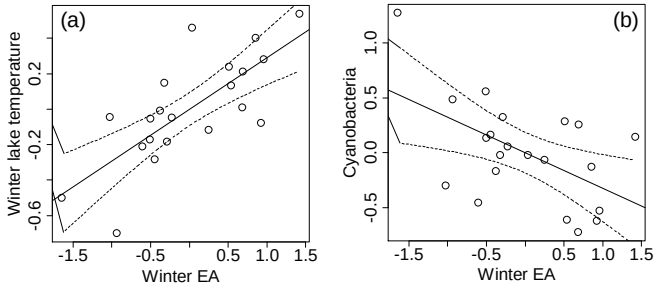


Fig. 1. Impact of the winter (Dec-Feb) East Atlantic pattern on (a) the late winter lake temperatures (February-March; 0-100 m; $p$ < 0.01) and (b) the biomass of cyanobacteria between June and December ($p$ = 0.01) in Lake Garda. Dotted lines are 95% confidence bands. Before the analyses, the variables were linearly de-trended.

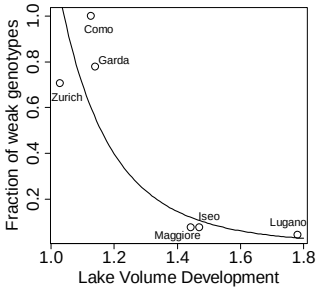


Fig. 2. Relationship between the fraction of *P. rubescens* genotypes synthesizing weak gas vesicles and the "Volume Development" ($V_d$) ($p$ < 0.01). $V_d$ > 1 are typical of concave lakes, i.e. characterized by a lower fraction of shallow areas. From D'Alelio et al. (2011), modified.

The morphometric features of the deep subalpine lakes and the deep mixing dynamics were proved to represent also a strong factor selecting different genotypes of *P. rubescens* adapted to different hydrostatic pressures. This species is able to control the vertical positioning through the synthesis of gas-vesicles, i.e. cellular structures which provide positive buoyancy. After summer metalimnetic development, in winter *P. rubescens* is entrained by convective mixing into the deeper water column, where gas vesicles can collapse due to increasing hydrostatic pressure, resulting in a decrease of buoyancy and population abundance. D'Alelio et al. (2012) showed that the proportion of the stronger strains (i.e. those with the genes able to synthesize stronger gas-vesicles) was greatest in deep basins with high depths and concave slopes (as exemplified by the "volume development", $V_d$, a parameter which estimates the departure of the shape of a lake basin from a cone, where $V_d$=1), i.e. in lakes where the effects of deeper penetrative mixing events were higher and extended over a greater area (Fig. 2).

The results of these recent investigations contribute to put in a new perspective the impact of the physical environment (climate and internal physical processes) on the development of algal assemblages. Physical drivers can act not only at the level of population and at different time-scales (with different time-lags), but also at the level of genotypes. Implications for the use of predictive models based on taxonomic or functional groups will be finally discussed.

**REFERENCES**

D'Alelio, D., A. Gandolfi , A. Boscaini, G. Flaim, M. Tolotti, N. Salmaso (2011), *Planktothrix* populations in subalpine lakes: selection for strains with strong gas vesicles as a function of lake depth, morphometry and circulation, *Fresh. Biol.*, **56**, 1481–1493.

Salmaso, N., F. Buzzi, L. Cerasino, L. Garibaldi, B. Leoni, G. Morabito, M. Rogora, M. Simona (2014), Influence of atmospheric modes of variability on the limnological characteristics of large lakes south of the Alps: a new emerging paradigm, *Hydrobiologia*, **731**, 31–48.

# Extended abstracts

# Modelling climate and storage volume influences on a subtropical reservoirs' circulation characteristics

E. Bertone[1]*, R.A. Stewart[1], H. Zhang[1] and K. O'Halloran[2]

[1] *Griffith School of Engineering, Griffith University, Gold Coast, Australia*
[2] *Scientific Services and Data Systems, Seqwater, Brisbane, Australia*

**Corresponding author, e-mail edoardo.bertone@griffithuni.edu.au*

**KEYWORDS**
Lake circulation; water treatment; climate change; water storage; lake nutrients.

## EXTENDED ABSTRACT

### Introduction

As stated by the Intergovernmental Panel of Climate Change (IPCC) in 2007, the anthropogenic increase in greenhouse gases emissions is having an effect on the most recent climate change (CC) that goes well beyond the natural causes. The main consequence is a substantial increase in temperature, with calculations predicting a rising global average surface temperature up to 5.4 °C by 2099 (IPCC, 2007). Water reservoir thermal stability and mixing patterns are expected to change as a result of future climate (Hondzo and Stefan, 1993; Stefan et al., 1998); this might imply the mixing regime shifting from polymictic to dimictic, dimictic to monomictic, or monomictic to oligomictic (Boehrer and Schultze, 2008; Livingstone, 2008). In winter 2013, the warm monomictic Advancetown Lake reservoir (Gold Coast region, Australia) was affected by a warmer than usual winter and did not fully mix (Bertone et al., 2014). However, the reservoir was recently upgraded and reached, for the first time, its new full capacity (310,730 ML) during the previous wet summer, thus requiring more work to break down the thermal stability. The current study aims, through the use of a numerical model, to assess the relative importance of storage volume and CC in triggering or limiting the lake circulation, in order to understand if a transition from monomixis to meromixis will be permanent.

### Materials and methods

Through an effective collaboration with Seqwater, the main bulk water supplier in South East Queensland (SEQ), physical data were made available for Advancetown Lake, the main source of potable water for the Gold Coast region. Meteorological data were also collected from different sources, as well as downscaled seasonal CC predictions till 2090 as detailed in Helfer et al. (2012). Finally, six scenarios regarding different possible increases in population and associated water demand for the Gold Coast region were taken from recent studies (Sahin et al., 2013).

Because of the high residence time and slow horizontal velocities of the reservoir, a one-dimensional model was considered to be appropriate for this study. The model used was "General Lake Model", a hydrodynamic model developed by University of Western Australia that conducts a lake water and energy balance and computes vertical profiles of temperature, salinity and density. Since the main focus of this research was on thermal stratification/destratification, the model's parameters calibration was conducted in order to optimize the variable $\Delta Tw$, intended as the water temperature differential between top and bottom of the reservoir. Once the parameters were calibrated for the period 2008-13, the

model was applied to the period 2014-2090, where the input time series were repeated and changed by systematically applying the prediction coefficients. Six different scenarios were run considering the different projections in water demand; however, the results from different simulations were clustered together, by associating the mixing behavior to the winter reservoir's volume for different periods into the future.

## Results and discussion

Figure 1 shows how, without CC (blue bar), the monomictic regime would persist regardless of the volume. However, if CC-modified input variables are applied, then the lake's volume plays a central role: whenever the volume will be low (e.g. increased water demand, El-Nino events), then CC will not impede a full circulation (Figure 1a). However, if the volume will be close to the maximum capacity (e.g. following La-Nina events, or the installation of new bulk supply sources such as desalination plants which will satisfy increased water demand) then the increased stability induced by both CC and the high volume will often be too strong to be fully broken in future winters (Figure 1b). As a result, Advancetown Lake will fully circulate only around half the time between 2076 and 2090.

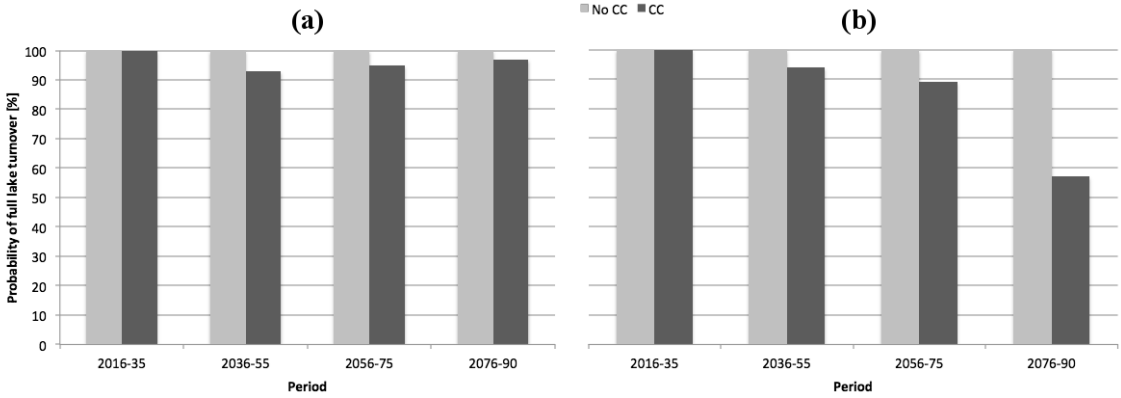


**Figure 1.** Probability of full reservoir destratification; low (a) or high (b) storage volume years**.**

Another important CC effect, shown by the model in any future scenario, is the increase in water temperature both in the epilimnion and in the hypolimnion, leading to stronger and longer summer stratifications. Such stratifications will have an impact on the traditional biogeochemical processes of the lake, potentially presenting new water quality issues (e.g. increased algal blooms and nutrients release) to manage.

### REFERENCES

Bertone, E., Stewart, R.A., Zhang, H., O'Halloran, K., Analysis of the mixing processes in the subtropical Advancetown Lake, Australia, *Journal of Hydrology* (under review; submitted January 2014).

Boehrer, B., Schultze, M., (2008), Stratification of lakes, *Rev. Geophys*., **46**(2), doi:10.1029/2006RG000210

Helfer, F., Lemckert, C., Zhang, H. (2012), Impacts of climate change on temperature and evaporation from a large reservoir in Australia, *Journal of Hydrology*, **475**, 365-378.

Hondzo, M., Stefan, H. (1993), Regional water temperature characteristics of lakes subjected to climate change, *Climatic change*, **24**, 187-211.

IPCC (2007), Climate Change 2007: the Physical Science Basis, *Contribution of Working Group I to the 4th Assessment Report of the Intergovernmental Panel of Climate Change* [Solomon, S., Qin, D., Manning, M., Chen, Z., Marquis, M., Averyt, K.B., Tignor, M. and Miller, H.L. (eds.)]. Cambridge University Press, Cambridge, UK and New York, USA, 996 pp.

Livingstone, D.M. (2008), A change of climate provokes a change of paradigm: taking leave of two tacit assumptions about physical lake forcing, *Internat. Rev. Hydrobiol*., **93**, 404-414.

Sahin, O., Stewart, R.A., Helfer, F. (2013), Bridging the water supply-demand gap in Australia: a desalination case study, *European Water Resources Association (EWRA) 8th international conference, Porto, Portugal*.

Stefan, H.G., Fang, X., Hondzo, M. (1998), Simulated climate change effects on year round water temperatures in temperate zone lakes, *Climatic change*, **40**, 353-381.

# Thermobaric stratification in very deep Norwegian fjord lakes

B. Boehrer[1*], L. Golmen[2,3], J. E. Løvik[4], K. Rahn[1] and D. Klaveness[5]

[1] *Helmholtz-Centre for Environmental Research - UFZ, Magdeburg, Germany*
[2] *Norwegian Institute for Water Research (NIVA), Bergen, Norway*
[3] *Runde Environmental Centre, Runde, Norway*
[4] *Norwegian Institute for Water Research (NIVA). Ottestad, Norway*
[5] *University of Oslo, Department of Biosciences, Oslo, Norway*

**Corresponding author, e-mail Bertram.Boehrer@ufz.de*

**KEYWORDS**
Deep lakes; thermobaricity, compressibility, water density, physical limnology

## EXTENDED ABSTRACT

### Introduction

The temperature dependence of compressibility of water (thermobaricity) leads to a shift of the temperature of maximum density by 0.02 °C/bar. Hence the temperature of maximum density can be drawn as a profile against depth $T_{md}(z)$ and reaches about 3.0°C at the base of a 500m deep lake (see below). These water properties affect the circulation and stratification in very deep freshwater lakes (Lake Baikal: Weiss 1991, Crawford and Collier 1997). For horizontally homogeneous lakes, this effect has been investigated previously (see Boehrer et al. 2008). In this contribution, we look at lakes long enough to allow for longitudinal temperature gradients.

### Materials and methods

We show measurements taken in five Norwegian fjord lakes early at a time when the lakes have just started into the summer stratification 2006. All lakes were deeper than 200m. We measured profiles of temperature, electrical conductivity, dissolved oxygen and pH.

### Results and discussion

Results confirm the thermobaric stratification, i.e. temperatures in the deeper waters lie below 4°C even during the summer stratification period (see Fig. 1). The temperature gradient in the lakes Mjøsa, Tinnsjø and Tyrifjord corresponds to

$$\frac{\partial T}{\partial z} = 0.6 \frac{\partial T_{md}}{\partial z}, \qquad (1)$$

which is close to a stability criterion promoted by Eklund in 1965. A closer check of the conditions indicate that the Eklund criterion does not apply in these conditions, and in deed, two lakes (Hornindalsvatn and Breimsvatn) oppose the stability criterion (Figure 1).

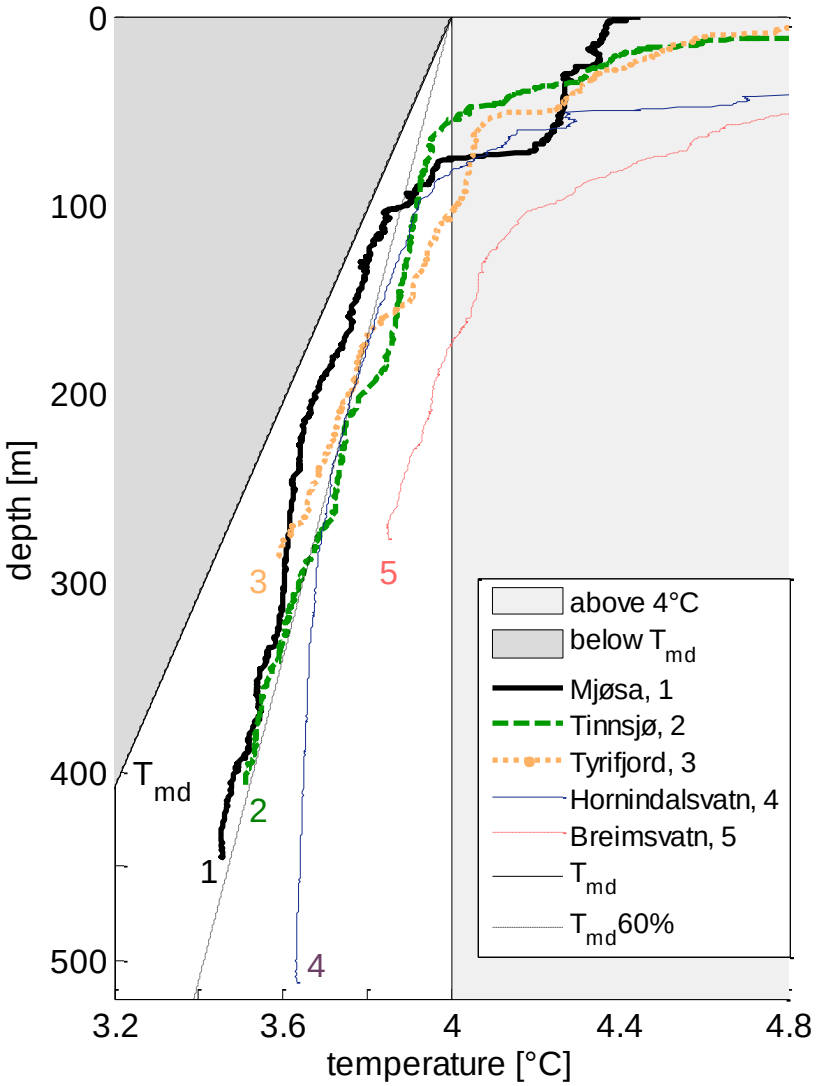


**Figure 1**. Temperature profiles from five Norwegian fjord lakes in spring 2006 (from Boehrer et al., 2013).

A length ranking of the lakes corresponded perfectly with the ranking of bottom temperatures. As long lakes provide better conditions for horizontal temperature gradients, I is reasoned that the temperature profiles that establish in very deep lakes are the result of longitudinal gradient before the onset of summer stratification.

**REFERENCES**

Boehrer, B., Fukuyama, R., Chikita, K. (2008), Stratification of very deep, thermally stratified lakes. *Geophys. Res. Lett.* **35**, L16405. http://dx.doi.org/10.1029/2008GL034519

Boehrer B., Golmen L., Løvik J.E., Rahn K., Klaveness D. (2013), Thermobaric stratification in very deep Norwegian freshwater lakes, *J. Great Lakes Res.*, **39**, 690–695, http://dx.doi.org/10.1016/j.jglr.2013.08.003

Crawford, G.B., Collier, R.W. (1997), Observations of deep mixing in Crater Lake, Oregon. *Limnol. Oceanogr.* **42**, 299–306.

Eklund, H. (1965), Stability of lakes near the temperature of maximum density, *Science* **149**, 632-633.

Weiss, R.F., Carmack, E.C., Koropalov, V.M. (1991), Deep-water renewal and biological production in Lake Baikal. *Nature*, **349**, 665–669.

# Process-based modelling of Lake Geneva

D. Bouffard[1]*, R. Schwefel[1], A. Gaudard[1], U. Lemmin[2] and A. Wüest[1]

*[1] Physics of Aquatic Systems Laboratory – Margaretha Kamprad Chair,*
*[2] Ecological Engineering Laboratory,*
*ENAC, Ecole Polytechnique Fédérale de Lausanne EPFL, Lausanne, Switzerland*

**Corresponding author, e-mail damien.bouffard@epfl.ch*

**KEYWORDS**
Lakes; near bed currents; modelling.

## EXTENDED ABSTRACT

### Introduction

Lake Geneva, the largest perialpine lake, is still recovering from excessive phosphorus loading 50 year ago and has one of the highest measured hypolimnetic oxygen depletion rates in Europe (areal hypolimnetic mineralization rate, AHM ~1.4 g/($m^2$d) (Müller et al. 2012)). Oxygen depletion is to a large extent driven by sediment oxygen uptake which in turn depends on the flow velocity in the bottom boundary layer. Therefore, a key objective is to predict the dynamics of the bottom currents as a response to external forcing. Influenced by the surrounding mountains, the wind field over Lake Geneva is strongly heterogeneous which modifies and complicates the lake's dynamics.

### Materials and methods

We used a 3-D hydrodynamic model (Deft3D-FLOW) to investigate the spatial and temporal dynamics of the lake circulation as well as the basin-scale internal waves, both inducing bottom currents. This model has recently been successfully implemented to model the dynamics of a bay on Lake Geneva (Razmi et al. 2013). In our case, the basin was discretized by using a maximum grid size of 500 m horizontally and 100 z-layers in the vertical. The vertical resolution was chosen to accurately resolve the surface boundary conditions with a vertical resolution of 0.25 m near the surface, gradually increasing to 1 m at 60 m depth. This choice was the best for considering external forcing and reproducing thermocline oscillations. The model was forced by a 2.2 km meteorological mesh grid (COSMO 2) allowing to take into account the spatial variability of the wind field over the partly mountain-sheltered Lake Geneva (Fig. 1). We run the model using a k-ε turbulence closure with a 1 min time step for different years (2011 and 2012).

For 2011 and 2012, the model was validated in temperature with (i) monthly temperature profiles at the center of the lake (SHL2, Fig. 1), (ii) hourly surface and bottom temperature data near the shore (Buchillon, Fig.1 ) and (iii) lake water surface temperature from Advanced Very High Resolution Radiometer satellites (Oesch et al. 2008). Currents were validated over a few months of acoustic Doppler current profiler (ADCP) measurements at two different locations (Fig. 1). Given the size of the lake compared to the only two locations we used for field validating the currents, we tested the possibility to process-based validate a model by comparing the spectral response and statistical distribution of the current intensity and direction from the model with historical long-term (~2 months) current measurements from previous years. We restricted our analysis to the stratified period and only used near-bed current (2 m above the bottom). We finally used current data from 7 different sites (Fig. 1).

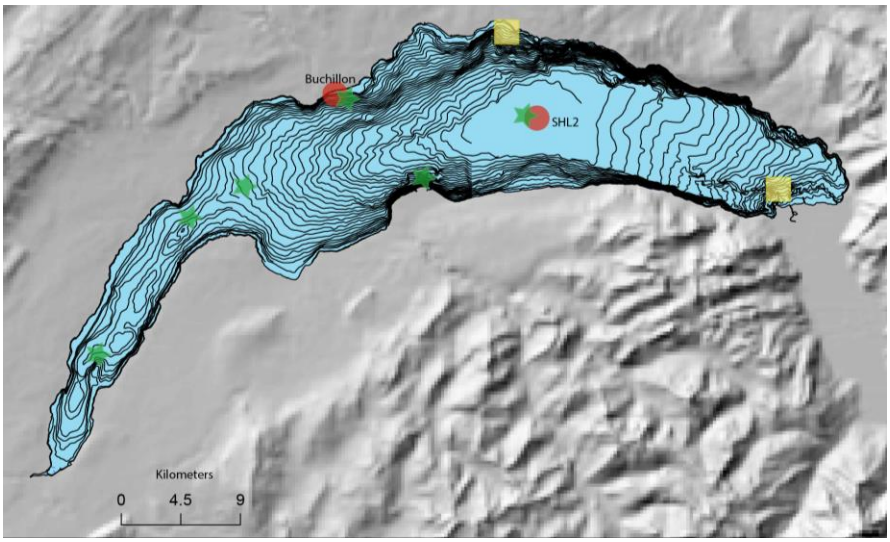


**Figure 1.** Bathymetric map of Lake Geneva including 10 m depth contours from 0 to 310 m. Red dots indicate temperature measurements and yellow square ADCPs measurements for the year 2011, 2012. Green stars indicate the location of other current measurements taken over the last 10 years on Lake Geneva.

## Results and discussion

The model has been successfully validated both in temperature and currents by using the data from the years 2011 and 2012. Interestingly, this study also demonstrates that statistical and spectral information inferred from historical data can be used to gain more confidence in the large scale hydrodynamic model (Fig. 2). This validated model is now applied together with field measurements (oxygen micro-profiler from Unisense and 2 MHz ADCP from Nortek) to correlate in space and time the sediment oxygen uptake and the bottom boundary layer velocity to the external forcing.

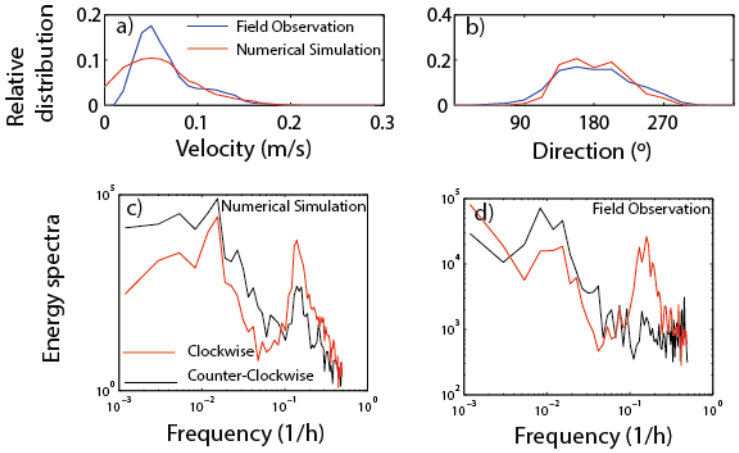


**Figure 2.** Comparison for two summer months of model output and observation concerning the statistical distribution of the near-bed current intensity (a) and direction on a nearshore site (b). Panels (c) and (d) show the spectral response of near-bed current from the model and the observation on an offshore site. The clockwise peak - a typical signature of a Poincaré wave - is well reproduced in the model.

## REFERENCES

Müller, B., L. D. Bryant, A. Matzinger, and A. Wüest (2012), Hypolimnetic oxygen depletion in eutrophic lakes. *Environ. Sci. Technol*. **46**(18): 9964-9971.

Oesch, D., J. M. Jaquet, R. Klaus, and P. Schenker (2008), Multi-scale thermal pattern monitoring of a large lake (Lake Geneva) using a multi-sensor approach. *Int. J. Remote Sens*. **29**: 5785–5808.

Razmi, A. M., D. A. Barry, R. Bakhtyar, N. Le Dantec, A. Dastgheib, U. Lemmin, and A. Wüest (2013), Current variability in a wide and open lacustrine embayment in Lake Geneva (Switzerland). *J. Great. Lakes Res*. **39**: 455–465.

# Sediment dynamics in shallow micro-tidal environments

L. Carniello[1]* and A. D'Alpaos[2]

[1] *Department of Department of Civil, Environmental and Architectural Engineering, University of Padova, Italy.*
[2] *Department of Geosciences, University of Padova, Italy.*

**Corresponding author, e-mail luca.carniello@dicea.unipd.it*

**KEYWORDS**
Lagoons; sediment transport; wind waves; modelling.

## EXTENDED ABSTRACT

### Introduction

A precise description of sediment dynamics (resuspension and re-distribution of sediments) is crucial when investigating the long term evolution of the different morphological structures characterizing tidal landscapes.

It has been demonstrated that wind waves are the main responsible for sediment resuspension in shallow micro-tidal lagoons where tidal currents, which produce shear stresses large enough to carry sediments into suspension only within the main channels, are mainly responsible for sediment redistribution (Carniello et al., 2011).

### Materials and methods

A mathematical model has been developed to describe sediment entrainment, transport and deposition due to the combined effect of tidal currents and wind waves in shallow lagoons considering both cohesive and non-cohesive sediments. The model was calibrated and tested using both in situ point observations and turbidity maps obtained analyzing satellite images (Carniello et al., 2011, 2012, 2014).

Once calibrated the model can integrate the high temporal resolution of point observations with the high spatial resolution of remote sensing, overcoming the intrinsic limitation of these two types of observations.

The model was applied to the specific test case of the Venice lagoon simulating an entire year (2005) which was shown to be a "representative" year for wind and tide characteristics. The time evolution of the computed total bottom shear stresses (BSS) and suspended sediment concentration (SSC) was analyzed on the basis of a "Peaks Over Threshold" method once a critical value for bottom shear stress (i.e. the critical shear stress) and turbidity (i.e. a value censoring turbidity which cannot be ascribed to storm events) were chosen.

### Results and discussion

The analyses of the numerical results enabled us to demonstrate, using the Kolmogorov-Smirnov goodness of fit test at significance level $\alpha = 0.05$, that resuspension events analyzed both in term of BSS (D'Alpaos et al., 2013) and SSC can be modeled as marked Poisson processes being the interarrival time between two consecutive resuspension occurrences an exponentially distributed random variable (Figure 1). The same analyses performed considering both the intensity of peak excesses and their duration enabled us to show that also these quantities are exponentially distributed random variable.

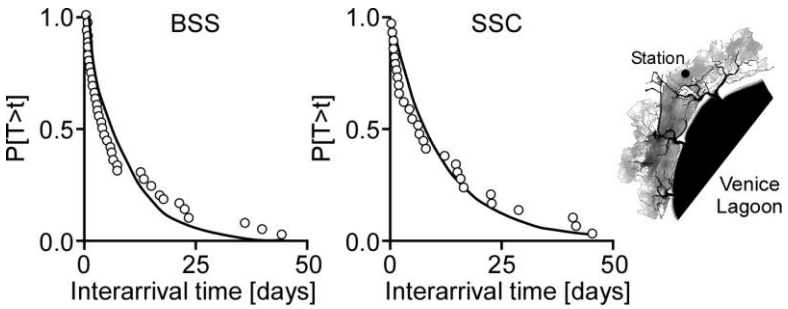


**Figure 1**. Probability distributions of interarrival times computed considering model results in term of BSS and SSC at one specific location within the Venice Lagoon.

Figure 2 shows the spatial distribution of the mean interarrival time of events exceeding the prescribed threshold values for BSS and SSC respectively. The two processes can be described as marked Poisson processes in almost all of the lagoon excluding (black areas) salt marshes, where very shallow water depth and the presence of vegetation prevent resuspension by waves, and the main channels where resuspension is exclusively due to tidal currents.

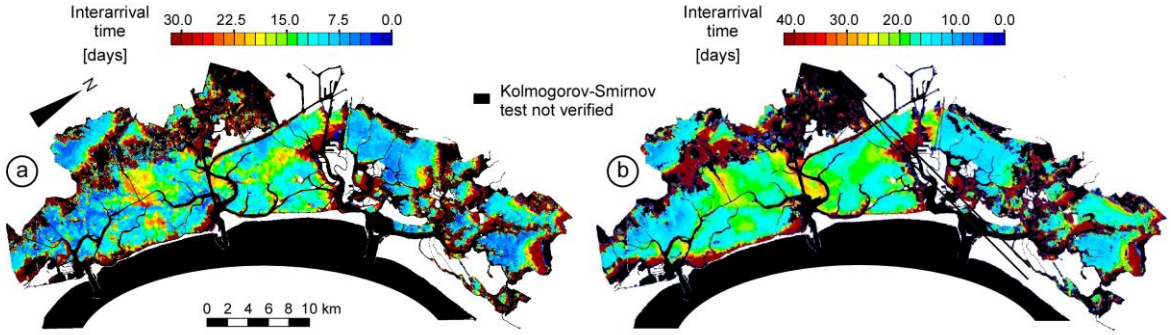


**Figure 2**. Spatial distributions of mean interarrival times for BSS (a) and SSC (b). In black: areas where Kolmogorov-Smirnov goodness of fit test in not verified.

Interestingly the central and southern part of the lagoon are those characterized by shorter interarrival times as well as higher intensities and durations of over thresholds events which is indirectly confirmed by the intense erosive process that this portion of the lagoon has been experiencing since the beginning of the last century (D'Alpaos, 2010).

The main finding of the present analyses consists in having demonstrated that wind driven resuspension events in a shallow microtidal basin analyzed both considering the driving process (BSS) and its effect (SSC) can be classified as marked Poisson processes. We speculate that our results are relevant for long-term morphodynamic studies as they can be used to generate Poissonian sequences of forcings through which Monte Carlo realizations of relevant morphological evolutions can be computed.

**REFERENCES**

Carniello, L., A. D'Alpaos and A. Defina (2011), Modeling wind waves and tidal flows in shallow micro-tidal basins, *Estuarine Coastal Shelf Sci.*, **92**, 263–276, doi:10.1016/j.ecss.2011.01.001.

Carniello, L., A. Defina and L. D'Alpaos (2012), Modeling sand-mud transport induced by tidal currents and wind waves in shallow microtidal basins: Application to the Venice Lagoon (Italy), *Estuarine Coastal Shelf Sci.*, **102**, 105–115, doi:10.1016/j.ecss.2012.03.016.

Carniello, L., S. Silvestri , M. Marani, A. D'Alpaos, V. Volpe and A. Defina (2014), Sediment dynamics in shallow tidal basins: in situ observations, satellite retrievals, and numerical modeling in the Venice Lagoon. *J. Geophys. Res.* doi: 10.1002/2013JF003015.

D'Alpaos, A., L. Carniello, A. Rinaldo, (2013), Statistical mechanics of wind wave-induced erosion in shallow tidal basins: Inferences from the Venice Lagoon. *Geophysical Research Letters*, **40**, doi:10.1002/grl.50666.

D'Alpaos, L. (2010), Fatti e misfatti di idraulica lagunare. La Laguna di Venezia dalla di-versione dei fiumi alle nuove opere alle bocche di porto, Istituto Veneto di SS.LL.AA., Memorie, Classe di scienze fisiche, matematiche e naturali, Vol. XLIV, Venezia.

# CALYPSO - an operational network of HF radars for the real-time monitoring of surface currents in the Malta-Sicily Channel

S. Cosoli[1*], F. Capodici[2], G. Ciraolo[2], A. Drago[3], A. Maltese[2], M. Gacic[1], C. Nasello[2], J. Azzopardi[3], A. Gauci[3], P. Poulain[1] and G. La Loggia[2]

[1] *Istituto Nazionale di Oceanografia e di Geofisica Sperimentale, Italy*
[2] *Dipartimento di Ingegneria Civile Ambientale, Aerospaziale, dei Materiali, Università degli Studi di Palermo, Italy*
[3] *International Ocean Institute - Malta Operational Centre, University of Malta*

**Corresponding author, e-mail scosoli@ogs.trieste.it*

**KEYWORDS**
Sea surface currents; oil spill; HF radar system.

## EXTENDED ABSTRACT

Following the case in several other areas of the Mediterranean basin, the Sicily Channel is under pressure due to 1) significant migration fluxes (Figure 1, left panel); and 2) intense traffic of commercial vessels (right panel).

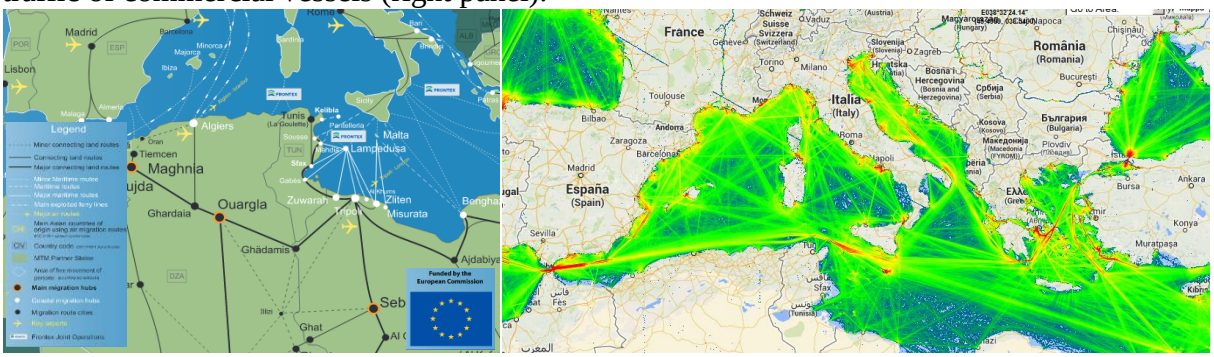


**Figure 1.** Immigration fluxes along the Central Mediterranean and East Africa Routes (left panel; source: 2012 MTM Mao on Irregular and Mixed Migration Routes); and, vessel traffic density map at 11 UTC of 11th April, 2014 (source: https://www.marinetraffic.com/it/).

Illegal migration often results in dramatic loss of lives that can be avoided with timely Search and Rescue (SAR) interventions; such SAR services require accurate information such as on sea-state and operational tools such as trajectory forecasting for floating objects at sea. The maritime transport of oil crossing this region accounts for 25% of the global maritime traffic and for nearly 7% of the world oil accidents over the last 25 years. In combination with localized oil extraction plants existing in the shelf zones this situation presents a serious threat to both the open-sea and coastal-zone habitats, with consequent impacts on local economic activities as tourism and fisheries, impacts on ecosystems and losses in revenue. In the case of both accidental/deliberate oil spills or drifting-vessel emergency, an operative response chain must include both the detection and the trajectory prediction steps, that take advantage of the most appropriate methodologies and data availability such as: updated meteorological information, near-surface current measurements, and hydrodynamic models with oil spill weathering processes modules. Indeed, both the knowledge of initial positions and an accurate, effective and prompt prediction of their future pathways are of fundamental importance to optimize response activities, shortening the intervention time and increasing their efficacy. In the particular case of oil spills, the knowledge of spill trajectories is very important to anticipate impacts on economic and environmental assets on threatened coasts; the provision of accurate information to decision makers together with training in best practices and damage recovery methods need to be adopted in order to minimize spill impacts.

In this framework, a reliable knowledge of sea-surface currents is a fundamental prerequisite. In both cases of SAR and pollutant mitigation, the detection process is just the first step in the response chain, whereas the most important steps deal with interception and mitigation. Hydrodynamic numerical models require forcing data from other numerical models, that provide the proper meteorological forcing and the initial and boundary conditions. Computer models are however prone to errors due for instance to parametrization of subgrid scale processes. Numerical models can be improved if actual measurements that can map the spatial distribution of the sea surface currents is provided. Indeed, observed sea surface currents can be used i) to provide boundary and initial conditions; ii) for calibrating / validating hydrodynamic numerical models; iii) within a data assimilation process, to drive or correct the model outcome. High-Frequency (HF) coastal radars provide useful information to support sea safety and monitoring, as they are capable of measuring sea-surface currents with high temporal (10 minutes – 3 hours) and spatial (500 m – 6 km) resolution. Designed originally for research purposes, their use ranges from search-and-rescue activities to water quality monitoring in coastal regions where, for instance, wastewater treatment and industrial plants could affect the health of the sea. The use of HF radars is nowadays well established worldwide: sea surface currents on both the eastern and western coasts of the United States are continuously monitored through HF radar networks. In Europe, the number of installations is increasing: several HF networks were already installed in Galicia (North-west Spain), Ría de Vigo (Galicia, Spain), Strait of Gibraltar, Iberian Peninsula, Irish Sea and Northern Scotland. Recently, a network of HF radars was installed in the Malta-Sicily Channel, as part of the CALYPSO project (www.capemalta.net/calypso), conducted under the partial fundingof the EU 2007-2013 Italia-Malta Programme. This project involved the University of Malta (Physical Oceanography Unit, IOI-Malta Operational Centre, in the role of Lead partner), the University of Palermo (Sicilian project focal point), and the expert advice of the Istituto Nazionale di Oceanografia e di Geofisica Sperimentale (OGS). The CALYPSO network is providing hourly sea surface current maps with a spatial resolution of 3 km since September 2012 (Figure 2).

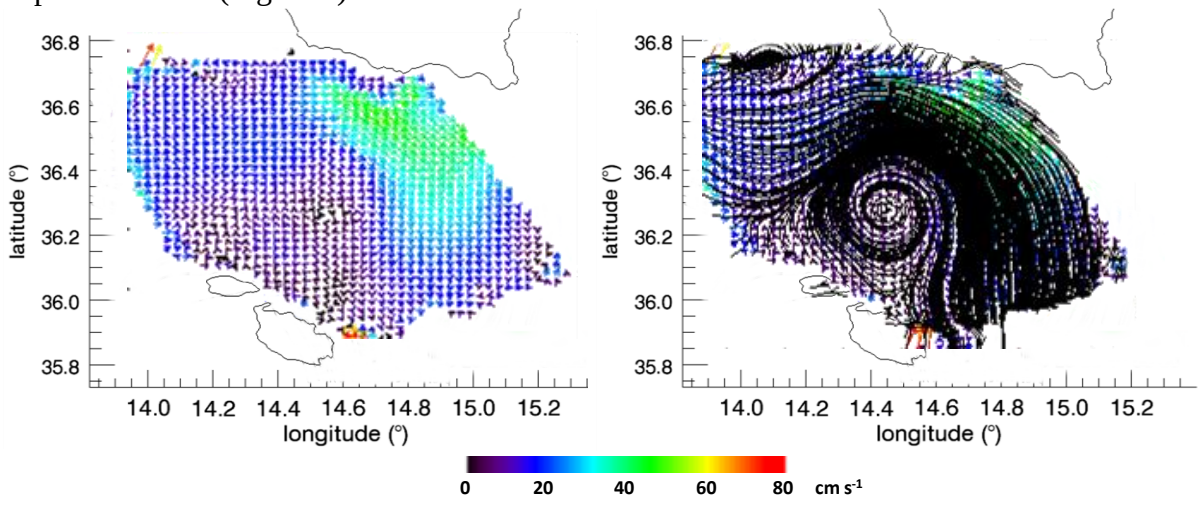


**Figure 2.** Average currents between 1 and 31 of January, 2014 (left panel) and their streamlines (right panel).

Here in this paper we provide a general review of data collected by the CALYPSO (CALYPSO-HF Radar Monitoring System and Response against Marine Oil Spills in the Malta Channel) system, its validation by means of *in situ* current data collected during 2012-2014 both by drifters and ADCP (Acoustic Doppler Current Profiler), also showing the importance of circulation processes at larger scale on the local dynamics in the Malta-Sicily Channel.

# Observations of turbidity currents and internal waves in Lake Ohau, South Island, New Zealand

R. Cossu[1]*, A.L. Forrest[1,2], P. Stumpner[2], H. Roop[3,4], G.B. Dunbar[3], R.H. Levy[4], M.J. Vandergoes[4] and S.G. Schladow[2]

[1]*Australian Maritime College, University of Tasmania, Launceston, TAS, Australia*
[2]*Environmental Research Center, Department of Civil and Environmental Engineering, University of California, Davis, CA*
[3]*Antarctica Research Center, Victoria University of Wellington, Wellington, NZ*
[4]*GNS Science, Department of Paleontology, Lower Hutt, Wellington, NZ*

**Corresponding author, e-mail remo.cossu@utas.edu.au*

**KEYWORDS**
Glacial lakes; turbidity currents; internal waves; mixing dynamics; sediment transport.

## EXTENDED ABSTRACT

### Introduction

In glacial lakes, processes such as turbidity currents, internal waves and convective instabilities drive mixing and sediment transport. These processes arise from inflow of rivers, wind stresses and diurnal and seasonal heating, respectively. We found evidence that all of these mechanisms are present in Lake Ohau (South Island, New Zealand, 44.234°S, 169.854°E) over an annual cycle, demonstrating the lake to be a very complex, dynamic system with large seasonal variations. Despite their episodic nature, we were able to measure and profile several turbidity current events, which play a major role in the ecosystem dynamics of the lake. In particular, detailed field observations of density currents are important, as the present understanding of river inflows in stratified lakes and reservoirs is far from complete.

### Materials and methods

Our observations were obtained near the head of the lake at water depths of 25m and 50m using a combination of instruments, including fast response thermistor chains (recording at 5 s intervals) and acoustic Doppler current profilers (ADCPs) and (recording at 30 min intervals) over an annual cycle (January 2012–January 2013) as well as data from a nearby weather station.

### Results and discussion

Here we focus on the stratified season during summer as this period generally showed stronger thermal gradients and larger river inflow rates. Figure 1 summarizes a portion of our main findings during the late spring-summer period (November 2012 - February 2013). The air temperature reveals a diurnal pattern with mean temperatures around 16 ºC (Figure 1a). Several rainstorms, with precipitation exceeding (>5 mm), were recorded during the experiment (Figure 1b) that were usually followed by increased inflow rates (200-1000 $m^3 s^{-1}$, Figure 1c). In addition, the spring-summer season showed a frequent occurrence of strong wind events (>8 m $s^{-1}$; Figure 1d). The resulting thermal structure is stratified after DOY 350 with mean temperatures of 14°C in the epilimnion and 8°C in the bottom waters but also exhibits many intermittent periods of cooling and destratification (Figure 1e). Increased river water inflow events are in broad agreement with large horizontal velocities of 0.15 - 0.40 m $s^{-1}$ (Figure 1f) and downward vertical velocities of 0.025 m $s^{-1}$ (Figure 1g) at heights up to

10 m above the bottom. These events can last up to several days (shown by the black arrows in figure 1f and 1g). In addition, high values of acoustic backscatter data (Echo intensity, Figure 1h) show that these inflows have sufficiently high sediment concentrations that the flow progresses as turbidity current along the bottom of the lake and observations of sediment traps reveal that particles are transported to more distal parts in the lake.

After DOY 320 the water column is characterized by frequent and rapid changes of temperature, which we attribute to the presence of internal waves with amplitudes >10 m when inflow rates are relatively low. The large inflow events around DOY 1 and DOY 10 caused increased mixing and completely destratified the water column demonstrating the significance of turbidity currents in this system for mixing processes. However, such intense inflow events ($Q > 1000\ m^3\ s^{-1}$) have been measured less than 10 times since the beginning of the discharge record in the 1920s. Differentiating the relative importance of turbidity currents caused by river inflow or internal waves as driving mechanisms in Lake Ohau during the summer is a source of continued work.

Our observations and analysis are important to relate physical characteristics such as turbidity currents to recently obtained sediment cores and to studies that aim to explain regional climate and the associated infill stratigraphy of lakes in New Zealand. On a larger scale, this work will contribute to better understanding of lake dynamics in the Southern Hemisphere, which have been poorly studied compared to their Northern Hemisphere counterparts in Europe, Asia and North America.

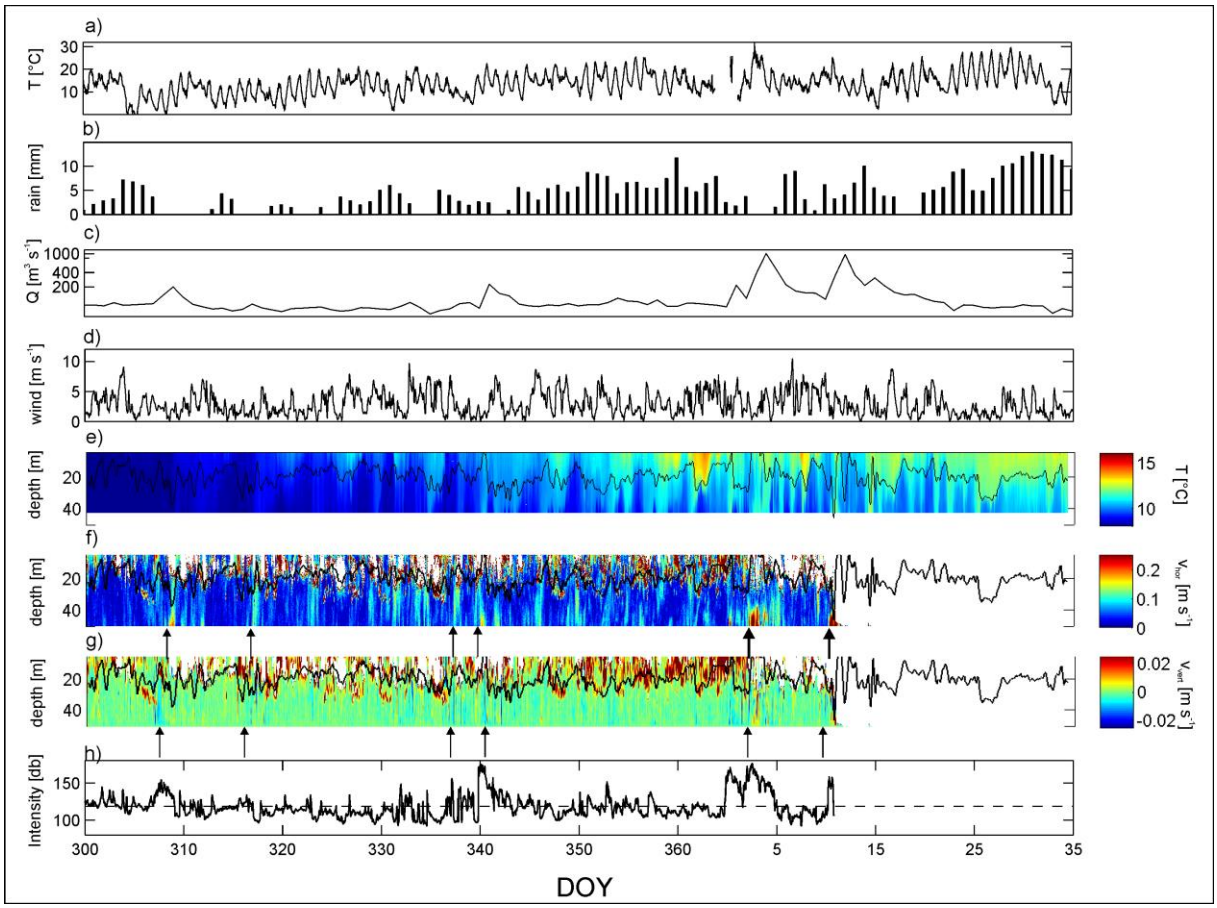


**Figure 1:** Observations of weather conditions, temperatures and currents in Lake Lake Ohau during summer: a) Air temperature; b) Recorded precipitation; c) Daily averaged river inflow rate (Q) at the head of the lake; d) Wind speed at 5 m above the ground; e) Thermal stratification is shown with colour contours, with the position of the thermocline marked in black; f) Colour contours of horizontal ADCP-velocities in the water column; g) Colour contours of vertical ADCP-velocities in the water column; and, h) Averaged Echo intensity of the ADCP pings at 5 m above the bottom.

# The analysis of turbulent structure of Ivankovskoye Reservoir (Russia)

E. Debolskaya* and G. Saminski

*Institute for Water Problems of the Russian Academy of Science, Moscow, Russia*

**Corresponding author, e-mail e_debolskaya@yahoo.com*

**KEYWORDS**
Turbulent structure; environment; water quality; modelling.

## EXTENDED ABSTRACT

### Introduction

To analyze turbulent structure of Ivankovskoye Reservoir (Russia) three-dimensional model GETM was applied. The main objectives of the work were: the identification of conditions and factors for the development of environmentally adverse structures; the obtaining of evaluation criteria for these structures; the development of methods for their determination.

### Materials and methods

The object of our research is the Ivankovskoye reservoir (Figure 1) being the main drinking water source of Moscow, supplying 70% of the total water consumption. The Ivankovskoye reservoir was built in 1937 to improve common and industrial water supply, navigation, hydroenergy, fish industry development and recreation use. However within the recent years the ecological condition of the reservoir itself and its coastal area causes more and more threats. The area of the reservoir is 41 000 km2, with a water mirror of 327 km2, a volume of 1.12 km3. At its greatest width it is 8 km, has an average depth of 3.4 m, the greatest depth is 19 m. The Ivankovskoye reservoir refers to the riverbed type and is one of the shallowest. Hydrological regime of the reservoir is determined by the natural conditions of the catchment area, weather conditions, the morphological structure of the reservoir, the water regime in the Moscow Canal and Konakovskaya State Power Station. The regime of currents in the reservoir is determined mainly by the work of Konakovskaya station and wind.


**Figure 1**. Ivankovskoye reservoir (on the Volga River).

To obtain the necessary data the following types of measurements were carried out: the mapping using GPS- navigation system with electronic data processing, the instrumental observations of meteorological characteristics, the methods of hydrography (echo sounding, measuring of temperature and current velocity).

To calculate the characteristics of the thermodynamic and turbulent structure of Ivankovskoye reservoir the three-dimensional mathematical model GETM was adapted.

**Results and discussion**

Expression characterizing ratio of averaged flow to turbulent flow can be written as $Rtur = uh / \nu_T$, similar to the streaming Reynolds number. Difference is in the denominator. It is not molecular but turbulent viscosity. In contrast to the streaming Reynolds number values of velocity and turbulent viscosity are needed not be averaged over the total depth of the flow, i.e. parameter *Rtur* depends not only on the horizontal but also on the vertical coordinates. It is shown (Figure 2) that there are significant areas were *Rtur* <1, which mainly located in shallow coastal areas.

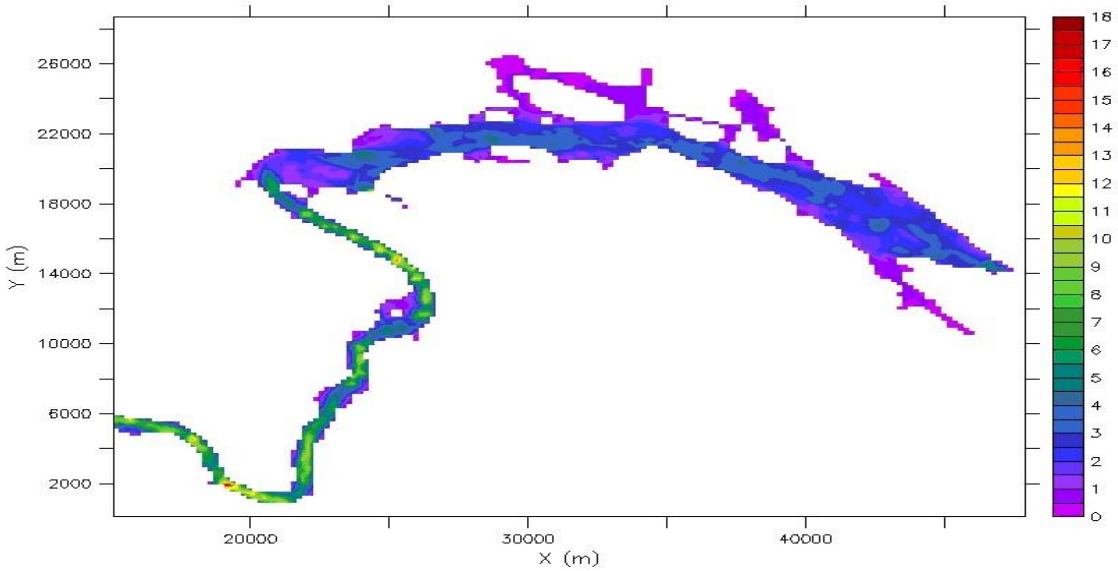


**Figure 2**. The distribution of the parameter *Rtur* averaged over depth and time for the weekly period in the reservoir water area.

Unlike the Reynolds number *Rtur* has one more (besides the flow velocity and depth) variable parameter - coefficient of eddy viscosity. Moreover it is necessary to involve another independent relation between the parameters characterizing the turbulence to characterize state of the flux. Namely size comparison of the vortices of different scales is needed. If the dimensions of the Kolmogorov eddies $L_{Kol}$ and vortices of integral scale $L_{int}$ will close at the same points and the same moments of time while $Rtur < 1$ it will confirm the hypothesis of the existence in this area only dissipative small-scale vortices. Considerable shallow areas are characterized by values $Rtur < 1$. At the same time in these areas $L_{int}$ and $L_{Kol}$ values are close. Sometimes there is a situation characterized by the implementation of inequality $L_{int} < L_{Kol}$, as a rule, in the absence of wind action, when the flow velocity and turbulent parameters tend to zero, and the coefficient of turbulent exchange close to the molecular. Thus, in the areas of flow, characterized by the value of the parameter $Rtur < 1$ in the absence of wind action only small-scale dissipative eddies exist. It is shown also that these areas can occur in the deep zones of the reservoir.

The proposed method allows you to define the conditions of appearance of areas with low turbulent exchange, i.e. unfavorable from an environmental standpoint.

# The duration of summer stratification - routine temperature measurements in two dimictic lakes of Northern Germany

C. Engelhardt* and G. Kirillin

*Department of Ecohydrology, Leibniz-Institute of Freshwater Ecology and Inland Fisheries, Müggelseedamm 310, 12587 Berlin, Germany*

**Corresponding author, e-mail engelhardt@igb-berlin.de*

**KEYWORDS**
Temperate lakes; Onset of stratification; Breakup of stratification; Stability threshold; High-resolution data.

## EXTENDED ABSTRACT

### Introduction

The ecological conditions of temperate lakes during stratification differ substantially from those during the preceding and following periods of complete overturn. Hence, the duration of stratification is of crucial ecological importance (e.g. De Stasio et al., 1996; Kirillin et al., 2012). Because timing and the strength of lake stratification are driven by atmospheric forcing, climate change influences these characteristics by increasing stability and duration of summer stratification in the temperate zone (e.g. Robertson and Ragotzkie, 1990; Peeters et al., 2007). One possibility to estimate the envisaged trends in duration of summer stratification from observational data is to determine experimentally the onset and the end of stratification with the help of long-term measurements. Different diagnostic indices characterizing stratification (Read et al., 2011) were proposed over the last decades. To define temporal limits of the stratified period one should assume that the lake is either mixed or stratified, whereas, in reality, stratification is a gradual process (Stainsby et al., 2011). For two temperate lakes, we demonstrate that the transition time from mixed to stratified water column in spring and vice versa in autumn can last from several days up to about two weeks. Regardless of this common feature, the transition processes at the beginning and at the end of the summer stratification differ in their nature. The formation of stratification in spring is an unstable, fragile process, often interrupted by setbacks of mixing. In contrast, the termination of the stratified period in autumn is distinguished by a gradual, monotonous loss in stratification stability.

### Materials and methods

In Lake Arendsee and Lake Stechlin, two dimictic lakes in Northern Germany, high-resolution time series of water temperature were measured over the past decade with the help of various moored temperature loggers. These buoy data were compared with profiling data from biweekly monitoring utilized in a former approach (Kirillin et al., 2013). To maximise the methodological transparency and comparability the authors used the Lake Analyzer program suit (Read et al., 2011) for computing the values required to test the criteria for stratification onset and breakup. For the date of the stratification onset three different criteria were examined for each year under investigation. The stratification duration was defined as a continuous period for which one of the following criteria is fulfilled: (i) the Schmidt stability is greater than a fixed value (ii) the difference between surface and bottom temperature is smaller than a fixed value, and (iii) the surface temperature is higher than a certain threshold.

## Results and discussion

We demonstrate that the end of summer stratification can be detected precisely with the help of a single temperature logger mounted near the lake bottom (Fig 1).

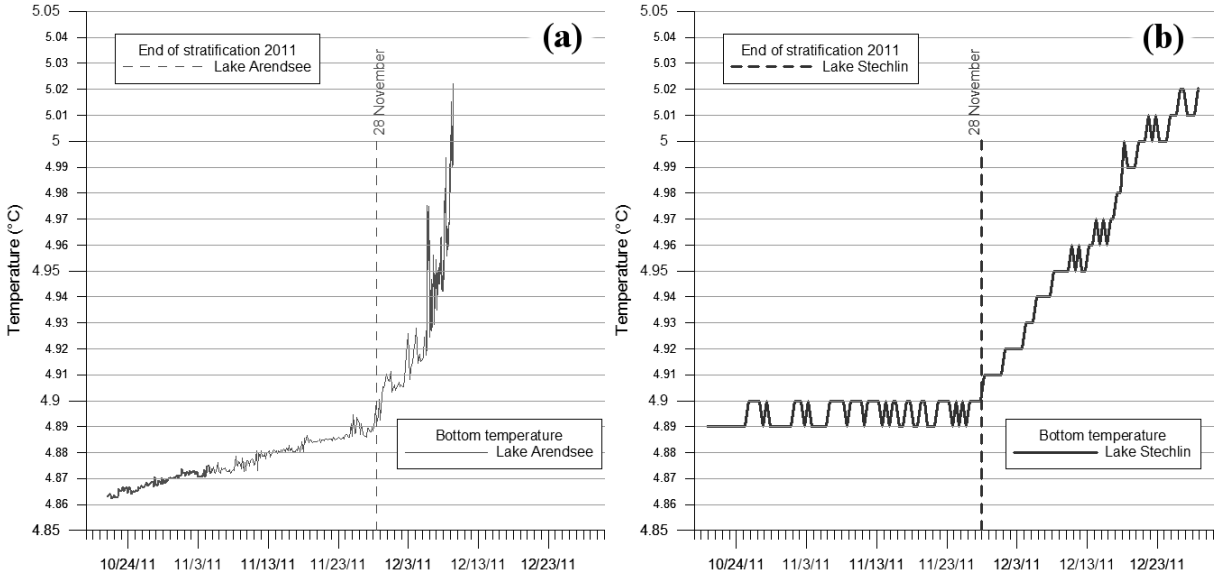


**Figure 1**. The end of thermal stratification in 2011: (a) Bottom logger data of a moored buoy in Lake Arendsee (RBR Ltd, Canada; measuring interval 20 seconds, thermal resolution 0.005°C) and (b) Bottom logger data from optodes moored in Lake Stechlin (Zebra-Tech Ltd, New Zeeland; measuring interval 0.5 hours; temperature resolution 0.01°C). The onset of mixing (shown here by a dotted line) is indicated by a rapid bottom temperature enhancement.

Furthermore, it is shown that the result of the experimental detection of stratification duration depends on the frequency of data collecting. The number of sensors (spatial resolution of measurements) and the choice of thresholds are of lesser importance than the temporal resolution of routine temperature measurements. At least, daily data (measured by high-resolution sensors mounted at moored buoys or by profiling) are necessary to detect experimentally the length of the stratified period with accuracy sufficient to estimate long-term shifts in these characteristics (Elo et al., 1998; Kirillin, 2010).

**REFERENCES**

De Stasio Jr., B.T., D.K. Hill, J.M. Kleinhans, N.P. Nibbelink, and J.J. Magnuson (1996), Potential effects of global climate change on small north-temperate lakes: physics, fish, and plankton, *Limnol. Oceanogr*., **41**, 1136 –1149.

Elo, A.-R. (2005), Modelling of summer stratification of morphologically different lakes, *Nord. Hydrol.*, **36**, 281–294.

Kirillin, G. (2010), Modeling the impact of global warming on water temperature and seasonal mixing regimes in small temperate lakes, *Boreal Environ. Res.*, **15**, 279–293.

Kirillin, G., H.-P. Grossart, and K. W. Tang (2012), Modeling sinking rate of zooplankton carcasses: Effects of stratification and mixing, *Limnol. Oceanogr*., **57**, 881–894, doi:10.4319/lo.2012.57.3.0881.

Kirillin, G., T. Shatwell, and P. Kasprzak (2013), Consequences of thermal pollution from a nuclear plant on lake temperature and mixing regime, *J. Hydrol.*, **496**, 47–56.

Peeters, F., D. Straile, A. Lorke, and D.M. Livingstone (2007) Earlier onset of the spring phytoplankton bloom in lakes of the temperate zone in a warmer climate, *Glob. Change Biol.*, **13**, 1898–1909.

Read, J. S., D.P. Hamilton, I.D. Jones, K. Muraoka, L.A. Winslow, R. Kroiss, C.H. Wu, and E. Gaiser (2011), Derivation of lake mixing and stratification indices from high-resolution lake buoy data, *Environmental Modelling & Software*, **26**, 1325–1336.

Robertson, D.M. and R.A. Ragotzkie (1990), Changes in the thermal structure of moderate to large sized lakes in response to changes in air temperature, *Aquat. Sci.*, **52**, 360-380.

Stainsby, E. A., J. G. Winter, H. Jarjanazi, A. M. Paterson, D. O. Evans, and J. D. Young (2011), Changes in the thermal stability of Lake Simcoe from 1980 to 2008, *J. Great Lakes Res.*, **37**, 55–62.

# Critical bed shear for passive transport of a benthic bivalve

A.L. Forrest[1,2]*, T.J. Mathis[2], M.E. Wittmann[3] and S.G. Schladow[2]

[1] *Australian Maritime College, University of Tasmania, Launceston, TAS, Australia*
[2] *University of California Davis Tahoe Environmental Research Center, Incline Village, NV, USA*
[3] *Department of Biological Sciences, University of Notre Dame, Notre Dame, IN, USA*

**Corresponding author, e-mail alex.forrest@amc.edu.au*

**KEYWORDS**
Passive transport; hydraulic flume; bed shear; *C. fluminea*; Asian clam.

## EXTENDED ABSTRACT

### Introduction

Dispersion of the benthic bivalve *Corbicula fluminea* (Asian clam) is driven by a number of transport mechanisms including vertical dispersion of the pediveliger larvae in the water column and lateral transport of adult individuals (Williams and McMahon, 1986). Populations of *C. fluminea* have been found at water depths of 20–40 m in Lake Tahoe, CA-NV at significant densities (up to 500–1000 clams $m^{-2}$). These populations are found distributed along the steep slopes (>20°) that characterize the lake and are considerably deeper than the shallow (0–10m deep) shelf where most individuals are located (up to 6400 clams $m^{-2}$). While *C. fluminea* individuals will spend much of their lives burrowed at depths up to tens of centimeters in the substrate, they have been shown to migrate to the substrate surface when exposed to environmental stressors (e.g. low water temperatures or dissolved oxygen levels; Wittmann et al., 2012). Once on the lakebed surface, adult individuals are potentially vulnerable to hydrodynamic transport induced by currents. The main aim of this study was to characterize the flow conditions whereby critical bed shear might be great enough to induce passive transport.

### Materials and Methods

Current velocities were measured at the 25 m isobath at Nevada Beach, Lake Tahoe, CA-NV between September 2011 and March 2012 using an upward looking RDI-1200 kHz ADCP Workhorse Monitor. These measurements were used to determine the range of bed velocities over areas where known populations of *C. fluminea* are established. Experimental runs were subsequently conducted with individual clams (5–24 mm shell length) in a hydraulic flume over the range of observed field velocities. In each experiment, two clams were initially placed at the center of the flume and the flow was increased until the velocity set point was reached. The distance that each clam was displaced was recorded until they stopped moving for more than 5 minutes. The episodic displacement of clams, in a manner analogous to particle saltation, was recorded as sets of multiple individual motions. At the end of each experiment, a new experiment was commenced with different clams. In total, approximately 240 *C. fluminea* individuals were tested in this manner.

### Results and Discussion

During storm events in the study period, peak horizontal and vertical (downwards) velocities reached 25 cm $s^{-1}$,and 4 cm $s^{-1}$, respectively. While near-bed sediment load wasn't measured directly, the acoustic backscatter increased significantly during storm events

indicative of material being transported. Based on these field observations, four velocity classes (ranging from 10 – 25 cm $s^{-1}$; Figure 1) were selected to group the experimental runs into. A critical shell length of 7.1, 8.3, 13.5 and 15.1 mm (i.e., the first evidence of downstream transport) was determined for each of the velocity classes.

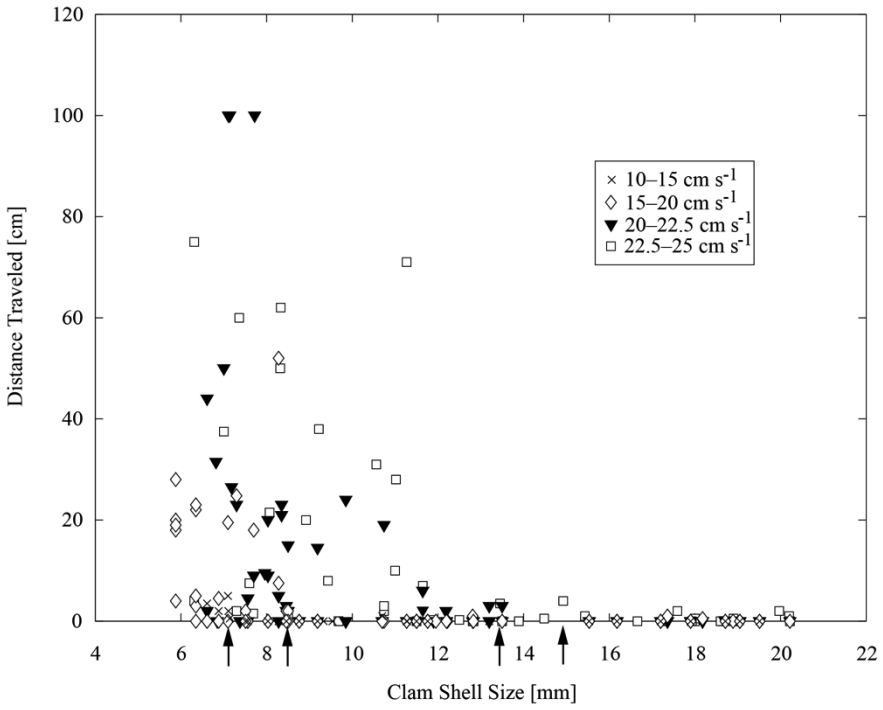


**Figure 1**. Experimental results of distance traveled as function of clam shell size and sorted into four velocity classes: 10–15 cm $s^{-1}$ (black x), 15–20 cm $s^{-1}$ (diamonds), 20–22.5 cm $s^{-1}$ (filled inverted triangles), and 22.5–25 cm $s^{-1}$ (squares). Arrows indicate critical shell length for each velocity class.

By conducting a force balance on the measured average dimensions for each of these critical shell lengths in a similar fashion to Dey (2003), an experimental relationship was derived between the critical shell length and associated bed shear stress and velocity. Relating this back to observed water column velocities, it was concluded that individuals up to 15 mm in size during average storm events, and all size classes during peak storm events, would undergo lateral transport. This indicates a strong potential for downslope recruitment as a result of the downwards vertical velocities associated with the peak flow events. Horizontal water column velocities that supported the transport of clams in the flume experiment (up to 25 cm $s^{-1}$) were similar to those observed through fall cooling and winter stratification in the lake, suggesting the potential for physical clam transport during these time periods. This work shows that passive transport of adult *C. fluminea* individuals is a potentially important dispersal mechanism within in this lake and other systems given similar conditions. This has significant ecological implications for the dispersion of introduced species.

**REFERENCES**

Dey, S. (2003), Incipient motion of bivalve shells on sand beds under flowing water. *Journal of engineering mechanics* **129**(2), 232-240, DOI 10.1061/ASCE0733-9399.

Williams, C. J. and R.F. McMahon (1986), Power station entrainment of *Corbicula fluminea* (Mueller) in relation to population dynamics, reproductive cycle and biotic and abiotic variables. *American Malacological Bulletin* **2**, 99–113.

Wittmann, M.E., S. Chandra, J.E. Reuter, S.G. Schladow, B.C. Allen, K.J. Webb (2012), The control of an invasive bivalve, *Corbicula fluminea*, using gas impermeable benthic barriers in a large natural lake. *Environmental Management Online Issue*. 1-11, DOI 10.1007/s00267-012-9850-5.

# Optical properties of Lake Vendyurskoe: ice-covered period and open water

G. Gavrilenko*[1], G. Zdorovennova[1] , R. Zdorovennov[1],
N. Palshin[1], S. Golosov[2] and A. Terzhevik[1]

[1] *Northern Water Problems Institute, Russian Academy of Sciences, Petrozavodsk, Russia*
[2] *Institute of Limnology, Russian Academy of Sciences, Saint-Petersburg, Russia*

**Corresponding author, e-mail south.sun.cr@gmail.com*

**KEYWORDS**
Ice-covered lake; environment; euphotic zone; irradiance; attenuation coefficient.

## EXTENDED ABSTRACT

### Introduction

Solar radiation penetrating into the water column in the open-water period and passing through the snow-ice sheet during winter is one of the most important factors that determines the functioning of lake ecosystems (Lei et al, 2011). Parameterisation of the attenuation of solar radiation in the snow-ice sheet and in a water column is an essential tool in research of shallow boreal lakes (Arst et al, 2008). The aim of our study is to analyse dynamics of underwater irradiance in a small shallow lake during open-water and ice-covered periods.

### Materials and methods

The optical properties of Lake Vendyurskoe (Karelia, Russia, 62°10N, 33°10'E, ) were investigated during four surveys (April 2012, April, May, and June 2013). Lake Vendyurskoe is a mesotrophic polymictic shallow lake of glacial origin (surface area 10.4 $km^2$, volume $54.8 \cdot 10^6$ $m^3$, maximal and average depths 13.4 and 5.3 m, respectively). The obtained data consist of (1) the water temperature, (2) downwelling and upwelling planar irradiances at the surface of water and ice, downwelling planar irradiance beneath the ice, (3) photosynthetically active radiation (PAR) at different depths under the ice or water surface down to 7.2 m, and (4) Secchi disc depth.

There were used such equipment: (1) TR – 1060 (RBR Ltd., Canada), (2) star-shaped pyranometer (Theodor Friderich & Co, Meteorologishe Gerate und Systeme, Germany), and (3) Ultra-miniature Light Intensity Recorder (Alec electronics, Japan).

### Results and discussion

The PAR vertical profiles shows maximum value in 0-1 m depth and rapid decrease with depth to zero values in 5 m depth. The maximum value was marked in the end of April- early May 2013 (Fig. 1, A).

The attenuation coefficients was calculated, revealing maximum values (1.5-2.5 $m^{-1}$) in 0-1 m depth and minimum (0.5-1 $m^{-1}$) in 3-4 m during all surveys. On 21.04.2013 the value of attenuation cofficient increased to 1.5 $m^{-1}$ on 4-6 m depth (Fig 1, B).

The Secchi disc depth was 2.9 – 3.7m in April and 2.7-2.8 m in May 2013.

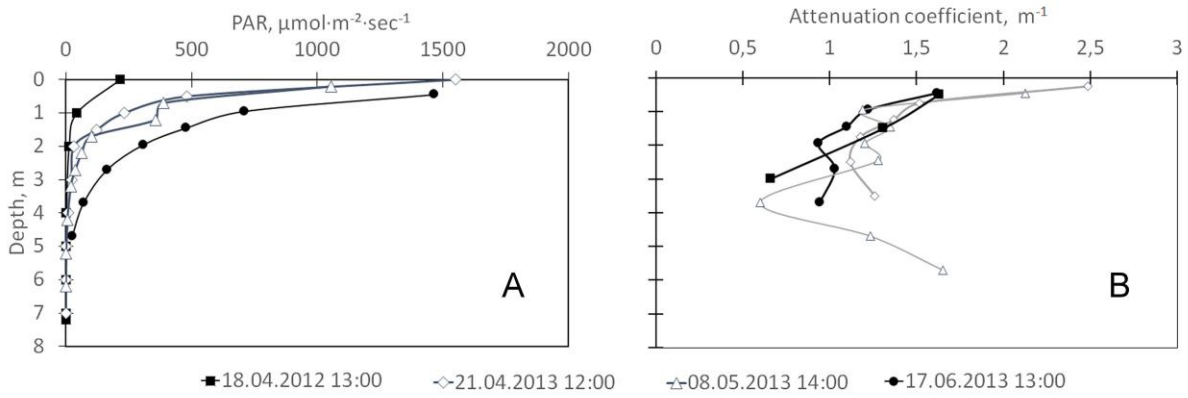


**Figure 1.** Vertical profiles of PAR (A) and attenuation coefficient (B) on 17.06.2013, 18.04.2013, 21.04.2013 and 08.05.2013.

Water transparency decreasing in surface waters of shallow lake in early summer may lead to the development of strong thermal stratification. These procceses lead to development of a seasonal dissolved oxygen deficit in near-bottom layers of shallow lake.

**Acknowledgments.** The present study was supported by the Russian Academy of Science, The Russian Fund of Basic Research (project 13-05-00338).

**REFERENCES**

Arst H. et al. (2008), Optical properties of boreal lake waters in Finland and Estonia. *Boreal environment research*, **13,** 133-158.

Lei R. et al (2011), Field investigatioms of apparent optical properties of ice cover in Finnish and Estonian lakes in winter 2009. *Estonian Journal of Earth Sciences*, **60,** 50-64.

# Under-ice, basin-scale circulation in an Arctic lake

K. Graves[1]*, A.L. Forrest[2], B.E. Laval[1] and G. Kirillin[3]

[1] *Department of Civil Engineering, University of British Columbia, Vancouver, Canada*
[2] *Maritime Engineering, Australian Maritime College at the University of Tasmania, Launceston, Tasmania, Australia*
[3] *Leibniz-Institute of Freshwater Ecology and Inland Fisheries, Germany*

**Corresponding author, e-mail kellygraves@civil.ubc.ca*

**KEYWORDS**
Lakes; ice-cover; density anomaly; cyclogeostrophic; Rossby number.

## EXTENDED ABSTRACT

### Introduction

During winter, ice-cover prevents momentum transfer from the wind to the water column; therefore, it is assumed basin-scale circulation is insignificant in seasonally ice-covered lakes that are not subject to large inflows. However, recent field observations (Rizk et al., 2014; Forrest et al., 2013) and computer simulations (Huttula et al., 2010) have indicated significant basin-scale circulation under ice. This study presents field observations immediately prior to ice-off in the seasonally ice-covered, arctic Lake Kilpisjärvi. This data set shows an approximately 500-meter-wide density anomaly in the centre of the lake that is consistent with an anti-cyclonically rotating density anomaly in a cyclogeostrophic balance.

### Materials and Methods

Lake Kilpisjärvi (69°01'N, 20°49'E) is located in northwestern Finland where Finland, Sweden and Norway meet. There are two basins (north and south) and the north basin was the focus of this study. It is located 473 m above sea level, has mean and maximum depths of 19.5 and 57 m and a surface area of 37.1 square kilometers (km²) (Leppäranta et al., 2012). During the study period, Lake Kilpisjärvi was subject to 24 hours of daylight.

A RBR conductivity, temperature and depth (CTD) profiler collected vertical CTD profiles between May 25th and 27th. These profiles were spaced every 50 m across a high-resolution transect of the lake and every 100 m across a perpendicular transect. A bottom-mounted, 600 kHz Acoustic Doppler Current Profiler (ADCP) measured water column velocities between 5 and 25 m depth for the same period of time as the CTD profiles were collected and was located near one end of the high-resolution transect.

### Results and Discussion

The CTD transects show a 500m-diameter mass of warmer, denser water near the centre of the lake that is surrounded by cooler, less dense water (Figure 1). There is a 0.04 °C temperature difference between the inner core and surrounding water that leads to a density difference of 0.04 kg $m^{-3}$. We hypothesize this density anomaly to be in cyclogeostrophic balance.

A system is in cyclogeostrophic balance when the Coriolis and centripetal forces are comparable in size, which is represented by a Rossby number ($R_o = u_{max} / r \times f$) of approximately 1. Here $u$ is a velocity scale, $r$ is a horizontal length scale (typically taken to be the anomaly radius), and $f$ is the Coriolis parameter ($f \sim 1.36 \times 10^{-4}$ $s^{-1}$ for a latitude of 69°N). Using the maximum azimuthal ADCP velocity 0.05 m $s^{-1}$ as the velocity scale, and the observed density anomaly radius of 250 m as the length scale gives a Rossby number of order 1, suggesting both Coriolis and centripetal forces balance the pressure force caused by the

density difference.

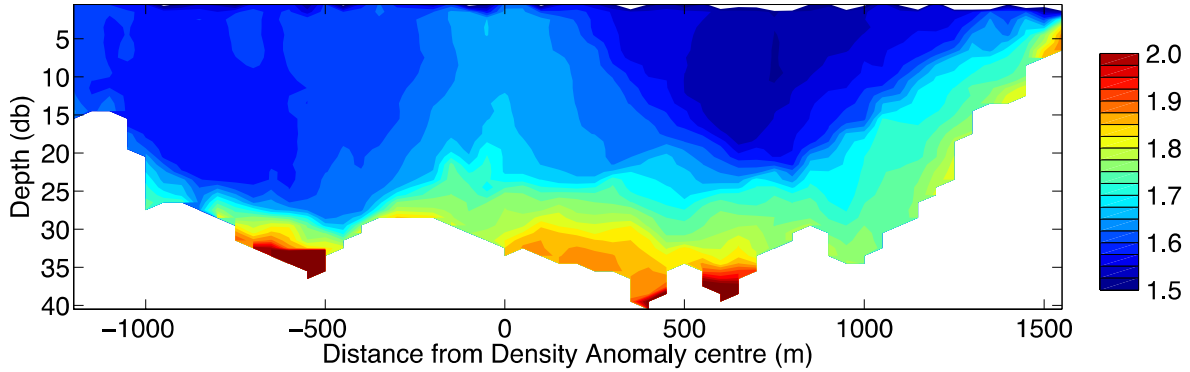


**Figure 1.** High-resolution temperature transect referenced from the anomaly centre with contour interval of 0.025°C.

A dense-core anomaly, as observed here, in cyclogeostrophic balance will have radial symmetry with an outwards pressure force, resulting in anti-cyclonic motion. The high-resolution and perpendicular transects suggest radial symmetry, and the direction of the ADCP measured velocity is consistent with anti-cyclonic motion. Solving the equation of motion, including pressure, Coriolis and centripetal forces and assuming no motion at the water surface, the density field was used to calculate a velocity field. This velocity field is approximately radially symmetric about the centre of the anomaly and shows anti-cyclonic motion over most of the lake with a counter-rotating region near the lakeshore.

The repeated high-resolution transect shows that this anomaly persisted for the three days before likely being destroyed along with the ice-cover over a period of three days. Ice break-up occurred from strong wind events and a rapid temperature increase. If the ice cover had remained, it is estimated, from the time scale of adjustment of rotating flow that the gyre would persist for approximately 20 days before it decayed. This comes from the time scale of adjustment of a rotating fluid, $T_{rot} = (E^{1/2} f)^{-1}$, where $E$ is the Ekman number, $E = \nu / (f \times h^2)$, where $\nu$ is the viscosity, assumed to be molecular ($\nu$=$10^{-6}$ m$^2$ s$^{-1}$), and $h$ is the height of the anomaly 22.5 m.

Observations of rotating density anomalies under-ice are common in the Arctic Ocean, such as the eddies in the Canada Basin of the Arctic Ocean. These rotate at velocities that range from 0.09 – 0.26 m s$^{-1}$ and their Rossby radii are of the order of 10 of kilometres (Timmermans et al. 2008). Whereas, observations of rotating densities anomalies under lake-ice are extremely rare. Forrest et al. observed a cyclonically rotating density anomaly, gyre, in Pavilion Lake, Canada (2013). This gyre had an observed radius of ~ 110 m, and rotated at a maximum of 0.021 m s$^{-1}$. This gyre persisted unchanged for the observation period of 6 days. Rizk et al. (2012) observed cyclonic and anti-cyclonic rotating gyres under lake-ice in Lake Pääjärvi, Finland, that rotated at maximum velocity of 0.001 m s$^{-1}$ and persisted throughout the winter. These observations are comparable to our observations in Lake Kilpisjärvi with a persistent density anomaly with velocity of the order ~ 0.05 m s$^{-1}$.

**REFERENCES**

Forrest, A., B. Laval, R. Pieters, and D. Lim (2013), A cyclonic gyre in an ice-covered lake, *Limnol. Oceanogr*., **58**(1), 363-375.

Huttula, T., M. Pulkkanen, B. Arkhipov, M. Leppäranta, V. Solbakov, K. Shirasawa, and K. Salonen (2010), Modelling circulation in an ice-covered lake, *Est. J. Earth Sci*., **59** (4), 298-309.

Leppäranta, M., K. Shirasawa, and T. Takatsuka (2012) Ice season on Lake Kilpisjärvi in Arctic Tundra, 21st *IAHR International Symposium on Ice*, Dalian, China, June 11 to 15, 11.

Rizk, W., G. Kirillin, and M. Leppäranta (2014), Basin-scale circulation and heat fluxes in ice-covered lakes, *Limnol. Oceanogr*., **59**(2), 445-464.

Timmermans, M.-L, J. Toole, A. Proshutinsky, R. Kirshfield, and A. Plueddemann (2008) Eddies in the Canada Basin, Arctic Ocean, Observed from Ice-Tethered Profilers, *J. Phys. Oceanogr*., **38**(1), 133-145.

# Modelling Temporal Evolution of Dredging Induced Turbidity in Far Field

J. Guo[1], D. Shao[1]*, A.W.K. Law[2] and T. Sun[1]

[1] *State Key Laboratory of Water Environment Simulation & School of Environment, Beijing Normal University, Beijing, China*
[2] *School of Civil and Environmental Engineering & DHI-NTU Centre, Nanyang Environment and Water Research Institute, Nanyang Technological University, Singapore*

**Corresponding author, e-mail ddshao@bnu.edu.cn*

**KEYWORDS**
Dredging; turbidity plume; far-field transport; environmental impact assessment.

## EXTENDED ABSTRACT

### Introduction

It has long been recognized that the increase in turbidity resulting from dredging can cause many adverse effects on the aquatic ecosystem, and even create unfavorable public response occasionally (Bray, 2008). Simplified analytical model that allows quick and first-order assessment of the fate and transport of the sediment plume can be used as an economical and effective tool to address the associated environmental impact. In the present study, a mathematical model concerning the transport of the dredging-induced turbidity in the far field was developed. Unlike the majority of the existing models that are based on the steady state assumption (Kuo and Hayes, 1991, Je et al., 2007), the present model retains the transient term, $\partial c/\partial t$, such that the temporal evolution of the spatial extent and concentration of the sediment plume can be predicted.

### Materials and methods

Assuming the sediment plume to be well mixed in the vertical direction, the governing equation for the depth-averaged sediment transport model is:

$$\frac{\partial c}{\partial t} = D_x \frac{\partial^2 c}{\partial x^2} + D_y \frac{\partial^2 c}{\partial y^2} - u \frac{\partial c}{\partial x} - \frac{w_s c}{h} \quad , \tag{1}$$

where $c$ denotes depth-averaged concentration of total suspended sediments (TSS) (mg/L), $t$ denotes elapsed time (s), $D_x$, $D_y$ denotes turbulent diffusion coefficient in the $x$ and $y$ direction, respectively ($m^2$/s), $u_x$ denotes the velocity of the tidal current (m/s), $w_s$ denotes bulk sediment settling velocity (m/s), and $h$ denotes water depth (m). We further assumed that the tidal currents are represented by a small constant component, $V$ (normally referred as residual or drift current), plus a periodic part, $U_0 sin\omega t$, i.e.,

$$u_x(t) = V + U_0 sin\omega t \quad , \tag{2}$$

where $U_0$ is the amplitude of the oscillatory current and is typically much greater than the magnitude of the residual current, $V$; $\omega = 2\pi/T$ ($T$ is the tidal period) is the angular frequency of the oscillatory current.

The solution to equation (1) can be written in the form of a convolution integral, and solved by numerical integration (Shao et al., 2008). The parameters adopted in the present study follow that in Je et al. (2007).

**Results and discussion**

We first assume a mean tidal current velocity, i.e., $u_x = v$. After calibrating the unknown source strength using the field observation data from Je et al. (2007), and further determining the appropriate turbulent diffusion coefficient in the longitudinal direction, $D_x$, to adhere to the real situation with negligible longitudinal diffusion, the complete transient model formulation was used to predict the approach of the excess turbidity to the steady state and the ultimate turbidity level at the steady state under the mean tidal currents, as well as the dependence of the model predictions on the key modelling parameters, i.e., $h$, $D_x$, $D_y$, $u$ and $w_s$. As an example, Figure 1 shows the approach of the turbidity to the steady state at $x$=1000m.

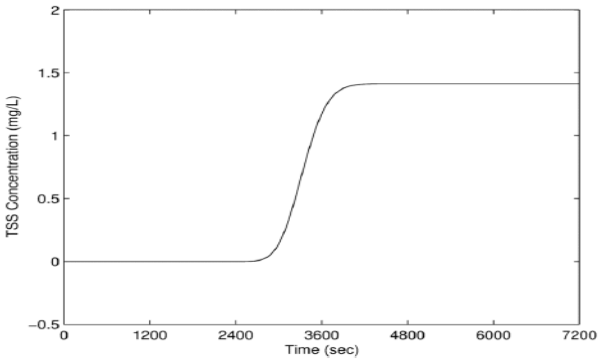


**Figure 1** Temporal pattern of turbidity build-up at x=1000m

When the oscillatory tidal current was accounted for, the behaviour of the turbidity plume, e.g., the convergence to the quasi-steady state in which the concentration fluctuates periodically between fixed upper and lower bounds exhibits a different pattern as shown in Figure 2 and 3.

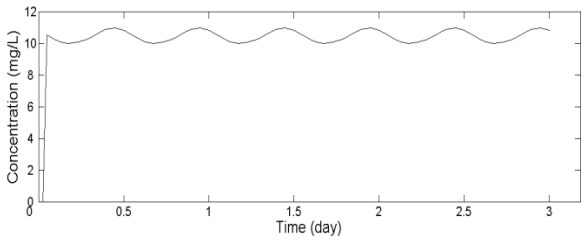


**Figure 2** Temporal patterns of turbidity build-up

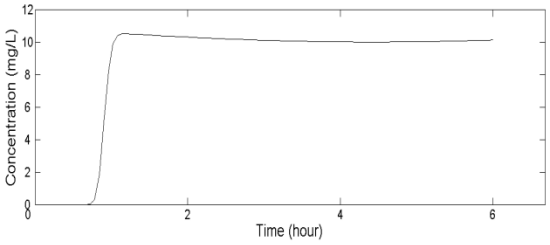


**Figure 3** Close up of initial development

The dependence of the model predictions on four dimensionless parameters, namely, the velocity ratio, $\nu = V/U_0$, the Li and Kozlowski (1974)'s parameter, $\lambda = U_0^2/4\omega D_x$, the diffusion coefficient ratio, $\alpha = \left(D_x/D_y\right)^{1/2}$, and the time ratio, $\phi = w_s/\omega h$, is further analysed.

The developed semi-analytical model that incorporates tidal effects can be used for first-order assessment of the far-field transport of the sediment plume generated by dredging operations in a tidal environment.

**REFERENCES**

Bray, R. N. (2008), *Environmental aspects of dredging*, Taylor & Francis, London.

Je, C. H., Hayes, D. F., and Kim, K. S. (2007), Simulation of resuspended sediments resulting from dredging operations by a numerical flocculent transport model, *Chemosphere*, **70**(2), 187-195.

Kuo, A. Y., and Hayes, D. F. (1991), Model for Turbidity Plume Induced by Bucket Dredge, *J. Waterway, Port, Coastal, Ocean Eng.*, **117**(6), 610-623.

Li, W. H., and Kozlowski, M. W. (1974), Do-Sag in Oscillating Flow, *J. Env. Eng. Div.*, **100**(4), 837-854.

Shao, D. D., Law, A. W. K.., and Li, H. Y. (2008), Brine discharges into shallow coastal waters with mean and oscillatory tidal currents, *J Hydro-Environ Res*, **2**, 91-97.

# Using mass transport instead of concentration transport in coupled physics/ecosystem models

B.R. Hodges

*Department of Civil, Architectural, and Environmental Engineering,*
*University of Texas at Austin, Austin, TX, USA*

*e-mail hodges@utexas.edu*

**KEYWORDS**
Lakes; environment; water quality; modelling; internal waves.

## EXTENDED ABSTRACT

### Introduction

A challenge for modelling the coupled physics and transport for an ecosystem model is the computational cost associated with transporting a large number of ecosystem state variables (e.g. different speciation of phytoplankton, zooplankton and nutrients). Where the number of ecosystem state variables exceeds 10 or so, the transport computational cost will typically exceed the costs of solving both the shallow water equations and the ecosystem state equations. There are two underlying issues: (1) high velocities in a small region can require subtime-stepping of the transport equations to avoid CFL stability constraints (e.g. Dawson et al, 2013), and (2) there are often large regions of background values where the model is simply shuffling background concentrations into/out of grid cells, thus wasting computational effort. As an approach to solving these problems, we can change our conventional paradigm of transporting dilute concentrations to coupled transport of mass and volume. It can be shown that this simple idea allows the different faces of a single grid cell to have transport at different subtime steps without requiring ad hoc numerical schemes at the boundaries between regions with different time steps. Thus, a small region requiring smaller time steps does not require the entire model to be subtime cycled. This new idea also allows regions of background concentrations to be dynamically masked from regions where concentrations are evolving, so that transport concentrations are only carried out where the results will be significant

### Materials and methods

The conventional transport approach requires treating any scalar as a dissolved concentration, c, with a conservative advection-diffusion equation of the form:

$$\frac{\partial c}{\partial t} = -\frac{\partial u_j c}{\partial x_j} + \kappa \frac{\partial^2 c}{\partial x_j \partial x_j} + S, \tag{1}$$

where $x_j$ and $u_j$ are Cartesian coordinates and velocity components, respectively, is a diffusivity, and $S$ is a net source/sink. Discretized on a model grid that allows a moving free surface (hence the volume changes for grid cell $i$), a generic time advance from the $n$ to the $n+1$ time level can be written as

$$c_i^{n+1} = \frac{V_i^n}{V_i^{n+1}} c_i^n + \frac{\Delta t}{V_i^{n+1}} G(q, c, \kappa, S), \tag{2}$$

where $G$ is a conservative discretization function and $q$ represents volume fluxes through cell faces. An entirely equivalent scheme can be obtained by transport of mass, volume, and diagnostic recovery over concentration as

$$m_i^{n+1} = m_i^n + \Delta t\, F(q, c, \kappa, S), \quad V_i^{n+1} = V_i^n + \Delta t\, H(q), \quad c_i^{n+1} = m_i^{n+1} / V_i^{n+1}, \qquad (2)$$

where $F$ and $H$ are discretizations that are consistent with continuity (Gross et al, 2002).

## Results and discussion

The advantage of the mass transport form is the ability to break a single time step, $\Delta t$, into a series of subtime steps that are independent on each face of a grid cell. This allows a cell face with a high velocity (i.e. high CFL) to be treated with stable subtime steps while other faces use the full time step. Development of the full discrete form is shown in Hodges (2014), but the concept can be understood by imagining each grid cell as a balloon with multiple orifices. The volume of an individual grid cell "balloon" increases or decreases during the subtime steps, depending on the flux balance through faces that have (do not have) fluxes in a given subtime step (Figure 1). Since the mass and volume are consistently transported during the subtime step, the concentration always remains consistent with the fluxes.

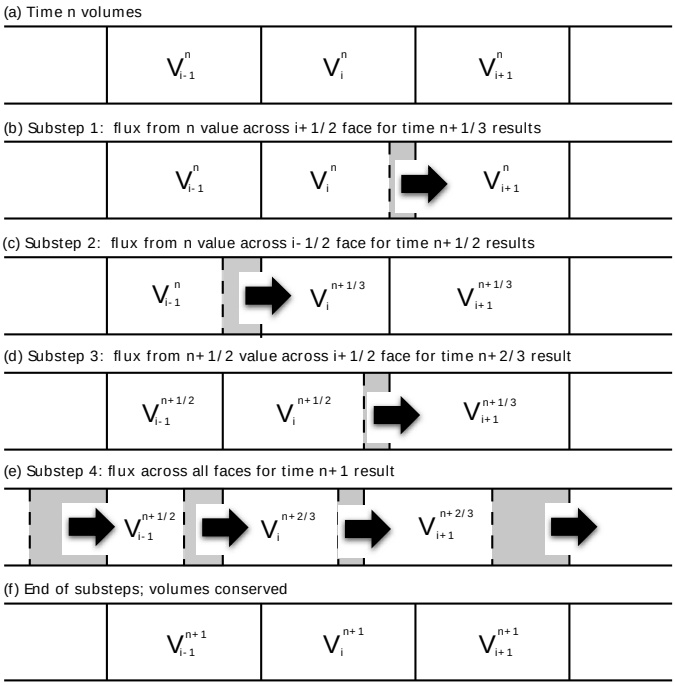


**Figure 1**. Sequence of subtime stepping for three grid cells in a 1D system. The i+1/2 face uses 3 subtime steps while the i-1/2 face uses 2 subtime steps and outer cell faces use the full time step. The volume of the *i* cell alternately decreases and increases during the subtime stepping. The final result is a conservative volume change. Figure from Hodges (2014).

**Acknowledgments**. This material is based upon work partially supported by the U.S. National Science Foundation under Grants No. 0710901, CFF-1331610, and in part by the BP/The Gulf of Mexico Research Initiative and the Research and Development program of the Texas General Land Office Oil Spill Prevention and Response Division under Grant No. 13-439-000-7898.

## REFERENCES

Dawson, C., Trahan, C. J., Kubatko, E. J., Westerink, J. J., (2013). A parallel local timestepping Runge-Kutta discontinuous Galerkin method with applications to coastal ocean modeling. *Computer Methods in Applied Mechanics and Engineering*, **259**, 154–165.

Gross, E. S., Bonaventura, L., Rosatti, G., (2002). Consistency with continuity in conservative advection schemes for free-surface models. *International Journal for Numerical Methods in Fluids*, **38** (4), 307–327.

Hodges, B.R. (2014). A new approach to the local time stepping problem for scalar transport. *Ocean Modelling*, **71**, 1-19. http://dx.doi.org/10.1016/j.ocemod.2014.02.007

# River modeling - keeping it physical for river basins

B.R. Hodges[1]* and F. Liu[2]

[1] *Department of Civil, Architectural, and Environmental Engineering, University of Texas at Austin, Austin, TX, USA*
[2] *IBM Research Austin, Austin, TX, USA*

**Corresponding author, e-mail hodges@utexas.edu*

**KEYWORDS**
Rivers; Saint-Venant equations; numerical models.

## EXTENDED ABSTRACT

### Introduction

For river networks in large basins, we often despair of modeling the full river physics and resort to kinematic wave, diffusive wave, or neural network models. Thus, there is a disconnect between these larger scales and our more complete Navier-Stokes modeling of lakes, estuaries, and short river reaches. The reduced- (or non-) physics approaches are applied over river networks because the conventional wisdom is that it is impractical to apply the full physical solutions (i.e. using momentum and mass conservation). Driving this perception are the need for geometric data (e.g. river cross-sections, roughness) and the computational requirements for the full equations. However, solutions for the geometrical data problem are rapidly advancing through use of advanced digital elevation models, lidar, and multibeam sonar, although application of sufficient resources remains an issue (Hodges, 2013). Furthermore, it makes logical sense to calibrate unknown geometry into the full physical equations; i.e. *why reduce the modeled physics if geometry is the problem?* The historic reasons for reduced physics models actually appear more closely associated with the perceived computational costs of solving coupled momentum and mass solutions for river networks. However, Liu and Hodges (2014) showed the computational ideas and methods developed in the design of computer microchips can be used to create extremely fast solutions of the Saint-Venant equations over large river networks. Cross-disciplinary ideas outlined in Hodges and Liu (2014) open up new opportunities for upscaling models previously used for short river reaches into physical models for large river basins – in short, pushing more physics into the traditional world of calibrated hydrological models.

### Materials and methods

The 1D Saint-Venant equations for continuity and momentum can be written as:

$$\frac{\partial A}{\partial t}+\frac{\partial Q}{\partial x}=q_L\,,\qquad \frac{\partial Q}{\partial t}+\frac{\partial}{\partial x}\left(\frac{Q^2}{A}\right)+gA\frac{\partial h}{\partial x}+\frac{gn^2P_w^{4/3}}{A^{7/3}}Q|Q|=gAS_0\,, \tag{1}$$

where $A$ is the channel cross-sectional area, $Q$ is the flow rate, $q_L$ is a lateral inflow rate, $n$ is the Gauckler-Manning-Strickler roughness, $P_w$ is the wetted perimeter, $h$ is the water depth and $S_0$ is the channel slope. The above equations are solved with an implicit Preissmann scheme and a Newton-Raphson nonlinear solver in the Simulation Program for River Networks (SPRNt), which is being released as an open-source code by IBM Research. This model has been demonstrated practical for $10^5$ computational elements for more than $15\text{x}10^3$

km of river network using only a desktop computer and achieving more than 300x faster than real time (Liu and Hodges, 2014).

## Results and discussion

Although the Saint-Venant system of eq. (1) is numerically solvable, computational convergence and solution efficiency are affected by smoothness. That is, a numerical solution of the partial differential equations inherently requires the resulting $Q$ and $A$ be Lipshitz smooth, which is a difficult proposition if the coefficients and auxiliary variables (i.e. $h$, $P_w$, $n$, $S_0$) are non-smooth. Unfortunately, increasing geometric data can actually exacerbate, rather than solve, such numerical problems. As illustrated in Figure 1, detailed survey cross-sections can lead to abrupt relationships between h and A, which results in convergence problems. Furthermore, shorter separations between river geometric data can enhance the variability in $A$ and $P_w$ relative to the channel length, leading to oscillatory numerical behaviour and poor convergence.

Thus a problem for Saint-Venant models is that as we include more detailed geometry, we create non-smooth equations that can make modelling impractical. These numerical effects are being driven by small-scale variability that arguably could be treated as a form of roughness. Indeed, where models are calibrated, the unknown variability in the channel cross section shape is inherently reduced to mere roughness. However, as complex geometric data becomes more readily available, we need to rethink the idea of "roughness." We cannot expect to naively include the detailed geometry and obtain a solvable equation set – instead, we need to develop new ideas for translating the difference between a computationally-efficient smooth geometry and the measured geometry into a new model term, perhaps a "shape roughness." Ideally, a shape roughness could be analytically estimated rather than empirically calibrated.

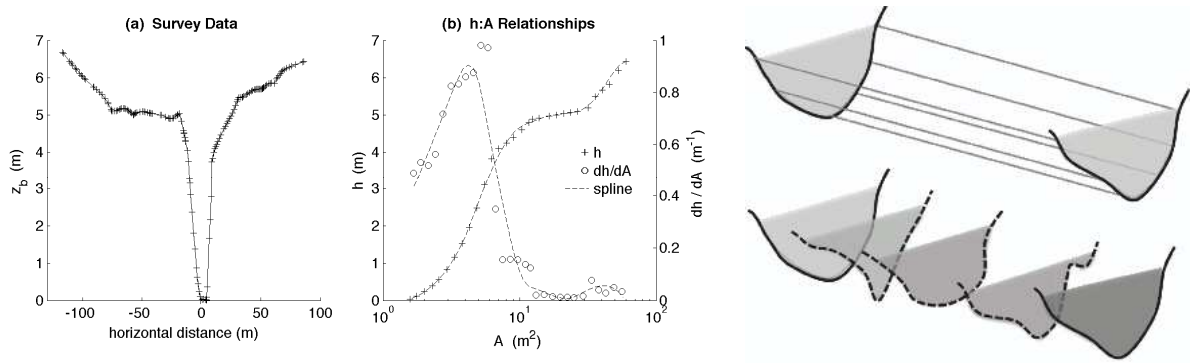


**Figure 1**. At left, detailed survey data and non-smooth relationships for $h$:$A$, which can be smoothed by splining. At right, increasing the density of cross section surveys can lead to increased variability (relative to separation length scale) in cross-section $A$ and $P_w$.

**Acknowledgments.** This material is based upon work supported by the U.S. National Science Foundation under Grant No. CCF-1331610.

**REFERENCES**

Hodges, B.R. Challenges in continental river dynamics, *Environmental Modelling & Software*, **50**, 16-20.

Hodges, B.R., and F. Liu (2014), Rivers and electrical networks: Crossing disciplines in modeling and simulation, *Foundations and Trends in Electronic Design Automation*, **8**(1), 1-116.

Liu, F. and B.R. Hodges, (2014), Applying microprocessor analysis methods to river network modeling, *Environmental Modelling & Software*, **52,** 234-252.

# Local dispersion of invasive Asian clam by wind-driven lake currents

A.B. Hoyer[1,2]*, S.G. Schladow[3,4] and F.J. Rueda[1,2]

[1] *Water Research Institute, University of Granada, Granada, Spain*
[2] *Department of Civil Engineering, University of Granada, Granada, Spain*
[3] *Department of Civil & Environmental Engineering, University of California, Davis, CA, USA*
[4] *Tahoe Environmental Research Center, University of California, Davis, CA, USA*

**Corresponding author, e-mail abhoyer@ugr.es*

**KEYWORDS**
Lake model; Individual-based model; wind-driven currents; dispersion; invasive species.

## EXTENDED ABSTRACT

### Introduction

The spread of aquatic invasive species is one of the major ecological and economic threats to lakes and waterways worldwide (Wilcove et al., 1998; Pimentel et al., 2005). In the US alone there are about 50,000 invasive species established that cause economic losses estimated at more than $120 billion per year (Pimentel et al., 2005). Invasive species may cause dramatic changes in the ecosystems through perturbations to the inter-specific competition, predator-prey interactions, food web structure, nutrient dynamics, hydrologic cycle, and sedimentation rates. Those changes typically lead to the displacement of native species from their natural habitats. The pressure posed by invasive species on native organisms is of such magnitude that their introduction has been ranked second only to habitat loss in the factors that threaten native bio-diversity at the global scale (Wilcove et al., 1998).

Asian clam (*Corbicula fluminea)* is among the most aggressive freshwater invaders worldwide (McMahon, 1999). Passive (*natural*) hydraulic transport by water currents is considered to be the main mechanism for the local dispersal of Asian clam (McMahon, 1999). Our goal is to characterize the transport pathways of young life stages of Asian clams from existing beds to other near-shore areas by wind-driven currents, and analyze the development of the clam population, using Lake Tahoe (CA-NV, USA) as a test case. Since its introduction in Lake Tahoe in 2002, Asian clam has increased to nuisance levels with highest population density in a bay (Marla Bay) at the south-eastern shore. We establish the mechanisms of larvae dispersion from the existing population patch of Asian clam, the variability of dispersion in time, the linkage existing between local and basin-scale lake circulation, and the spatial variability of the clam population.

### Materials and methods

A three-dimensional (3D) Lagrangian, individual-based dispersion model has been developed to simulate the dispersion of Asian clams in their larval stages by wind-driven lake currents. The model consists of three modules representing the main disperion processes of **R**elease, **T**ransport and **S**urvival (RTS model). This model is driven by advection and turbulence produced by two external computational models: a wave model and a hydrodynamic model. The simulations correspond to a 2 month period in 2008, when environmental conditions in the lake are known to be suitable for the reproduction and release of Asian clam larvae.

**Results and discussion**

The lake bottom in near-shore areas is frequently perturbed by wind-waves and wind-driven lake currents, inducing shear above the sediment and, leading to resuspension of sediments and non-attached living organisms (such as benthic larvae). Large fluctuations in the number of resuspended larvae are driven by the episodic nature of the wind regime. Larvae dispersion and migration occurs in form of pulses in response to episodic strong wind forcing. The dispersion of suspended larvae over the existing population patch is driven predominantly by wind-driven shear and strain deformation rates in the flow field. The initial dispersion rates largely control whether the suspended larvae settle in the area of the existing population patch, travel within the coastal boundary layer and follow along-shore transport paths, or, if they, in turn, move off-shore drifting with basin-scale currents.

Bays that are characterized by low current velocities and re-circulation act as traps for suspended benthic larvae. During periods of low physical forcing, the suspended larvae tend to remain within the area of the existing beds, partly as a result of the low displacement rate of the negatively buoyant larvae, but also as a result of the re-circulation in Marla Bay, which will tend to trap the suspended larvae inside the bay. The trapping effect of shoreline irregularities could favor the preservation of existing population patches at those sites, given that newly produced and trapped larvae can contribute to replenish of the existing population, balancing mortality rates.

In lake systems, the size of the population patch increases in form of pulses induced by the physical (wind) forcing that drives the dispersal mechanisms of suspension and transport. The predictions of the spatial extension of habitats reached by viable larvae are highly sensitive to the settling velocity specified for larvae in the model. High sedimentation rates decrease the chance of dispersion. Further, the expansion of a population restricted to shallow near-shore areas is bounded by the shore-line on one side and deeper waters on the other side. Off-shore transport routes are unfavorable for larval survival, given that they end up on long-transport paths and sedimentation in deep and unsuitable habitats. In this sense, local dispersion of benthic invasive species within a bounded aquatic system differs from unbounded overland dispersion between systems or terrestrial dispersion, where the square root of the population area may increase linearly in time (Skellam, 1951).

**Acknowledgments.** Funding was provided by the US Forest Service under the Southern Nevada Public Lands Management Act (SNPLMA). The parallel version of the hydrodynamic model was developed under the project CGL2008-06101 funded by the Spanish Government (*Ministerio de Innovación y Ciencia de España*).We are grateful to Marion Wittmann, (University of Notre Dame), Todd Steissberg and Kristin Reardon (UC Davis) for providing some of the field data. We would like to thank William Fleenor (UC Davis) and Simon Hook (NASA) for providing the meteorological information. We also thank Oliver Ross (CSIC) for his contribution to the particle tracking model. The first author was supported by a PhD grant (*Formación del Profesorado Universitario*) from the Spanish Government.

**REFERENCES**

McMahon, R.F. (1999), Invasive characteristic of the freshwater bivalve Corbicula fluminea. Pages 315-345 of: Nonindigenous Freshwater Organisms: Vector, Biology and Impacts. CRC Press LLC.

Pimentel, D., R. Zuniga and D. Morrison (2005), Update on the environmental and economic costs associated with alian-invasive species in the United States. *Ecol. Econ*., **52**, 273–288.

Skellam, J.G. (1951), Random dispersal in theoretical populations. *Biometrica* **38**: 196-218.

Wilcove, D., D. Rothstein, J. Dubow, A. Phillips and E. Losos (1998), Quantifying threats to imperiled species in the United States. *BioScience*, **48**, 607-615.

# Acoustic methods for registration and estimation of meso-scale perturbations (internal waves, seiches, temperature fronts) in natural shallow waters

B. Katsnelson

*Department of Marine Geosciences, University of Haifa, Mt Carmel, 31905, Israel*

*e-mail bkatsnels@univ.haifa.ac.il*

**KEYWORDS**
Shallow water, meso-scale perturbations, acoustic sensing, internal waves.

## EXTENDED ABSTRACT

### Introduction

In the paper analysis of methods of remote acoustic sensing for monitoring of meso-scale perturbations (both stationary and non-stationary) is presented as rather prospective method of monitoring of aquatic systems (Jagannathan et al., 2009). Different types of these perturbations are shown in Dickey (2003). It is well known that sound signals, propagating through water medium in shallow water waveguide (oceanic shelf, lake etc) are very sensitive to variation of water layer and bottom properties (Katsnelson et al., 2011; Lynch, 2011). In dependence on distances of interest different frequency ranges should be used (low frequency < 1 kHz for long distances ~ a few tens of km, and mid frequency < 10 kHz for a few km). Parameters of the sound signal, which can be used for registration and estimation of perturbation placed or moving between source and receiver are concerned with interference pattern.

### Acoustical methods

*Spatial interference on horizontal and/or vertical line arrays* can be used for registration/estimation of perturbation in horizontal plane. In the fig.1 example of formation of interference pattern on horizontal/vertical line array (HVLA) is shown. If there is area with another properties in horizontal plane (sound speed $c_2$ ) with some boundary, having radius of curvature about a few km-tens of km then we can observe interference pattern between "direct" ray (DR) and reflected ray (RR) in horizontal plane forming some angle between directions of propagation and in turn interference pattern in horizontal plane (and measured on HVLA). Parameters of this interference pattern can give information about properties of mesoscale perturbation including velocity and direction of propagation. Similar experiment was carried out in shallow water area of Atlantic coast of US (SW06), see Badiey et al (2011), where moving front of nonlinear internal waves was registered using horizontal refraction at the distance about 25 km.

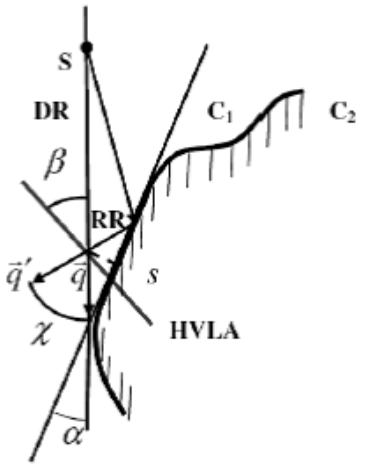


**Figure 1.**

*Frequency shift of interference pattern* can be used for diagnostics of perturbation using single hydrophone and wide-band source. In particular this method can be used for registration of basin scale waves (Kelvin waves, Poincare waves) in lakes for acoustic tracks of the length about 5-10 km for mid-frequency sound signals (Katsnelson et al., 2014).

*Interference pattern in frequency domain* measured by single receiver (hydrophone); This method can be used in particular for estimation of bottom parameters (such as density, porosity, attenuation) because mentioned properties changes spectrum of signal propagating on comparatively long distances. In the Fig.2 spectra of wide-band signals (20-90 Hz) are shown for experiment in the Barents sea on the acoustic track ~ 14 km. Continuous line (1) denotes modeling, dashed line (2) denotes experimental data. Porosity within the framework of two component model of sediment, and the corresponding values of sound speed, density and attenuation coefficient are in a good agreement with data, obtained by other methods.

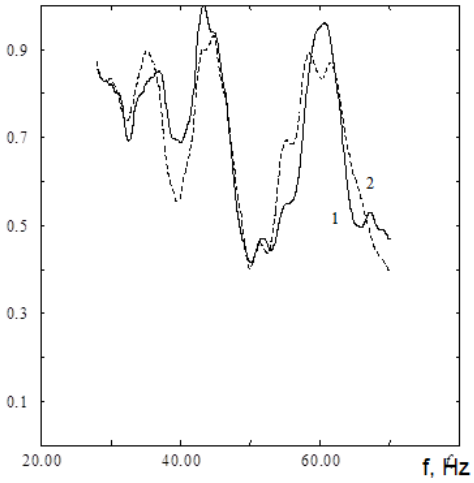


**Figure 2.**

*Pulse shape and arrival time* on long-range acoustic tracks also can be used for solution of "inverse problem" – estimation of parameters of perturbation or parameters of shallow water.

*Noise interferometry* is one of the most prospective invasive method of estimation of shallow water parameters, even non-stationary, with comparatively long time variability.

## Results and discussion

Analysis and some examples of variation of the sound field in the presence of meso-scale perturbations of different nature (for example nonlinear internal waves or variation of bathymetry and bottom parameters) are presented obtained both in experiments and using numerical modeling. It is shown that measurements of parameters of sound signal, mentioned above can give us estimation of parameters of perturbations, for example velocity and direction of propagation of nonlinear internal waves. Experimental observations in Shallow Water 2006 experiment (Atlantic shelf of US) are discussed, theoretical modeling of the sound variations for internal seiches in lake are presented as well.

**REFERENCES**

Badiey M., B. Katsnelson, Y.-T. Lin, J. Lynch (2011), Acoustic multipath arrivals in the horizontal plane due to approaching nonlinear internal waves, *J. Acoust. Soc. Am*., **129**(4), EL141-EL147.

Dickey, T. D. (2003), Emerging ocean observations for interdisciplinary data assimilation systems, *Journal of Marine Systems*, **40-41**, 5-48.

Jagannathan S., I. Bertsatos, D. Symonds, T. Chen, et al. (2009), Ocean acoustic waveguide remote sensing (OAWRS) of marine ecosystems. *Marine Ecology Progress series*, **395**, 137-160.

Katsnelson, B., V. Petnikov, J. Lynch (2011), Fundamentals of shallow water acoustics. Springer, 540 p.

Katsnelson, B., A. Lunkov, I. Ostrovsky (2014), Acoustic remote sensing of spatio-temporal dynamics of internal waves in a stratified lake. Proceedings of 2nd Underwater acoustics Conference, Greece, 2014

Lynch, J. (2011), Acoustical Oceanography and Shallow Water Acoustics. Proceedings of ACOUSTICS 2011, 2-4 November, Gold Coast, Australia, pp 1-4.

# Standing waves during ice breakup in an arctic lake

G. Kirillin[1*], C. Engelhardt[1], A. Forrest[2], K. Graves[3], B. Laval[3], M. Leppäranta[4] and W. Rizk[1]

[1] *Leibniz-Institute of Freshwater Ecology and Inland Fisheries, Germany*
[2]*Australian Maritime College at the University of Tasmania, Australia*
[3]*University of British Columbia, Canada*
[3]*University of Helsinki, Finland*

**Corresponding author, e-mail kirillin@igb-berlin.de*

**KEYWORDS**
Ice break-up, seasonal lake ice, surface seiches.

## EXTENDED ABSTRACT

### Introduction

There is evidence that strong wind events play a critical role in seasonal ice breakup in lakes and marginal seas (Kirillin et al., 2012). However, the process of ice breakup, i.e. breaking of the ice sheet and of the stable boundary layer beneath with subsequent fast melting remains poorly investigated. There are two apparent mechanisms associated with wind that accelerate the ice breakup: the drag force moving and disjointing the ice sheet, and wind-produced shear turbulence destroying the strongly stratified boundary layer in the warm atmosphere above the cold ice surface and intensifying the downward heat flow.

We demonstrate that, apart from these mechanisms, wind drag also produces strong basin-scale standing waves (seiches) under ice, whose amplitudes under breaking ice exceed those in the open water conditions. We hypothesize that seiches contribute to the acceleration of the breaking and melting of the seasonal ice cover.

### Materials and methods

An extensive dataset on the lake physical properties during the ice breakup was acquired in spring 2013 in polar Lake Kilpisjärvi, Finland (69°01'N 20°49'E; Fig. 1). Kilpisjärvi is a mid-size (surface area 37 km$^2$, max. depth 57 m) polar lake with the longest ice-covered

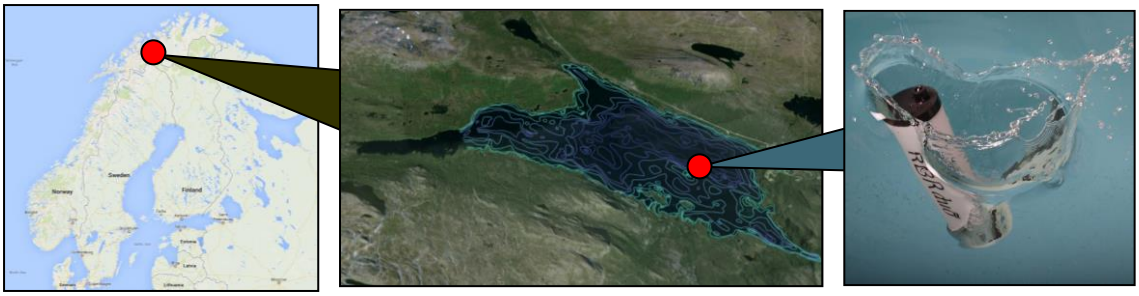

**Figure 1**. Study site: (left) geographical location, (center) bathymetry and pressure sampling position, (right) the pressure logger RBR DUO wave.

period among the West-European lakes (Lei et al. 2012). Various hydrophysical parameters were sampled from May 25 to June 6, 2013, including high-frequency pressure variations in the water column recorded by the pressure logger 'RBR Duo Wave'. The latter dataset is discussed below.

### Results and discussion

*Ice breakup*: During the campaign period, the lake area was exposed to sunlight for nearly 24 hours a day, with no observed clouds and wind speeds < 5 m s$^{-1}$ during the first six days of the study. These conditions followed a cold winter (the ice cover in winter 2012 to 2013 was ~10 cm thicker than the long-term mean, Finnish Environmental Service, pers.

comm.), with a relatively low snow pack: at the start of the campaign, no measurable snow layer persisted on the 60 cm thick ice cover. Despite a strong radiation flux and maximum air temperatures above 30° C, approximately 90% of the lake surface remained covered with 40-50 cm of ice, which underwent internal melting and reduced its thickness at the rate of 1-2 cm day$^{-1}$. On June 2, 2013 the wind speeds increased to ~7-10 m s$^{-1}$ and on June 3, 2013 the lake was completely ice-free.

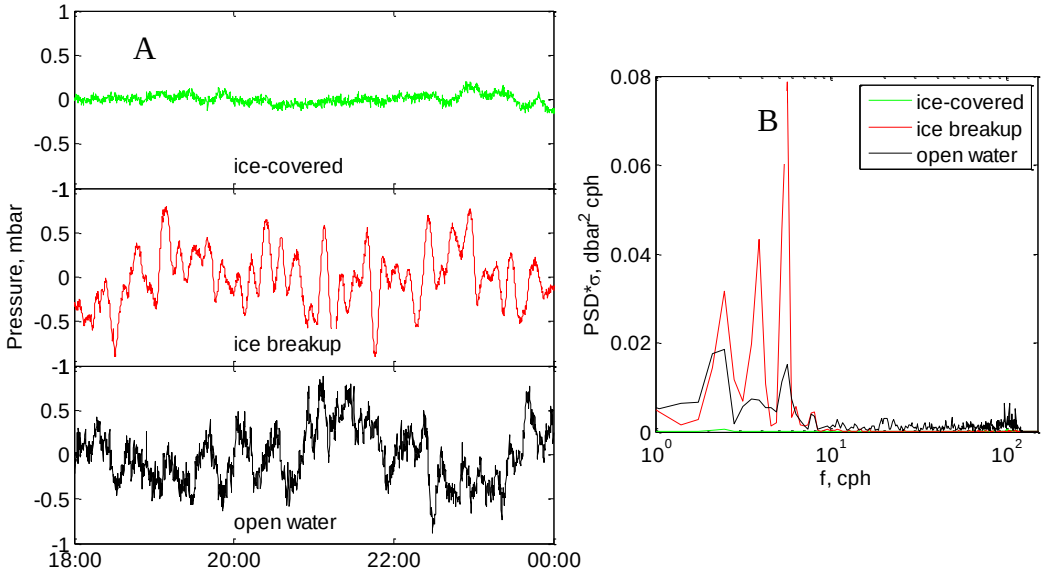


**Figure 2**. (A) 4-hour outtakes from the pressure oscillation records at different stages of the ice break-up. (B) Power spectral densities for the times series from (A).

*Pressure oscillations*: The high-resolution records of pressure, current velocities and water temperature revealed continuous oscillatory motions with periods of 10 to 25 min (Figure 2). The spectral energy peaks resided on frequencies corresponding to the first three eigenfrequencies of the lake indicating the oscillations are produced by the seiche movements at the lake surface. In agreement with previous studies, seiches persisted under the ice cover. During the period preceding the breakup, amplitudes of the lake surface oscillations under ice did not exceed 1mm. The ice breakup was associated with a strong wind event and a 10-fold increase of seiche amplitudes under ice. Despite the wind speed not changing significantly after the ice cover melting, the seiche amplitudes decreased, indicating a redistribution of the wind energy towards the surface waves and drift currents. We suggest that vertical motions of the soft ice sheet significantly accelerated ice melting, so that, from the point the lake surface was covered by up to 90% ice to completely ice-free was approximate 10-15 hours.

At the final stage of the ice-covered period, the ice sheet is detached from the shoreline, allowing wind to produce deflection of the free surface. Simultaneously, ice prevents the formation of wind waves and drift currents. Hence, most of the wind energy entering the lake is transformed into surface seiches, which appear to increase the rate of ice melting. One important seiche effect consists of destroying the stable water-ice boundary layer and bringing ice in contact with lake water at temperatures exceeding 0°C and strongly increases the melting rate. This mechanism provides a plausible explanation for the disappearance of ice cover within 1-2 windy days as observed in many temperate lakes worldwide.

**REFERENCES**

Kirillin, G., Leppäranta, M., Terzhevik, A., Granin, N., Bernhardt, J., Engelhardt, C., Efremova, T., Golosov, S., Palshin N., Sherstyankin, P., Zdorovennova G., and Zdorovennov, R. (2012). Physics of seasonally ice-covered lakes: a review. *Aquatic sciences*, **74**, 659–682.

Lei, R., Leppäranta, M., Cheng, B., Heil, P., and Li, Z. (2012). Changes in ice-season characteristics of a European Arctic lake from 1964 to 2008. *Climatic change*, **115**, 725–739.

# Sediment-water gas exchange in a small boreal lake measured by Eddy Correlation

J. Kokic[1]*, E. Sahlée[2] and S. Sobek[1]

[1] *Department of Ecology and Genetics/Limnology, Uppsala University, Uppsala, Sweden*
[2] *Department of Earth Sciences, Uppsala University, Uppsala, Sweden*

**Corresponding author, e-mail jovana.kokic@ebc.uu.se*

**KEYWORDS**
Lake sediments; carbon dioxide; turbulence; eddy correlation.

## EXTENDED ABSTRACT

### Introduction

Lakes in the boreal landscape are active sites for carbon (C) cycling acting both as sources and sinks of C, through greenhouse gas evasion such as carbon dioxide ($CO_2$) and lake sediment burial (Algesten et al., 2004, Molot and Dillon, 1996). Lake sediments are additionally sources of $CO_2$ to the water column where the fate of this $CO_2$ is controlled by turbulence in the bottom boundary layer. This factor is generally not accounted for in current estimates of sediment $CO_2$ fluxes, which largely are based on conventional enclosure techniques. Novel techniques such the Eddy Correlation (EC) provide us with noninvasive flux measurements of sediment-water gas exchange (Berg et al., 2003).

In this study we aimed to measure the turbulent oxygen ($O_2$) exchange at the sediment-water interface (SWI) with the EC technique. By use of the metabolic relation of $O_2$ and $CO_2$ (RQ: respiratory quotient) derived from a sediment incubation experiment with artificial turbulence, we present the first estimates of turbulent lake sediment $CO_2$ flux from a small boreal lake in southern Sweden (58.37 °N, 12.16 °E) with low turbulence (characterized by $U_{0.1m}$ horizontal velocity <2 cm $s^{-1}$).

### Materials and methods

The EC technique (UNISENSE, Denmark) is based on fast resolution measurements of 3D velocity components (horizontal u and v, vertical w) and $O_2$ concentration, measured by an Acoustic Doppler Velocimeter (ADV) and a Clark-type $O_2$ microsensor. We conducted measurements at 8 Hz sampling frequency in 1-2 meter water depth over organic rich soft sediment during October 2013 for three consecutive days. Under a set of restrictions, e.g. stationary condition and horizontal homogeneous surface, the turbulent part of the $O_2$ flux, $J$ may be expressed as:

$$\overline{J} = \overline{w' O_2'} \qquad (1)$$

derived by applying Reynolds decomposition on the scalar continuity equation, where w´ and $O_2$´ are the fluctuating components of vertical velocity and $O_2$ concentration respectively and overbars symbolize averaging over time. The turbulence statistics were calculated in 15 min blocks, detrended using a running average filter (15 min) as recommended by previous studies (Lorrai et al., 2010). Our dataset was corrected for time lag between the ADV and $O_2$ microsensor by finding the maximum correlation between the two signals for each 15 min period by step-wise shifting of the time series. A double rotation technique was applied to the ADV data to correct for possible misalignments of the sensor. As quality control, individual cospectra of $wO_2$ were manually checked for all data.

## Results and discussion

Figure 1a indicates a typical problem for this site with both positive and negative flux contribution at the lower frequencies, providing difficulty in directly calculating the turbulent flux through Eq. (1). As our measuring site was shallow and close to the shore, this flux might not represent the uptake/production at the SWI but instead the impact of internal waves carrying a different $O_2$ concentration, thus not a turbulent component and not related to the local gradient.

By calculating ogives (Figure 1b), a measure of cumulative flux for each frequency range (starting from the highest frequency) this presumably wave-related low frequency flux could be separated from the turbulent flux. We then manually checked the cospectra and a cut-off frequency, $n_c$, was selected where the turbulent part was deemed to be negligible. The flux represented by $n<n_c$ was then read from the corresponding ogive.

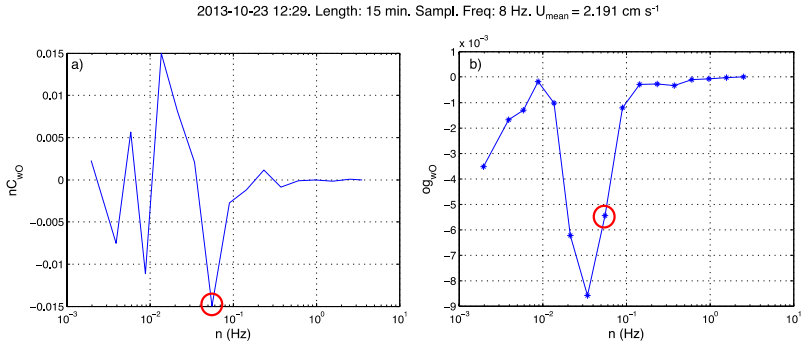


**Figure 1.** Example of (a) cospectra of w and $O_2$ ($nC_{wO}$) for a 15 min segment and (b) calculated ogive from the cospectra ($og_{wO}$). Red circles represent selected point for flux integration.

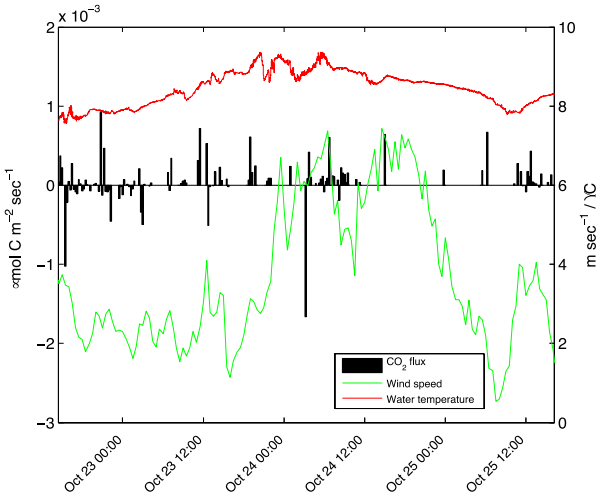


**Figure 2.** $CO_2$ flux at the SWI (µmol $m^{-2}$ $s^{-1}$), wind speed (m $sec^{-1}$) and water temperature (°C). Negative flux indicates uptake by the sediment.

Experimentally derived RQ of the sediment was close to 1, implying that in-situ $CO_2$ fluxes are of similar magnitude as the $O_2$ fluxes. $CO_2$ fluxes derived from our measurement were small (Figure 2) as expected for a low turbulent system, and show that the sediments could also consume $CO_2$, related to photosynthesis at this shallow water depth.

In our study we present a first trial of EC measurements for gas-exchange at the SWI in a small boreal lake. Since our flux rates are much less than previously presented we see a need for more measurements in small lakes. Further steps include a more detailed evaluation of our dataset, especially concerning the turbulence structure. Nevertheless, our results present an intriguing first look at the in-situ $CO_2$ flux from lake sediments, point towards the difficulties in EC measurements in low-turbulence environments, and are a first step to the ambition of improving the estimates of sediment contribution to $CO_2$ release from lakes.

### REFERENCES

Algensten, G., S. Sobek, S., A. Bergstrom, A. Agren, L. Tranvik, M. Jansson (2004), Role of lakes for organic carbon cycling in the boreal zone, *Global Change Biology*, **10,** 141-147.

Berg, P., H. Roy, F. Janssen, V. Meyer, B. Jorgensen, M. Huettel, and D. De Beer (2003), Oxygen uptake by aquatic sediments measured with a novel non-invasive eddy-correlation technique. *Marine Ecology-Progress Series*, **261,** 75-83.

Lorrai, C., D. McGinnis, P. Berg, A. Brand, A. Wüest, (2010), Application of Oxygen Eddy Correlation in Aquatic Systems, *Journal of Atmospheric and Oceanic Technology*, **27,** 1533-1546.

Molot, L. A., and P. J. Dillon (1996), Storage of terrestrial carbon in boreal lake sediments and evasion to the atmosphere. *Global Biogeochemical Cycles*, **10,** 483-492.

# Deep water ventilation of a fjord lake: 10 years of observation from Quesnel Lake, Canada

B. Laval[1]*, S. Vagle[2], J. Morrison[3] and E. Carmack[2]

[1] *Department of Civil Engineering, University of British Columbia, Vancouver, Canada*
[2] *Department of Fisheries and Oceans, Sidney, Canada*
[3] *Vynx Design, Sidney, Canada*

**Corresponding author, e-mail blaval@civil.ubc.ca*

**KEYWORDS**
Deep lakes; thermobaric instability; Quesnel Lake; field data.

## EXTENDED ABSTRACT

### Introduction

In deep temperate lakes, the temperature of maximum density ($T_{MD}$) decreases with depth approximately 1ºC per 500 m, complicating the annual cycle of overturn. Temperature profiles below about 200 m in deep temperate lakes are typically between $T_{MD}$ and 4 °C, with temperatures gradually decreasing with depth; for example, Crater Lake (Crawford and Collier, 2007), Lake Baikal (Killworth et al., 1996), and Shikotsu Lake (Boehrer et al., 2009). Although epilimnetic water cannot sink to the bottom by free convection, deep water can be renewed through a conditional instability known as thermobaric convection (Farmer and Carmack, 1981; Killworth et al., 1991; Weiss et al., 1991), which requires forced downward displacement of cold water by seiching to initiate.

Quesnel Lake is a fjord-type lake in British Columbia, Canada that is slightly more than 500 m deep (Figure 1). Here we expand on the lake-wide analysis of a single annual cycle (2003-2004) in Quesnel Lake described in Laval et al. (2012) to present water-column profile and moored thermistor data spanning 10 years to document the annual convective cycle.

### Materials and methods

Quesnel Lake is a fjord-type lake whose shape resembles a 'lazy Y' with West, North and East Arms (Figure 1). The lake is narrow and deep (maximum depth 511 m) with water deeper than 400m only found within the East Arm. Temperature data presented are from a series of field trips spanning 2003 to 2012. Data are from vertical profiles and thermistor chains at the deepest portion of the lake (station M9, Figure 1). Vertical profiles are from a Seabird Electronics SBE19 or 19plus. Thermistors are RBR TR-1000 or 1050.

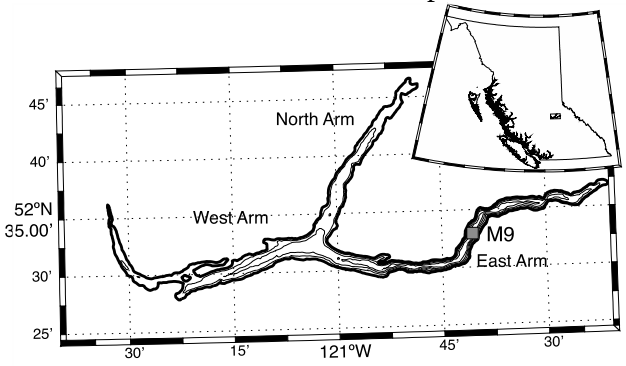


**Figure 1**. Map Quesnel Lake with inset showing its location within the province of British Columbia. Contour interval is 100m.

## Results and discussion

Four years of thermistor chain data are presented in Figure 2. "Turnover" occurs in January and April of each year, though water temperature does not cross $T_{MD}$ at all depths for all turnover events. Above 200m depth, water temperature crosses $T_{MD}$ twice annually due to vertical 1-D convective processes as is typical of dimictic lakes. At 300m depth, water temperature only crosses $T_{MD}$ in two of the four winters presented, but does become isothermal with shallower water in all years. This suggests an interannual variability in the depth to which inverse, winter stratification develops. At 400 and 500m depth, water is always warmer than $T_{MD}$.

At 500m depth, there is a steady temperature increase from April to October (~0.1ºC over 5-6 months), followed by a more rapidly increasing (and in some years highly variable) trend (~0.1ºC over 2 months). In January the water column nearly reaches near isothermal conditions (within 0.05ºC), followed by a rapid drop of 0.1–0.2ºC at 500m depth. February through April is characterized by a generally steady decrease in temperature (<0.1ºC over 2 months). This cooling at 500m depth is unlikely due to vertical, down-gradient, diffusive-type processes (c.a. Boehrer et al., 2009), because of the lake's long and narrow lake's geometry, which promotes seiching, and the presence of a mid-depth (observed at 400m) temperature maximum during winter stratification.

January turnover is characterized by near isothermal conditions followed by rapid change in temperature at 500m. Conversely, April turnover consistently has a significant temperature difference (~0.05ºC) between 400 and 500m, and no rapid temperature change in bottom water temperature. Exchange between surface and intermediate waters occurs twice annually, but deep-waters below 300m are primarily renewed during the generally stormy early-winter driving wind forced turbulent diffusion and gravitational convection triggered by isotherm displacement initiating thermobaric instability, which are required for deep-water renewal.

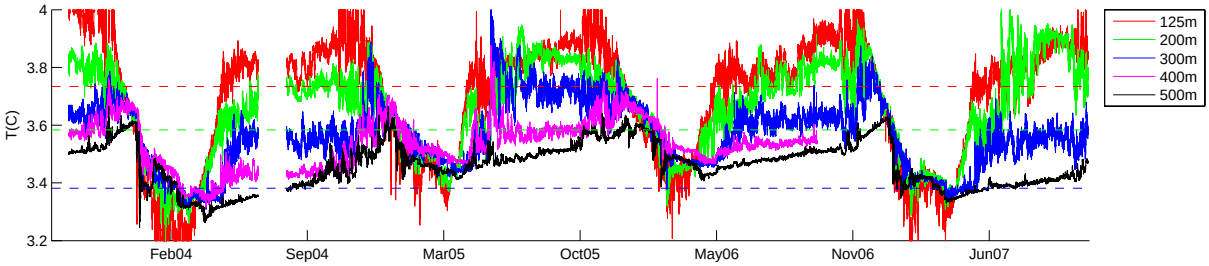


**Figure 2**. Four years of thermistor chain data in the east arm of Quesnel Lake. Horizontal dashed lines are temperature of maximum density at the depth given in the legend.

## REFERENCES

Boehrer, B., R. Fukuyama, K. Chikita and H. Kikukawa (2009). Deep water stratification in Japan's very deep caldera lakes Ikeda, Towada, Tazawa, Kuttara, Toya and Shikotsu, *Limnology*, **10**, 17–24. DOI 10.1007/s10201-008-0257-1

Crawford, G. B. and R. W. Collier 2007. Long-term Observations of Deepwater Renewal in Crater Lake, Oregon *Hydrobiologia*, **574**, 47-68. doi:10.1007/s10750-006-0345-3

Farmer, D. M. and E. C. Carmack (1981), Wind Mixing and Restratification in a Lake near the Temperature of Maximum Density. *J. Phys. Oceanogr*., **11**, 1516-1533.

Killworth, P. D., E. C.Carmack, R. F. Weiss and R. Matear (1996), Modeling deep-water renewal in Lake Baikal. *Limnol. Oceanogr*. **41**, 1520-1538.

Laval, B., D. J. Potts, E. C. Carmack, J. Morrison**,** C. James, S. Vagle, G. I. Sentlinger, F. A. McLaughlin and, M. Foreman (2012), The joint effects of riverine, thermal, and wind forcing on a temperate fjord lake: Quesnel Lake, Canada. *Journal of Great Lakes Research***, 38**(3), 540-549.

Weiss, R. F., E. C. Carmack and V. M. Koropalov (1991), Deep-water renewal and biological production in Lake Baikal. *Nature*, **349**, 665-669.

# Physical controls on lake evaporation across a variety of climates and lake types

J. D. Lenters[1]*, P. D. Blanken[2], N. C. Healey[3], K. M. Hinkel[4], J. B. Ong[5], C. S. Peake[6], B. L. Potter[6], D. Riveros-Iregui[7], C. Spence[8], K. Van Cleave[6] and V. Zlotnik[9]

[1] *LimnoTech, Ann Arbor, MI, USA*
[2] *Department of Geography, University of Colorado, Boulder, CO, USA*
[3] *Department of Biological Sciences, Florida International University, Miami, FL, USA*
[4] *Department of Geography, University of Cincinnati, Cincinnati, OH, USA*
[5] *Department of Civil and Environmental Engineering, University of Connecticut, Storrs, CT, USA*
[6] *School of Natural Resources, University of Nebraska-Lincoln, Lincoln, NE, USA*
[7] *Department of Geography, University of North Carolina, Chapel Hill, NC, USA*
[8] *National Hydrology Research Centre, Environment Canada, Saskatoon, SK, CA*
[9] *Dept. of Earth and Atmospheric Sciences, University of Nebraska-Lincoln, Lincoln, NE, USA*

**Corresponding author, e-mail jlenters@limno.com*

**KEYWORDS**
Lakes; evaporation; water temperature; energy budget; climate.

## EXTENDED ABSTRACT

### Introduction

Lake evaporation is a complex process that interacts with many aspects of a lake ecosystem, including water temperature, ice cover, vertical mixing, lake chemistry, stratification, and water levels. Although driven primarily by wind speed and vapour pressure gradient, evaporation is also an energy-consuming process. This not only leads to significant influences from net radiation, sensible heat flux, and other components of the surface energy balance, but it also results in important feedbacks on lake temperature, ice cover, and other evaporation-mediating processes. As such, defining the climatic variables that 'drive' lake evaporation is far from straightforward and often depends on timescale, lake depth, and characteristics of the regional climate.

### Materials and methods

In this study, we provide some insight into the drivers of lake evaporation by examining the energy budget of a variety of lakes across a range of climatic gradients and lake types. This includes an analysis of two deep, temperate lakes in the Laurentian Great Lakes region (Lenters et al., 2005; Van Cleave, 2012), a shallow, Arctic lake in northern Alaska (Potter, 2011), and a hypersaline lake in semi-arid western Nebraska (Zlotnik et al., 2012). Characteristics of each lake are listed in Table 1. Our analysis focuses on meteorological variables such as wind speed, net radiation, air temperature, and humidity, as well as the relative roles of sensible and latent heat flux in the lakes' surface energy balance.

**Table 1**. Geographic, morphometric, and climatic information for the four study lakes.

| Lake name | Latitude | Longitude | Elevation [m ASL] | Mean depth [m] | Max. depth [m] | Area [km$^2$] | Climate |
|---|---|---|---|---|---|---|---|
| Alkali | 41.8°N | 102.6°W | 1173 | 0.3 | 1.0 | 0.6 | Semi-arid |
| Emaiksoun | 71.2°N | 156.8°W | 8 | 1.8 | 2.6 | 1.86 | Polar |
| Sparkling | 46.0°N | 89.7°W | 495 | 11 | 20 | 0.64 | Temperate |
| Superior | 47.5°N | 87.5°W | 184 | 147 | 406 | 82,100 | Temperate |

Two approaches that are often used to calculate and diagnose the dynamics of lake evaporation include the mass transfer and energy balance relationships (Lenters et al., 2005):

$$E = k \cdot U \cdot (es - ea) \quad (1)$$

$$Rnet - H - LE = S, \quad (2)$$

where $E$ is evaporation rate, $k$ is the mass-transfer coefficient, $U$ is wind speed, $es$ is saturation vapour pressure (at the lake surface temperature), $ea$ is vapour pressure of the air, $Rnet$ is net radiation, $H$ is sensible heat flux, $L$ is the latent heat of vaporization, and $S$ is the rate of change in heat storage in the lake and underlying sediments. Often the Bowen ratio ($B = H/LE$) is employed to solve equation (2), which can then be used to estimate $k$ in equation (1).

## Results and discussion

Sample timeseries of $H$ and $LE$ for Lake Superior are shown in Figure 1, illustrating short-term and seasonal covariance between sensible and latent heat flux. This is commonly observed on lakes (Lenters et al., 2005; Blanken et al., 2011; Zhang and Liu, 2013), due to similar driving factors such as wind speed and air temperature. The mid-latitude location and extreme depth of Lake Superior also leads to significant temporal lags between net radiation and turbulent heat fluxes, due to large seasonal variations in heat storage (Spence et al., 2013). The presence of ice cover has strong interacting effects with $H$ and $LE$ (Lenters et al., 2013).

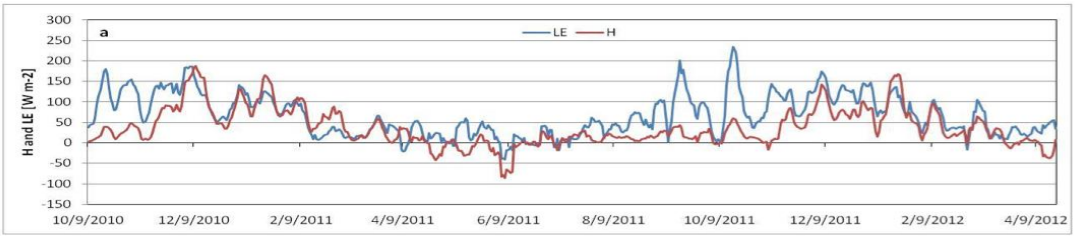


**Figure 1**. 7-day running mean sensible ($H$) and latent ($LE$) heat fluxes for Lake Superior based on eddy covariance measurements from Granite Island, October 2010 – April 2012 (Van Cleave 2012).

It turns out, however, that a strong correspondence between $H$ and $LE$ does not always apply to lakes in general. Alkali Lake (Table 1), for example, displays an out-of-phase relationship between $H$ and $LE$, due to its shallow depth and dry climate. Emaiksoun Lake, on the other hand, is also shallow but in a polar climate. As such, it shows significantly lower surface heat fluxes (compared to Lake Superior), but strong $H$ and $LE$ covariance (Potter, 2011). Examination of additional climatic drivers reveals a wide range of evaporative response to climatic forcing. This work highlights the need to expand our understanding, measurement, and modelling of lake evaporation across climatic gradients and lake types.

## REFERENCES

Blanken, P., C. Spence, N. Hedstrom, and J. Lenters (2011), Evaporation from Lake Superior: 1. Physical controls and processes. *J. Great Lakes Res.*, **37**, 707-716.

Lenters, J., T. Kratz, and C. Bowser (2005), Effects of climate variability on lake evaporation: Results from a long-term energy budget study of Sparkling Lake, northern Wisconsin (USA). *J. Hydrology*, **308**, 168-195.

Lenters, J., J. Anderton, P. Blanken, C. Spence, and A. Suyker (2013), Assessing the impacts of climate variability and change on Great Lakes evaporation. In: 2011 Project Reports. Brown, Bidwell, and Briley, ed.

Potter, B. (2011), Climatic controls on the summertime energy balance of a thermokarst lake in northern Alaska: Short-term, seasonal, and interannual variability. *Dissertations & Theses in Nat. Res*. Paper 39. 109 pp.

Spence, C., P. Blanken, J. Lenters, and N. Hedstrom (2013), The importance of spring and autumn atmospheric conditions for the evaporation regime of Lake Superior. *J. Hydromet.*, **14**, 1647-1658.

Van Cleave, K. (2012), Interactions among evaporation, ice cover, and water temperature on Lake Superior: Decadal, interannual, and seasonal variability. *Dissertations & Theses in Nat. Res*. Paper 52. 97 pp.

Zhang, Q., and H. Liu (2013), Interannual variability in the surface energy budget and evaporation over a large southern inland water in the United States. *J. Geo. Res.-Atmos*., **118**, 4290-4302.

Zlotnik, V., J. Ong, J. Lenters, J. Schmieder, and S. Fritz (2012), Quantification of salt dust pathways from a groundwater-fed lake: Implications for solute budgets and dust emission rates. *J. Geo. Res.-Earth Surf*., **117**.

# Variability of the kinetic energy of low-frequency currents in the Gulf of Finland

M.-J. Lilover

*Institute of Marine Systems,*
*Tallinn University of Technology, Tallinn, Estonia*

*e-mail madis-jaak.lilover@msi.ttu.ee*

**KEYWORDS**
Gulf of Finland; ADCP measurements; vertical kinetic energy variability; bottom-trapped topographic waves.

## EXTENDED ABSTRACT

### Introduction

The low-frequency current reversals are responsible for the appearance and disappearance of salt-wedge in the near bottom layer at the entrance area of the Gulf of Finland (GoF). The latter, in turn, is correlated with hypoxic and oxygenated conditions in the bottom layer. The aim of this study was to determine the depths of the GoF which were the most influenced by the low-frequency motions, to estimate the prevailing low-frequency bands and to reveal the possible processes behind the observed distribution of the kinetic energy.

### Materials and methods

Five bottom-mounted Acoustic Doppler Current Profilers (ADCP, 300 kHz, Teledyne RD Instruments) were deployed along the GoF at different locations (Figure 1). Three ADCP of five were deployed along the thalweg of the gulf whith the two outermost ADCPs measuring at the same time period (winter 2011/2012). The remaining two were located closer to the southern coastal slope of the GoF. Those ADCP were deployed at different time periods. The bottom-mounted ADCP takes the lowest reading at 5 meters above the seabed with the vertical increment of 2 meters. The uppermost readings were performed in the range of 5 to 10 meters depth depending on the depth of location. For the low-frequency analysis, the time series were filtered with a 36-h cutoff Butterworth filter. Such low-pass filtering almost removed the inertial, tidal and seiche-related current components.

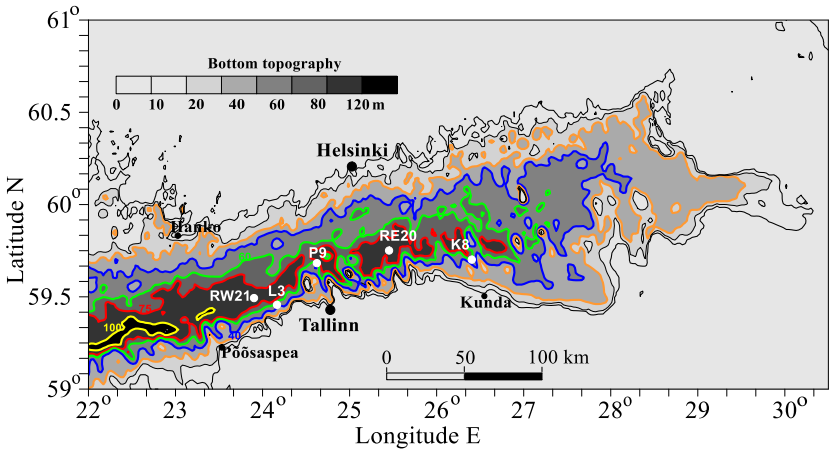


**Figure 1**. Current velocity measurement positions along the Gulf of Finland (white dots).

## Results and discussion

In three time series out of five the mean low-frequency kinetic energy had a secondary peak in the near bottom layer in addition to the near surface peak. In one time series the secondary maximum of the kinetic energy was observed directly in the bottom layer.

The dominating frequency bands vary with the gauge location and the sea depth. The observed kinetic energy can be divided into 2 relatively broad bands: with the characteristic time periods of 7 to 21 days (Sub LF band, SubLF) and of 2.1 to 6.6 days. In the latter band a sub-band of 4.2 - 5.2 days appears (Topographic LF band, TLF) which is observed in 3 out of 5 measurement series in the bottom layer (at locations RW21, L3 and RE20). Similarly, a narrow sub-band with shorter characteristic time periods of 2-3 days (Super LF band, SuperLF) is frequently observed.

The kinetic energy spectra at 2 westernmost stations showed more energy below the surface layer in the TLF sub-range (Figure 2). The maximum kinetic energy of that sub-range was observed at the depths of 20 – 35 meters (location depth 51 m) at measurement station L3 and in the bottom layer below 80 meters (location depth 90 m) at station RW21 respectively. In the stratified sea coastal-trapped waves were often observed (Huthnance, 1978) having the maximum kinetic energy in the region of coastal slope. Earlier measurements have shown the bottom–trapped waves in the GoF (Talpsepp, 2006). In the present case the possibility that the observed variability is result of topographically trapped waves - trapped by the coastal slope and by the bottom is considered.

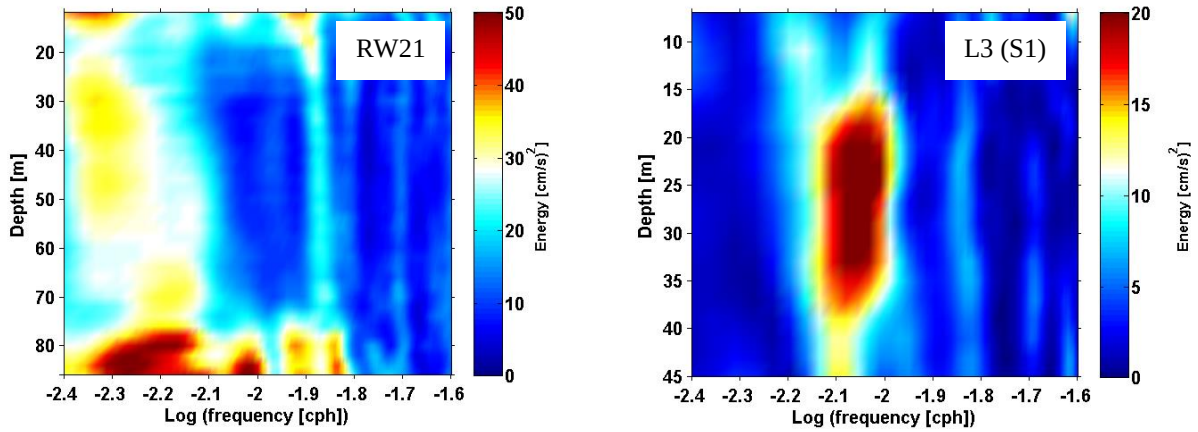


**Figure 2**. Vertical distribution of the energy spectra at locations RW21 and L3.

Probably the variability of dominating SW winds together with the attending barotropic forcing and changing bottom topography could be the factors behind of the observed phenomena (Elken et al., 2006).

**Acknowledgements.** We are grateful to Irina Suhhova for the assistance in ADCP data processing as well as to Aleksander Toompuu for the suggestions on the manuscript. This study was partly supported by the Estonian Science Foundation grant G9381.

**REFERENCES**

Elken, J., P. Mälkki, P. Alenius and T. Stipa (2006), Large halocline variations in the Northern Baltic Proper and associated meso – and basin-scale processes, *Oceanologia*, **48**, 91–117.

Huthnance, J. M. (1978), On coastal trapped waves. Analysis and numerical calculations by inverse iterations, *J. Phys. Oceanogr.*, **8**, 74−92.

Talpsepp, L. (2006), Periodic variability of currents induced by topographically trapped waves in the coastal zone in the Gulf of Finland, *Oceanologia*, **48**(S), 75−90.

# Mapping phycocyanin cells density of Planktothrix rubescens in freshwater reservoirs

A. Maltese[1]*, G. Ciraolo[1], F. Capodici[1], A. Granata[2] and G. La Loggia[1]

[1] *Dipartimento di Ingegneria Civile Ambientale, Aerospaziale, dei Materiali, Università degli Studi di Palermo, Italy*
[2] *Assessorato Territorio e Ambiente – Regione Siciliana, Italy*

**Corresponding author, e-mail antonino.maltese@unipa.it*

**KEYWORDS**
*Planktothrix rubescens*; phycocyanin cells density; reservoirs; remote sensing.

## EXTENDED ABSTRACT

### Introduction

In infested lakes, during periods of low solar irradiance when light weakly penetrates water and it cools, *P. rubescens* filaments float up to water surface forming red blooms. *P. rubescens* produces microcystins, which are harmful hepatotoxins. Water supply for civil purposes needs to be limited or suspended, as well as all recreational activities (*e.g.*, boating, fishing etc.) and cattle watering. Thus, mapping techniques are required to routinely, promptly and cheaply quantify microcystins density. Since, in recent years a toxic bloom of *P. rubescens* has occurred in several Sicilian reservoirs (Ancipa, Pozzillo, Nicoletti, Raia di Prizzi, Trinità di Delia), water samples were collected for counting phytoplankton cells and for analysing microcystins occurrence. In this framework, this manuscript setup empirical relationships, based on reflectance products, to evaluate phycocyanin cells density, $\delta_C$ ($10^6$ cells $l^{-1}$), from MODIS Terra (at a spatial resolution 250 m) and Landsat ETM+ images (at 30 m) using both Red and NIR ground spectral reflectances.

### Calibration/validation

*In situ* $\delta_C$ were correlated with the MODIS reflectances, $\rho_{RED} \bullet \rho_{NIR}$, and a linear trend line was retrieved using a least square regression analysis ($r^2$=0.67) to calibrate an empirical equation. Data dispersion does not highlight a clear trend for low values of $\delta_C$, where, moreover, the trend line lies below the cluster $\delta_C$ *vs.* $\rho_{RED} \bullet \rho_{NIR}$; thus underestimating $\delta_C$ for low cells density. The relationship was adapted to Landsat ETM+ images, given the sensors relative spectral responses (Maltese *et al.*, 2012). Thus, the algorithm was validated by comparing *in situ*, $\delta_C$, *vs.* values estimated by Landsat ETM+, $\delta_{CE} \pm \sigma_{CE}$ (spatial average ± standard deviation), on Prizzi reservoir although *in situ* data and satellite images were timely close but not simultaneous. Results show that $\delta_C$ was under-estimated by satellite maps, however it falls within the range individuated by the standard deviation.

**Table 1.** Measured *vs.* Landsat ETM+ estimated $\delta_C$ on Prizzi reservoir.

| *Prizzi* | *Date* | $\delta_C$ ($10^6$ cells $l^{-1}$) | $\delta_{CE}$ *mean* ($10^6$ cells $l^{-1}$) | $\sigma_{CE}$ ($10^6$ cells $l^{-1}$) |
|---|---|---|---|---|
| *In situ* | 19/04/2006 | ≈22.13 | - | - |
| *Landsat ETM+* | 04/04/2006 | - | ≈19.13 | ±3.67 |

### Diachronic analysis

A diachronic analysis was carried out on Landsat ETM+ images to show the potentiality of *P. rubescens* monitoring through remote sensing. The analysis performed on the *SS. Trinità*

*di Delia* reservoir highlighted that $\delta_{CE}$ reached up to ~$12.6 \cdot 10^6$ cells $l^{-1}$, where a bloom of *P. rubescens* was detected on December the 20th 2007, as consequence of the frost recorded by the Castelvetrano meteorological station during the nights of 6th and 15th December 2007.

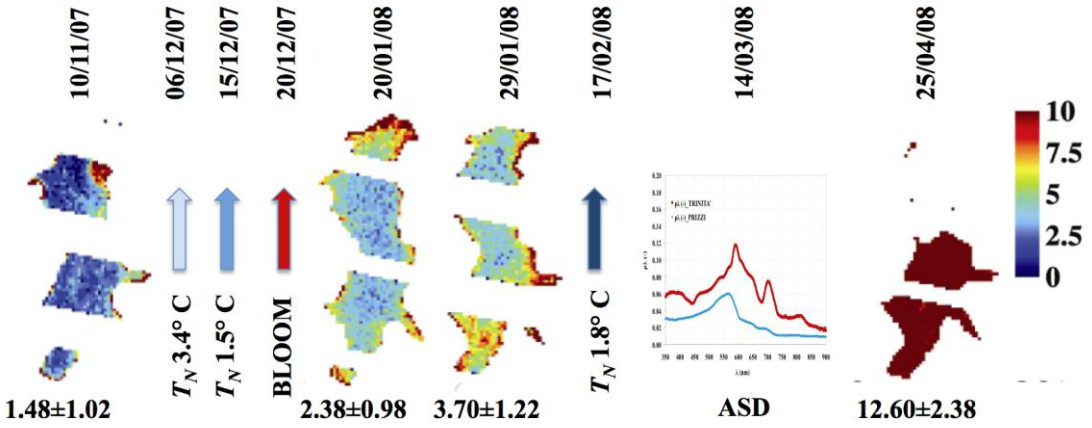


**Figure 1.** $\delta_{CE}$ ($10^6$ cells $l^{-1}$) maps derived from Landsat ETM+ images on the SS. Trinità di Delia reservoir; arrows highlight $T_N$ (°C) of frosts and the date when the bloom was observed; the graph represents also the spectroradiometric acquisition date; white stripes are due to the SLC-off acquisition mode of the ETM+ sensor.

## Discussion and conclusions

Empirical relationships were calibrated on Red and NIR reflectances of MODIS Terra and Landsat ETM+ by exploiting *in situ* $\delta_C$ and spectral acquisitions, to characterize the spatial distribution of phycocyanin cells density. Relationships assess accurately $\delta_C$ for high cells densities, whereas it is too sensitive to slight variation of reflectance within the low density ranges. The empirical equations tend to overestimate the actual values for low (or absent) surface filaments when the contribution of chlorophyll on surface reflectance is not distinguishable from that of cyanobacteria and their pigment (the phycocyanin), especially at early stage formation of cyanobacterial blooms.

Recently, during winter 2014, a bloom of *P. rubescens* has occurred in Pozzillo lake (Racalbuto district). The lake waters are sampled from 2012 by ARPA Sicilia (the Regional Environmental Protection Agency) and by CNR (the Marine Microbiology Institute of Messina). The lake water is used by the lake managing authority ENEL S.p.a. (the National Italian Electric utility company) and, by two land reclamation authorities (*Consorzi di Bonifica*), for irrigation water managing. On the 13th of January samplings are taken, while results revealing the *P. rubescens* infestation are transmitted on the 22nd of January; thus, on the 24th of February, a Major decree prohibited any water use for seek legal protection. A successive sampling of the 14th of April still revealed the bloom (> $100^6$ cells $l^{-1}$), thus the decree, on the 20th of April 2014, is currently maintained in force. These recent events highlight the modernity of the problem and the need of a prompt monitoring of the lakes.

New remote sensing sensors (*e.g.*, high spatial resolution LDCM, high temporal resolution VIIRS/NPP) could provide precious information to reservoir managers that should be used to alert water authorities and to limit (or stop) the water supply for civil purposes; hence, using these information to adapt the water treatment strategy and regulate or even forbidden cattle watering or any recreational activities.

**REFERENCES**

Maltese, A., F. Capodici,, G. Ciraolo, C. Corbari, A. Granata, G. La Loggia (2012). Planktothrix rubescens in freshwater reservoirs: The Sentinel-2 potentiality for mapping phycocyanin concentration, *European Space Agency, (Special Publication) ESA SP 707 SP*.

# Sedimentation in a large lake: Role of physical conditions and phytoplankton composition

I. Ostrovsky* and Y.Z. Yacobi

*Israel Oceanographic and Limnological Research, Yigal Allon Kinneret Limnological Laboratory, Migdal 1485000, Israel*

**Corresponding author, e-mail ostrovsky@ocean.org.il*

**KEYWORDS**
Lakes; sedimentation; re-suspension; photosynthetic pigments; primary production; export ratio.

## EXTENDED ABSTRACT

### Introduction

Sedimentation is a major process for removal of particulate material and important determinant accounting for the stability of aquatic ecosystems. The fluxes of particulate material are affected by numerous physical, chemical, and biological processes. The resulting patterns of particle deposition to bottom sediments depend on lake thermal and chemical structure, and the hydrological regime.

### Materials and methods

Gross sedimentation rates (GSR) in Lake Kinneret (Israel) regularly monitored from 1999 up-to-date. Sampling procedure and analyses see elsewhere (Ostrovsky and Yacobi, 2010).

### Results and discussion

Between 2003 and 2010 the annual GSR decreased about 3-4 fold at the lake center (Sta. A, 40 m). The decrease in GSR reflects changes in the rate of POM export from the epilimnion downwards. The strong positive correlation between GSR and the annual water inflow ($r=0.75$, $P<0.01$) implies that the allochthonous material exported from the watershed affect the sedimentological processes. The organic matter sedimentation rate (OMSR) measured in the middle of the quiescent hypolimnion provides the reliable assessment of POM flux from the upper productive layer (Ostrovsky and Yacobi, 2010). The POM sedimentation declines from February until October (Fig. 1a) and the ratio of this flux to primary production is the export ratio (ER) showing the proportion of primary production settled from the upper productive layer. Changes in the ER (Fig. 1b) are related with the composition of phytoplankton and physical regime in the lake. During January–March (holomixis), large celled algae (*Aulacoseira granulata*, *Peridinium gatunense*) dominate the phytoplankton and are hardly consumed by zooplankton. The high sinking velocity of such cells is a reason why high proportion of the phytoplankton reaches the lake bottom in still warm winter days when turbulent mixing is restrained. Increased turbulence that prevails throughout the well-mixed water column circulates algal cells between the euphotic zone and the trap locations. The latter is the reason for the overestimation of sedimentation flux of negatively-buoyant particles in the non-stratified water column (Yacobi and Ostrovsky, 2012). This accounts for the enlarged ER ratio during holomixis.

A drop in ER (Fig. 1b) occurs promptly after thermal stratification has established and the lower part of the water column became physically separated from the upper productive layer. The ER decline is explained by a shift in dominance in algal community from large to small slow-sinking phytoplankton species throughout thermal stratification (Ostrovsky et al., 2014). High turnover rates characteristic of small algal species enhance nutrient recycling within the euphotic zone and may be the reason for the lowest rate of phosphorous loss from the epilimnion in July-November (Ostrovsky and Yacobi, 2010). The seasonal timing of minimal ER and the greatest retention of limiting nutrients in the epilimnion is an outcome of adaptation of planktonic communities to stratification, when nutrient losses could not be replenished.

The fate of algal material was traced by the examination of photosynthetic pigments in particles prevailing in water and traps. Chlorophyll *a* (Chl *a*) is universally found pigment in all oxygenic photosynthesizers (algae and cyanobacteria). Upon degradation Chl *a* yields an array of degradation products, which reflect diagenetic processing of phytoplankton. Analysis of the seasonal variation of the ratio between Chl *a* -degraded products and intact Chl *a* in sediment traps helps to elucidate the trophic efficiency by which algal material in the water column is utilized (Ostrovsky and Yacobi, 2010). This ratio displayed maximum values of 0.4-0.6 during holomixis and nearly zero values in August-October (Fig. 1c), when algal community consisted of small species that possess low settling velocity, are easily consumed by zooplankton, and thus can be readily recycled within the epilimnion (cf. low ER). The maximum values of the ratio during the holomixis are related with dominance of the large algae that populate the entire water column, such that a high proportion of their fragments may be maintained in the well-mixed turbulent water for a long time. Moreover, large individual cells may have better ability to survive in the deep non-stratified water column with limited light, while the ability to retain and recycle in the upper euphotic stratified layer under conditions of nutrient limitation may well confer an evolutionary advantage to small or buoyant algal populations.

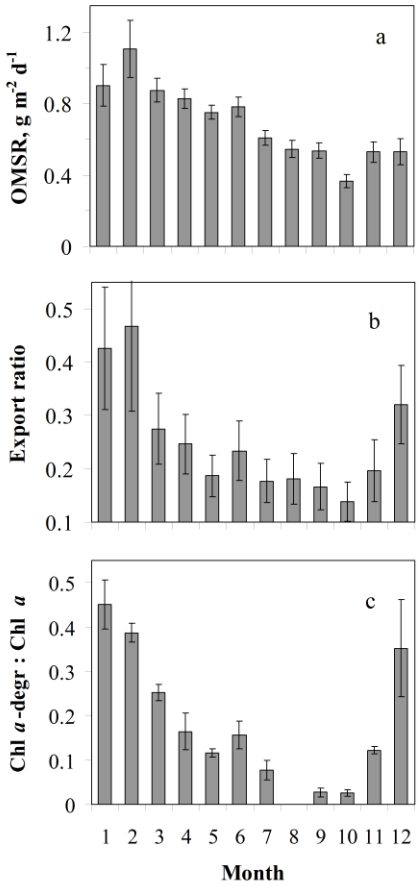


**Figure 1.** Seasonal changes in Lake Kinneret during 2005-2008: (a) organic matter sedimentation rate (OMSR), (b) export ratio, and (c) mass ratio of chlorophyll degradation product sedimentation rate to chlorophyll sedimentation rate (Chl *a*–degr : Chl *a*). The export ratio was calculated as a ratio between the monthly averages of OMSR and primary production at central station. Traps were positioned at ~11 m above the bottom to avoid oversampling of particulate material under turbulent conditions in the benthic boundary layer (Ostrovsky and Yacobi, 2010). Vertical bars show ± standard error.

**REFERENCES**

Ostrovsky, I., and Y.Z. Yacobi (2010), Sedimentation flux in a large subtropical lake: Spatiotemporal variations and relation to primary productivity, *Limnol. Oceanogr.* **55**(5), 1918–1931

Ostrovsky, I., Y.Z. Yacobi, and N. Koren (2014, in press), Sedimentation processes. In *Lake Kinneret: Ecology and Management* (Eds. T. Zohari, A. Sukenik, T. Berman, A. Nishri), Springer, Heidelberg.

Yacobi, Y.Z., and I. Ostrovsky (2012), Sedimentation of phytoplankton: role of ambient conditions and life strategies of algae, *Hydrobiologia*, **698**, 111-120, DOI 10.1007/s10750-012-1215-9.

# Characterization of deep water renewal in Lake Baikal: a numerical analysis

S. Piccolroaz* and M. Toffolon

*Department of Civil, Environmental and Mechanical Engineering, University of Trento, Trento, Italy*

**Corresponding author, e-mail s.piccolroaz@unitn.it*

**KEYWORDS**
Lake Baikal; deep ventilation; downwelling; thermobaricity; one-dimensional model.

## EXTENDED ABSTRACT

### Introduction

With a volume of 23′615 km$^3$ and a maximum depth of 1′642 m, Lake Baikal (Southern Siberia, see Figure 1) is the largest and deepest freshwater basin on Earth. Due to its huge depth, only the upper layer of the lake (approximately 250 m) follows the typical mixing dynamics of temperate lakes. Complete overturn in this layer occurs twice a year, in late May/early June and late December/early January, when surface water temperature approaches the mesothermal temperature maximum (i.e., the temperature where the temperature profile meets the temperature of maximum density). Differently, the hypolimnion is only occasionally subjected to a partial renewal of its waters, as a consequence of periodical deep downwelling events that are responsible for the displacements of water volumes from the surface down to the abyss of the lake. Direct observations (e.g., Weiss et al., 1991) showed that the key mechanism triggering deep downwellings is represented by the onset of buoyancy-driven instabilities, which are mutually controlled by thermobaricity (i.e., the combined dependence of water density on temperature and pressure) and external forcing (mainly wind). Despite deep downwellings have been widely observed in Lake Baikal, large uncertainty still exists with respect to their precise description and quantification.

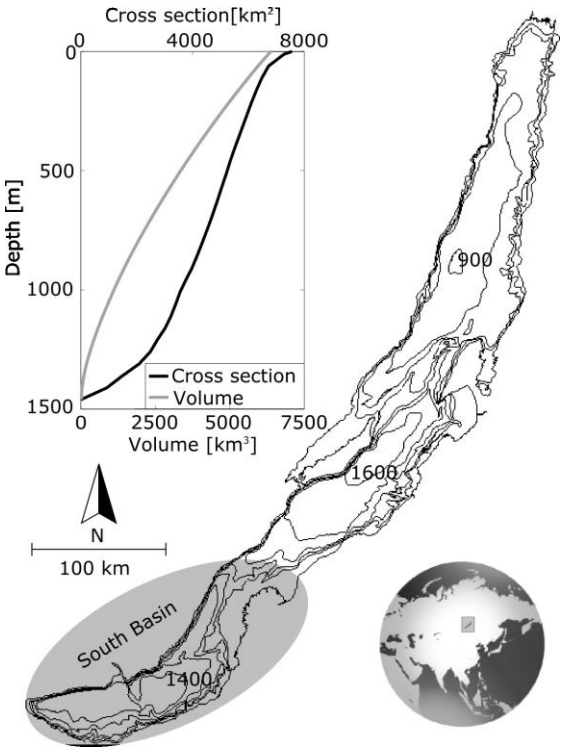


**Figure 1**. Bathymetric map and hypsometric curve of the SB of Lake Baikal.

### Materials and methods

Seasonal and episodic convective mixing in Lake Baikal has been investigated here by means of a simplified one-dimensional model recently proposed by Piccolroaz and Toffolon (2013). Three main algorithms are at the basis of the model: a reaction-diffusion equation for temperature and other tracers (e.g. dissolved oxygen), and two Lagrangian algorithms, the

first to handle buoyancy-driven convection due to density instability (including thermobaric effects) and the other to reproduce the deep downwelling mechanism.

**Results and discussion**

The calibration of the parameters has been obtained by performing a medium-term simulation over a historical period (40 years, from 1958 to 1998), for which measured temperature (courtesy of prof. A. Wüest), CFC-12 and dissolved oxygen profiles were available. Additionally, a long-term 1000-year simulation has been run by maintaining current climate conditions unchanged, which provided an indirect validation of the model. In both cases, numerical results have been shown to be in good agreement with observed data (see Figure 2), suggesting the suitability and robustness of the core algorithms and, in general, a proper performance of the model.

The analysis of the results obtained from the long term simulation allowed for a detailed description of the mixing regime and thermal dynamics of the lake (e.g. seasonality of temperature and diffusivity profiles), and a statistical characterization of deep ventilation, which mainly concerns: timing, typical volumes and temperatures, energy balance and vertical distribution of downwelling volumes. In particular, deep downwellings have been estimated to have a mean annual sinking volume of 91.6±73.0 $km^3$ and a mean annual temperature of 3.27±0.06°C. Concerning the vertical distribution of sinking volumes, nearly the 26% of deep downwelling have been found to reach depth greater than 1300 m, whereas the remaining percentage is mainly distributed between 150 and 900 m, with a peak at about 200-250 m that is due to the numerous shallow and relatively warm events that occur as soon as the water column approaches a nearly homogeneous temperature. Finally, results suggest a strong seasonality of the downwelling events. In this respect, some interesting insights can be raised about the role that the seasonal evolution of thermal conditions of the lake (e.g. thickness of the surface well-mixed layer, strength of the thermal stratification, depth of the mesothermal maximum) plays on the occurrence of deep water renewal.

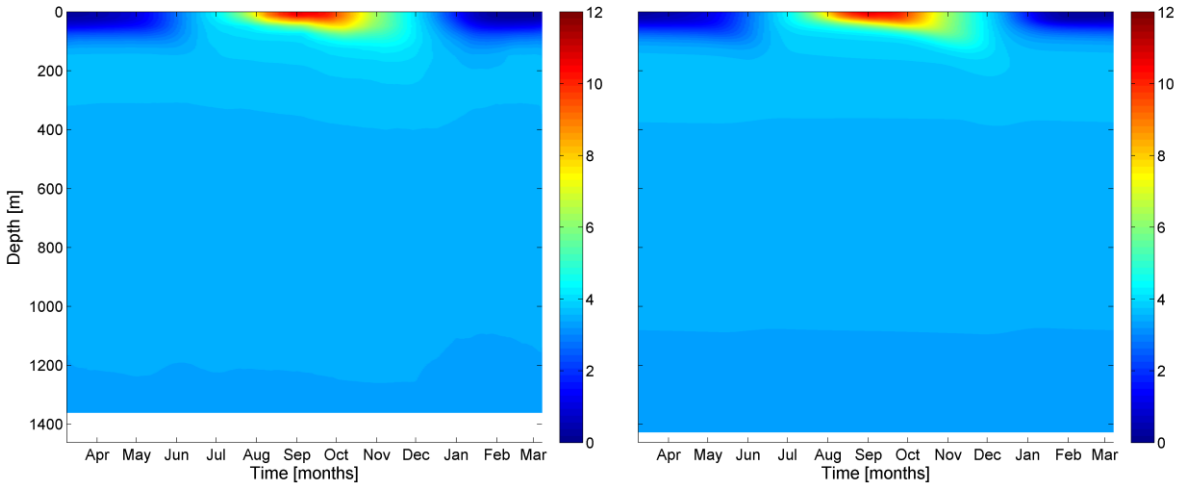


**Figure 2**. Comparison between the mean annual cycles of observed (left) and modelled (right) vertical temperature profiles (RMSE=0.07°C, Mean Absolute Error=0.03°C and Maximum Absolute Error=0.78°C).

**REFERENCES**

Piccolroaz, S. and M. Toffolon (2013), Deep water renewal in Lake Baikal: A model for long-term analyses, *J. Geophys. Res. Oceans*, **118**, 6717–6733, doi:10.1002/2013JC009029.

Weiss, R.F., E.C. Carmack and V.M. Koropalov (1991), Deep-water renewal and biological production in Lake Baikal, *Nature*, **349**, 665–669, doi:10.1038/349665a0.

# Explaining water temperature changes in Lake Superior by means of a simple lumped model

S. Piccolroaz, M. Toffolon* and B. Majone

*Department of Civil, Environmental and Mechanical Engineering, University of Trento, Trento, Italy*

**Corresponding author, e-mail marco.toffolon@unitn.it*

**KEYWORDS**
Lake Superior; water temperature; air temperature; climate change; heat budget.

## EXTENDED ABSTRACT

### Introduction

A significant warming has been noticed in the Great Lakes region during the last decades. One of the peculiar aspects is that water temperature in summer warmed up more rapidly than air temperature (+0.15 °C $yr^{-1}$ and +0.09 °C $yr^{-1}$, respectively, see Figure 1), based on measurements collected by several monitoring buoys and coastal stations in the period 1985-2011 (data from NOAA). Particularly interesting is the extraordinary summer warming that affected Lake Superior in 1998, which can be seen as an exceptional example of the amplified response of the lake system to increasingly warmer atmospheric conditions. This event is analysed by means of the recently developed lumped model *air2water* (Piccolroaz et al., 2013), which allows for simulating and predicting surface water temperature as a function of air temperature only. An explanation of the phenomenon is given based on the positive feedback with the stratification regime of the lake.

### Materials and methods

In spite of the simple formulation and the limited number of parameters (from 4 to 8 for different versions), the *air2water* model is able to satisfactorily capture the seasonal variations and the inter-annual dynamics in surface water temperature of lakes, thus representing a tool for both conceptual studies and real case analyses. The fact that the model is data-driven, while being based on physical grounds, allows for the direct acquisition of information about the studied system in the calibration phase, which is performed through a Monte Carlo approach. The model in its 8-parameter version (from $a_1$ to $a_8$) reads as follows:

$$\frac{dT_w}{dt} = \frac{1}{\delta}\left\{a_1 + a_2 T_a - a_3 T_w + a_5 \cos\left[2\pi\left(\frac{t}{t_y} - a_6\right)\right]\right\}, \tag{1}$$

$$\begin{cases} \delta = \exp\left(-\dfrac{T_w - T_h}{a_4}\right) & \text{for} \quad T_w \geq T_h \\ \delta = \exp\left(-\dfrac{T_h - T_w}{a_7}\right) + \exp\left(-\dfrac{T_w}{a_8}\right) & \text{for} \quad T_w < T_h \end{cases}, \tag{2}$$

where $T_w$ is water temperature, $T_a$ is air temperature, $\delta$ is a dimensionless number related with the depth of the surface volume affected by the heat exchange with the atmosphere, and $T_h$ is a reference value of the deep water temperature (approximately 4 °C for dimictic lakes).

## Results and discussion

The application of the model to Lake Superior suggests that the unusual water warming in summer 1998 can be explained by means of two combined factors: the extremely high air temperature and the increased strength of the stratification, which reduces the volume that effectively concurs to the variation of the surface water temperature (i.e., the parameter $\delta$) because of the reduction of the heat fluxes across the thermocline. Figure 2 shows an application of the model to two years (1997 and 1998): air temperature in 1998 is always higher than in 1997, but the abrupt change of slope in water temperature trend occurring at the end of June 1998 is mainly due to the strong decrease of $\delta$, which corresponds to a more isolated epilimnion and hence to a more intense warming of surface water. Conversely, in 1997, the decrease of $\delta$ occurs later, when air temperature has almost ceased to grow.

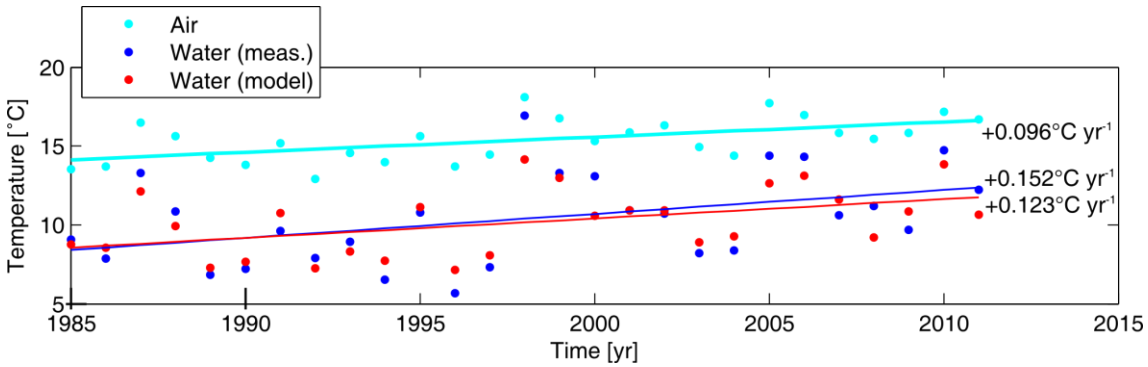


**Figure 1**. Long-term trends of summer average air and water temperatures within the period 1985-2011: observations of air and water temperatures, and modelled water temperature.

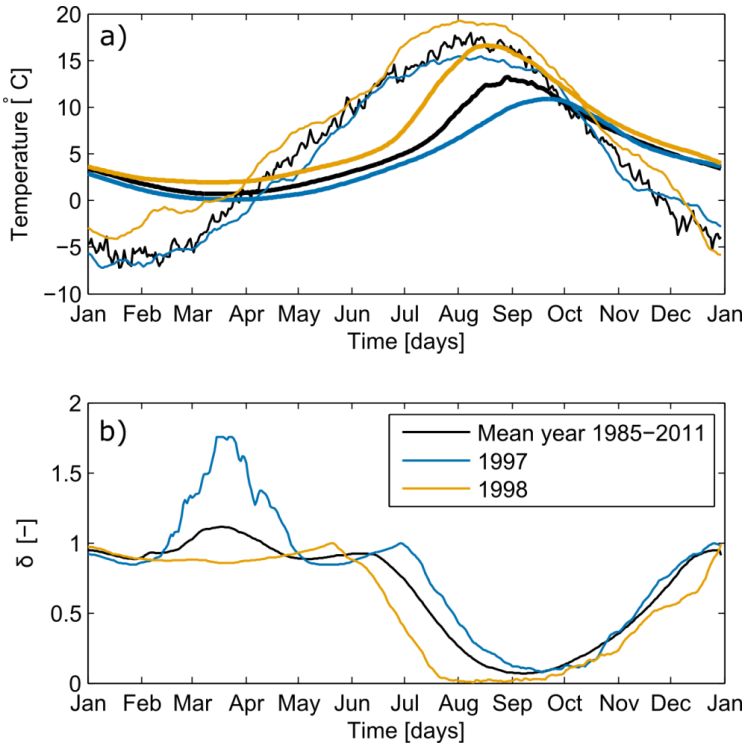


**Figure 2**. Comparison between the annual cycles of: a) measured air temperature (thin lines, smoothed for sake of clarity) and simulated water temperature (thick lines), and b) the dimensionless parameter $\delta$, for the mean year (1985-2011) and the two years 1997 and 1998.

**REFERENCES**

Piccolroaz, S., M. Toffolon, and B. Majone (2013), A simple lumped model to convert air temperature into surface water temperature in lakes, *Hydrol. Earth Syst. Sci.*, **17**, 3323-3338, doi:10.5194/hess-17-3323-2013.

# Turbidity in a drinking water reservoir

R. Pieters[1,2]*, L. Gu[3] and G. Lawrence[2]

[1] *Department of Earth and Ocean Sciences, University of British Columbia, Vancouver, Canada*
[2] *Department of Civil Engineering University of British Columbia Vancouver Canada*
[3] *Environmental Management and Quality Control Division, Metro Vancouver, Burnaby, Canada*

**Corresponding author, e-mail rpieters@eos.ubc.ca*

**KEYWORDS**
Reservoir, turbidity, interflow, intake, selective withdrawal.

## EXTENDED ABSTRACT

### Introduction

Construction of a 20 m dam at the outlet of Coquitlam Lake in 1911 resulted in the largest drinking water supply to Metro Vancouver in British Columbia, Canada. Coquitlam Reservoir is ultra-oligotrophic, receiving high rainfall on a granitic drainage, and is normally very clear (< 0.5 NTU). However, inflow from particular tributaries is occasionally turbid due to bank erosion or landslides in their catchments, especially during fall and winter rainstorms. The fate of these turbid inflows as they enter the reservoir has been examined and here one event is described.

### Study Site

Coquitlam Reservoir is located in the coastal mountains, 30 km northeast of Vancouver, Canada (49° 21′ N, 122° 46′W). The drainage area of the reservoir is 190 km$^2$, and receives high rainfall (3.7 m/yr). The largest tributary, Coquitlam River, drains 79 km$^2$ (45% of inflow) into the north basin (Fig. 1), which acts to isolate and dilute the effect of turbid inflow on the main lake. The second largest, Cedar Creek, drains 27 km$^2$ (15% of inflow) behind Coquitlam Island. Both of these tributaries are major sources of turbidity.

### Results

In fall, turbid inflows are isolated by temperature stratification; in winter turbid inflow tends to plunge to the deepest part of the reservoir, though splitting of the inflow

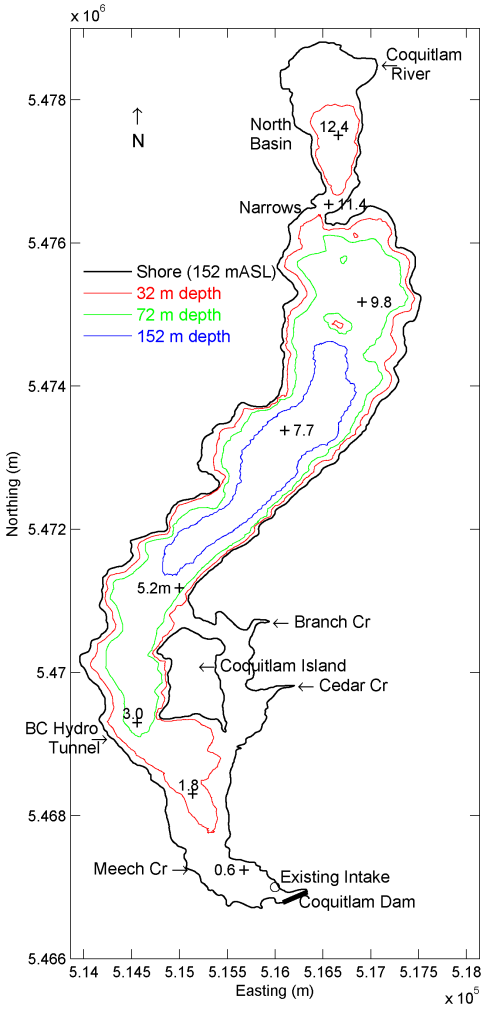


**Figure 1.** Map of Coquitlam Reservoir.

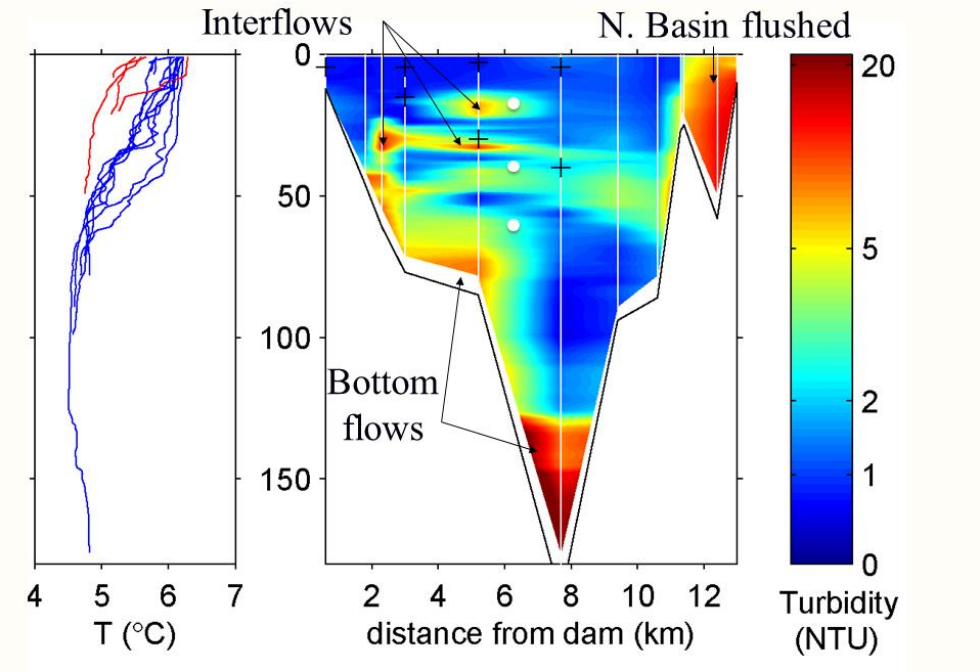


**Figure 2.** (a) Temperature and (b) turbidity on 14 Dec 2004. The (+) give the location of moored sensors. The (o) give the location of potential intakes.

as it plunges has been observed. We use survey and mooring data to describe the turbid inflow, trace its fate through the reservoir and examine which locations would be most suitable for a second drinking water intake.

As an example we show the results from a survey on 14 Dec 2004 following a large storm of 10 Dec 2004 (Fig. 2). The stratification is weak with temperature varying from just over 6 ºC at the surface to 4.5 ºC at 80 m depth (Fig. 2a). During the storm, the temperature of Cedar Cr. was 4-5 ºC, close to the temperature of maximum density, and TSS was high; as a result, the density of Cedar Cr. was significantly higher than the lake. From the turbidity (Fig. 2b) we observe the following:

- In the north basin, both the temperature and turbidity were dominated by Coquitlam River (affected by a landslide upstream). Water from the north basin plunged to approximately 60 m in the main basin and moved south. The plunge point was observed at the surface in the narrows.
- Lenses of turbidity are observed at various depths both at the north (5.5 km) and south (3.5 km) end of Coquitlam Island suggesting that these originate from Cedar Cr.
- Highly turbid water is observed in the deepest part of the lake. Note that the temperature increases toward the bottom; the temperature is stabilized by the turbidity. Increased oxygen levels were also observed at the bottom (not shown). The source of this high turbidity water is likely Cedar Cr.
- Of particular interest, the turbidity of the surface water remained < 1 NTU despite the dramatic effect of the storm on other parts of the basin.

The fact that turbidity is non-uniformly distributed through the depth has prompted a proposed three-level intake structure to selectively withdraw water of the highest quality.

# A simple way to compute the distribution of the age of water within thermally stratified natural lakes

M. Pilotti*, S. Simoncelli and G. Valerio

*Department DICATAM, Università degli Studi di Brescia - Via Branze, 43, Brescia, Italy*

**Corresponding author, e-mail marco.pilotti@ing.unibs.it*

**KEYWORDS**
Stratified lakes; water renewal time; inflow; modelling; CSTR.

## EXTENDED ABSTRACT

### Introduction

The water renewal time is an integrative indicator of the renewal capacity of a water body, which is also contemplated as a quality parameter in the Water Framework Directive. In spite of its wide use in limnology, it is commonly calculated in a too simple way, as the ratio $T_0$ between the volume of the whole basin and the long-term time average discharge of water passing through the lake. This definition, which provides a low order approximation to the time $T_{37}$ when 37% of the original water is still present within the lake, is based on a fully mixed hypothesis (CSTR) that completely neglects the most relevant features of the hydrodynamics of a stratified lake. To overcame this limitation, in this contribution we propose a simplified model for the calculation of the statistical distribution of the water age in a natural stratified lake (Bolin and Rodhe, 1973), which provides a straightforward way to compute $T_{37}$. This time can be regarded as a refined value of the water renewal time.

### Materials and methods

The presented model couples a 1D mass balance of the lake water (Piontelli and Tonolli, 1964) to an algorithm that provides the depth of intrusion of an inflows (Fischer et al., 1979). The model is presented as a system of ordinary differential equations along with a MATLAB script for its numerical solution (Pilotti et al., 2014). The input data required regard the annual evolution of the thermal stratification of the lake and the inflows regime, so that it can be easily applied to lakes where a minimum of limnological data are available, without the need of extensive meteorological data set and modelling expertise that an hydrodynamic model would require to the same purpose.

As an example of application, the algorithm was applied to refine the water renewal time of Lake Iseo, a deep pre-alpine Italian lake, characterized by a volume of about $7.9 \times 10^9$ $m^3$. The two main tributaries convey approximately the same average discharge of 27.5 $m^3/s$, which corresponds to a theoretical renewal time $T_0$ of 4.5 years. The recent monitoring of the inflows thermal regime (Pilotti et al., 2013) has shown that both the channels intrude under the lake surface from April to December. The lake is thermally stratified in most of the year, with a surface mixed layer that progressively deepens from May to October, approaching the hypolimnetic temperatures (6.4°C on average). Historically classified as warm monomictic, in the last 2 decades only two complete overturns occurred, so that its deep-waters underwent a drammatic process of progressive deoxygention (Ambrosetti e Barbanti, 2005).

**Results and discussion**

The proposed model was applied to lake Iseo in the period 1977-2011, using the historical time series of the daily-averaged discharges, the maximum mixing depths (Ambrosetti e Barbanti, 2005) and the reconstructed series of the inflows and lake temperatures. The resulted temporal trend of the concentration C(t) of the water initially present within the lake provided a value of $T_{37}$ of 6 years, which is significantly higher than the theoretical one. However C(t) is a stochastic process whose particular realizations reflect the time sequence of forcing terms and of maximum mixing depths. Therefore, in order to obtain statistically meaningful average results, one should include the natural variability of the hydrological and meteorological stressors so that the age distribution of water in the lake should be obtained as an average of a large number of C(t) equally likely realizations Accordingly, we repeatedly computed a set of 35 different C(t) series with different lengths, starting from year 1977, 1978, 1979 and so on until 2011. Under the hypothesis that the overall process is stationary, the obtained average C(t) curve is shown as a dotted line in Figure 1. The computed average value of $T_{37}$ is 7.1 years.

The same simulation was carried out by neglecting the intrusion of the inflows, obtaining a $T_{37}$ equal to 10.7 years. The comparison among the obtained results highlights the important role of the inflows in the mixing and renewal processes in lake Iseo. This supplements the findings of Valerio et al. (2014) regarding the role of the inflows on the thermal structure of the lake.

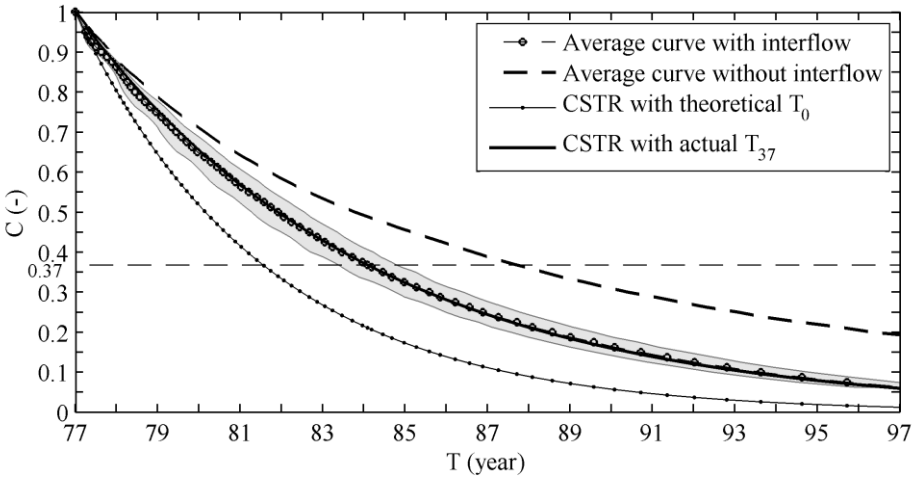


**Figure 1.** Average C(t) curve computed with (dotted line) and without (dashed line) interflow. The CSTR lines are the exponential curves that can be obtained with $T_{37}$= 4.5 years and $T_{37}$= 7.1 years, respectively.

**REFERENCES**

Ambrosetti, W., and L. Barbanti (2005), Evolution towards meromixis of Lake Iseo (Northern Italy) as revealed by its stability trend, *J. Limnol*., **64**, 1–11.

Bolin, B., and H. Rodhe (1973), A note on the concepts of age distribution and transit time in natural reservoirs, *Tellus*, **25**, 58–62.

Fischer H.B, E. J. List, R.C.Y. Koh, J. Imberger, and N.H. Brooks (1979), *Mixing in Inland and Coastal Waters*, Academic Press, New York, NY.

Pilotti, M., G. Valerio, and B. Leoni (2013), Data set for hydrodynamic lake model calibration: A deep pre-alpine case, *Water Resour. Res*., **49**, 1–5.

Pilotti, M., S. Simoncelli, and G. Valerio (2014), A simple approach to the evaluation of the actual water renewal time of natural stratified lakes, *Water Resour. Res*., **50**, doi:10.1002/2013WR014471.

Piontelli, R., and V. Tonolli (1964), Il tempo di residenza delle acque lacustri in relazione ai fenomeni di arricchimento in sostanze immesse, con particolare riguardo al Lago Maggiore, *Mem. Ist. Ital. Idrobiol.*, **17**: 247–266.

Valerio, G., M. Pilotti, S. Barontini, and B. Leoni (2014), Sensitivity of the multiannual thermal dynamics of a deep pre-alpine lake to climatic change, *Hydrological Processes*, in press, doi: 10.1002/hyp.10183.

# Measurements of Lake Greenhouse Gas Fluxes

E. Podgrajsek[1]*, E. Sahlée[1], A. Rutgersson[1] and D. Bastviken[2]

[1] *Department of Earth Sciences, Air, Water and Landscape Sciences*
*Uppsala University, Uppsala, Sweden*
[2] *Department of Thematic Studies, Water and Environmental Studies,*
*Linköping University, Linköping, Sweden*

**Corresponding author, e-mail eva.podgrajsek@geo.uu.se*

**KEYWORDS**
Lake fluxes; methane; carbon dioxide; eddy covariance; floating chambers; waterside convection.

## EXTENDED ABSTRACT

### Introduction

Methane ($CH_4$) and carbon dioxide ($CO_2$) are two important greenhouse gases and the knowledge of both anthropogenic and natural sources and sinks of these gases are important. Several studies, mostly using the floating chambers (FC) technique, have shown that lakes can be large sources of both methane and carbon dioxide (e.g. Bastviken et al., 2011; Cole et al., 2007). The FC method is an inexpensive and simple method used for direct flux measurements. For $CO_2$ measurements normally short sampling intervals are required, e.g. 20-40min, which makes this method labor intense. Another method that directly measures the gas flux is the eddy covariance (EC) method. This method requires expensive high frequency measuring instrumentation with high resolution. The EC flux measured will be continues and represents the flux from a relatively large upwind area (e.g. Foken, 2008).

### Materials and methods

Flux measurements presented are from lake Tämnaren in central Sweden (60°90'N, 17°20'E) which is a nutrient rich lake with a mean depth of 1.3m (maximum 2m) and an area of 38 $km^2$. Part of the high frequency water measurements where conducted in lake Erssjön in west Sweden (58°22'N, 12°09'E) which has an area of 0.07 $km^2$ and a mean depth of 1.3m (maximum 4.4m)

For more detailed descriptions of the measuring procedures and the quality of the EC data see Podgrajsek et al., (2014) and Sahlée et al., (2014).

### Results and discussion

Our EC measurement show that both $FCH_4$ and $FCO_2$ experience high nighttime fluxes for a large part of the data set ($FCH_{4night} \approx$ 300 nmol $m^{-2}$ $s^{-1}$ and $FCH_{4day} \approx$ 0 nmol $m^{-2}$ $s^{-1}$, $FCO_{2night} \approx$ 2µmol $m^{-2}$ $s^{-1}$ and $FCO_{2day} \approx$ -0.5 µmol $m^{-2}$ $s^{-1}$). For $FCH_4$ one possible interpretation is that convective mixing in the lake enhances the diffusive flux, in combination with the possibility that convection may bring methane-rich water from the bottom to the surface and trigger bubble release from the sediment (Podgrajsek et al., 2014). During 2012 $pCO_{2w}$ was measured simultaneous with $FCO_2$ and the transfer velocity could be calculated with equation. Analyzes of the transfer velocity show that convection will affect the gas transfer velocity, especially for moderate wind speeds.

During two field campaigns the gas fluxes were simultaneous measured with both the EC and the FC technique. A comparison between the EC and FC method shows that overall the

two methods yielded fluxes in the same order of magnitude. However, for some periods the discrepancy in the $FCO_2$ measurements is substantial, see Figure 1.

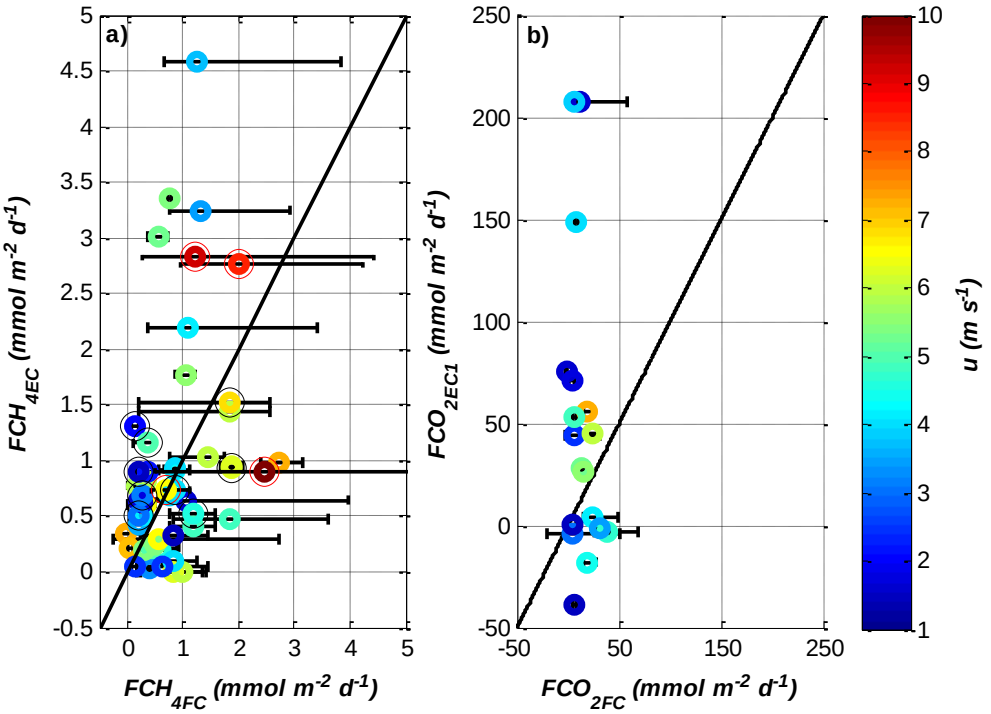


**Figure 1**. Mean values of 4-6 FCs deployed in the flux footprint compared to mean values of a) $FCH_{4EC}$ and b) $FCO_{2EC}$ during the same time. The bars represent the maximum and minimum FC measurement during one deployment. The colors in the figure show the mean wind speed during the FC deployment period. Red circles enclosing filled circles represent the four comparisons of EC2 and FC. Black open circles mark FCs with deployment time longer than 30 min. The black line shows a 1:1 relation. The total number of direct comparisons for $FCH_4$ are n=51 and for $FCO_2$ n=28

We suggest that this large discrepancy might be caused by heterogeneity of partial pressure of carbon dioxide in the EC flux footprint.

From May to September 2012 a new state of the art instrument measuring dissolved $CH_4$ was deployed together with measurements of dissolved partial pressure of $CO_2$ in lake Erssjön. These instruments give continuous measurements every half-hour showing short time dynamics of dissolved $CH_4$ and $CO_2$ previously not seen.

**REFERENCES**

Bastviken, D., L. Tranvik, and J. Downing (2011), Freshwater methane emissions offset the continental carbon sink, *Science*, **331**(6013), 50–50.

Cole, J. J., Y. T. Prairie, N. F. Caraco, W. H. McDowell, L. J. Tranvik, R. G. Striegl, C. M. Duarte, P. Kortelainen, J. A. Downing, J. J. Middelburg, and J. Melack (2007), Plumbing the Global Carbon Cycle: Integrating Inland Waters into the Terrestrial Carbon Budget, *Ecosystems*, **10**(1), 172–185, doi:10.1007/s10021-006-9013-8.

Foken, T. (2008), Micrometeorology, edited by N. C.J., Springer.

Podgrajsek, E., E. Sahlée, and A. Rutgersson (2014), Diurnal cycle of lake methane flux, *J. Geophys. Res. Biogeosciences*, **119**, 1–13, doi:10.1002/2013JG002327.

Sahlée, E., A. Rutgersson, E. Podgrajsek, and H. Bergström (2014), Influence from Surrounding Land on the Turbulence Measurements Above a Lake, *Boundary-Layer Meteorol.*, **150**(2), 235–258, doi:10.1007/s10546-013-9868-0.

# The contribution of hydraulics to a multidisciplinary study evaluating the effects of water abstraction from a high-integrity high-mountain lake for artificial-snow production

G. Rizzi[1]* and M. Cantonati[2]

[1] *CISMA Center for Engineering and Environmental Models Development, Via Malpaga 8, I-3812 Trento, Italy*
[2] *Museo delle Scienze- MUSE, Limnology and Phycology Research Unit, Corso del Lavoro e della Scienza 3, I-38123 Trento, Italy*

**Corresponding author, e-mail giuliano.rizzi@cisma.it*

**KEYWORDS**
Lakes; water quality; ecological integrity; modelling; Environmental Impact Assessment.

## EXTENDED ABSTRACT

### Introduction

The present work has been carried out in order to contribute to the Environmental-Impact Assessment of the possible water abstraction (of about 200'000 m³) for snowmaking facilities from a small high-mountain lake. Lake Ritorto is located on siliceous substratum in the Adamello-Brenta Nature Park (south-eastern Alps) at 2057 m a.s.l. of altitude, and has a volume of 111310 m³, an area of 91664 m², and very-low alkalinity waters. The lake-outlet system was under scrutiny, since the use of part of the lake water volume for artificial snow production had been proposed as an alternative to the construction of an artificial basin to use as a reservoir.

### Materials and methods

The response of the lake and the outflow stream system to this withdrawal has been investigated with a multidisciplinary approach, with contributions ranging from hydraulic issues and neo- / paleolimnology to a comparative evaluation aiming at discussing how such a project would have been evaluated in Switzerland in the light of the main legislation on the topic.

Due to the lack of meteorological data, temperature and precipitation measurements recorded by four weather stations placed on surrounding mountains and operating since 1992 had to be used for the hydrological part of the study. These data provide monthly total rain volumes with good correlation indices and deviations around 10%. Data provided by the Pradalago weather station, located at the same altitude of the lake, were considered as the main information source.

The investigation of the impact on the hydrological regime of the lake outlet, named Rio Colarin, has been carried out comparing estimates of annual natural floods obtained by using a geomorphological model and experimental formulas with the potential flow-rate that would be caused by the planned abstraction operations.

**Results and discussion**

As regards the lake, given that the estimate of the basin area performed with GIS tools is about 1'330'000 m², a rain amount of 150 mm would be needed to recharge the volume extracted. The hydraulic analyses showed that Lake Ritorto would recover the volume abstracted for the first treatment of the ski slopes only after snow melt. More precisely, the lake, after the sudden level drop due to spilling, would recover its average level not before April (statistically this would occur in the 40% of the cases) or May, depending upon climate conditions (it should be remembered that, even when deposition quantity is sufficient, lake refilling would occur only at snow melting during spring). Moreover, the hydrological recharge of the lake would be further delayed if a vital minimum flow had to be allowed for the outlet stream (it should be recalled that these freshwater environments are located in a Nature Park). Hydro-peaking in this stream would probably not have an extent greater than that of natural floods, and thermo-peaking could originate temperature waves of about 4 °C. This, however, implies that this stream would nevertheless be affected by lasting spates and occasional drying. Most importantly, the hydrological analyses also demonstrated that the proposed recharge of the lake with water pumped from the Sarca-di-Nambino stream would be virtually unavoidable, in spite of the fact that the environmental-assessment investigations demonstrated that this water doesn't meet the highest-quality standards of L. Ritorto, and that there would be an evident risk of allochthonous-microorganisms introduction.

The conclusions of the hydrological studies, suggesting severe impacts on the lake and its outflow, were mirrored and enhanced by considerations emerging from other parts of the environmental-assessment study. Both the comparison with multivariate techniques between near-natural and exploited (for hydropower purposes) lakes of the study area and the detailed paleolimnological study of two lakes showed that enhanced water-level fluctuations have clear negative effects on the micro- and macro- flora and fauna, in particular in the littoral zone. There are as well impacts on the overall functioning of these high-mountain ecosystems. Ecological and natural-history characterization showed that L. Ritorto and his outlet possessed high ecological integrity and value for biodiversity conservation. The main results of the different parts of the environmental-impact assessment all suggest that the use of water depleted from L. Ritorto would have deleterious effects on both the lake and its outlet from the ecological standpoint.

**REFERENCES**

Tomasi G. (1962), *Origine distribuzione catasto e bibliografia dei laghi del Trentino*, Museo di Storia Naturale, Trento.

Cantonati M., Tolotti M., Lazzara M. (2002), *I laghi del Parco Naturale Adamello-Brenta*, Documenti del Parco.

Strembo Tomasi G. (2004), *I trecento laghi del Trentino*, Artimedia, Trento

# Sediment resuspension within submerged model canopies under oscillatory flow

À. Ros, J. Colomer, T. Serra, D. Pujol, M. Soler and X. Casamitjana*

*Department of Physics, Campus Montilivi, Escola Politècnica Superior II University of Girona 17071 Girona (Spain)*

**Corresponding author, e-mail xavier.casamitjana@udg.edu*

**KEYWORDS**
Progressive waves, submerged aquatic vegetation, sediment dynamics, resuspension, sediment distribution.

## EXTENDED ABSTRACT

### Materials and methods

A set of laboratory experiments were conducted to study the effect of submerged aquatic vegetation in sediment resuspension under progressive waves. Three vegetation models composed of rigid, flexible and real plants (R. maritima), six wave frequencies (between F= 0.6- 1.6Hz) and four plant densities (Solid Plant Fractions, SPF between 1% 10%) were used The sediment bed properties corresponded to a salt marsh wetland, which was characterized by two sediment populations (population 1: particle diameters from 2.5 to 6.0 μm, and population 2: particle diameters from 6.0 to 100 μm).

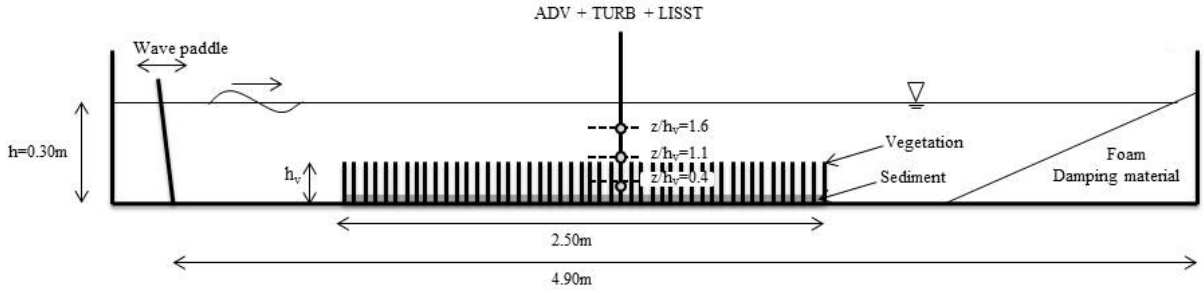


**Figure 1.** Scheme of the experimental set-up. Experiments were conducted in a 6 m long flume. The mean water depth, h, is 30 cm. The plant height in still water is $h_v$ = 14 cm. The model meadow was 250 cm long. The horizontal dashed lines indicate the position of the velocity (ADV) and sediment concentration measurements, both turbidity and particle sediment concentration (TURB+LISST).

### Results and discussion

For the rigid canopy model, in comparison to the unimpeded experiment, an increase in the turbulent kinetic energy (TKE) inside the canopy for smaller frequencies (F=0.6-1.2 Hz) was observed As a result, sediment resuspension for both sediment populations was higher than that of the unimpeded experiment however, at higher frequencies (F = 1.4 and 1.6 Hz) and higher plant densities (SPF 5%, 7.5% and 10%), the TKE inside the canopy decreases and sediment resuspension too. Therefore, surprisingly rigid vegetation at smaller frequencies acts promoting resuspension and reducing sheltering. This is due to the fact that, at higher frequencies the increase in the particle Reynolds number ($Re_w$>300) promotes TKE production.

For the flexible vegetation model in comparison with the unimpeded experiment a reduction in the TKE inside the canopy was nearly always found. Resuspended sediment concentrations were found to decrease as flexible canopy densities increased. For the flexible vegetation, $Re_w$<300, and therefore no TKE production appears. The movement of the blades absorb and dissipates the wave energy resulting in lower levels of TKE inside the flexible canopies. The real case or R. maritima behaves similarly to the flexible model.

Resuspension is controlled by the bottom shear stress (u'w'), which is normally well correlated with the TKE (Jansen and Reidenback 2012). Our results show that rigid canopies are not always effective in promoting the protection against resuspension. In Fig. 2 the cases with $\Delta C>0$ correspond to rigid canopies where resuspension is enhanced. Only a few cases for rigid canopies have $\Delta C<0$ (higher frequencies and higher SPF). On the contrary for all the flexible canopies and for the R. marina $\Delta C<0$ , indicating that flexible plants are more indicated for avoiding particle resuspension.

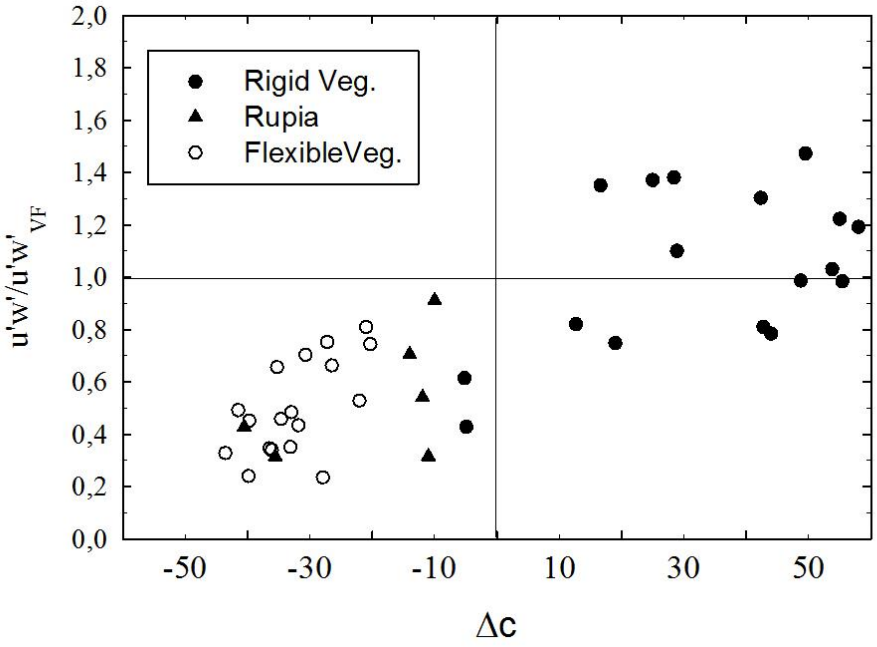


**Figure 2.** Ratio between u'w' for vegetated experiments and u'w' for the vegetation-free experiments against $\Delta C$, for experiments carried out with the three canopy models for the particles between 2.5 to 6.0 μm (A) and 6.0 to 100 μm particles (B)

**REFERENCES**

Jansen, J.C.R. and M.A. Reidenback (2012), Wave and tidally driven flows in eelgrass beds and their effects on sediment suspension, *Marine Ecology Progress series*., **448**, 271–287.

# Comparison of sea radiance coefficient spectra obtained by remote sensing in the Black, Baltic, Kara and Aral Seas

V. V. Rostovtseva*, I. V. Goncharenko, D. V. Khlebnikov and B. V. Konovalov

*P. P. Shirshov Institute of Oceanology RAS, Moscow, Russia*

**Corresponding author, e-mail vvrostovtseva@bk.ru*

**KEYWORDS**
Coastal sea waters, inland seas, sea radiance coefficient spectrum, remote sensing from board a ship, sea water admixtures concentration.

## EXTENDED ABSTRACT

Optical remote sensing from board a ship is of great importance for estimation of water content and admixtures distribution in inland seas and coastal regions of oceans. One of the most informative characteristics is the sea radiance coefficient spectrum Ro(λ) which we obtained with the special spectrophotometer developed for measuring the three values:

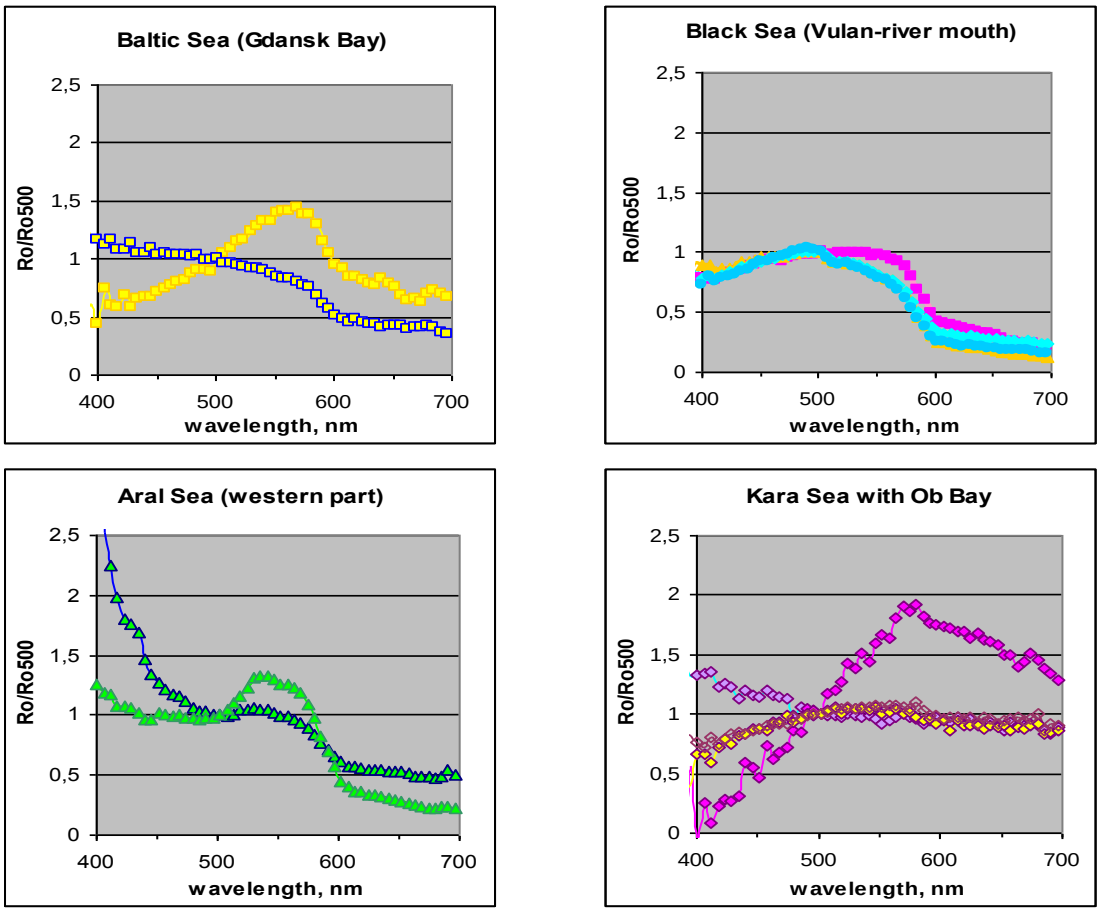


**Figure 1**. The sea radiance coefficient spectra normalized to the value of Ro(500) for the four different seas.

upward sea surface radiation, radiance of the adjacent sky area (it is the area that contributes most to the reflection part of the sea surface radiation) and radiance of the horizontal white screen (it estimates the total illumination of the sea surface). After subtracting the reflection part from the upward sea surface radiation and dividing the result by the total illumination of the sea surface we obtained the sea radiance coefficient spectra. The measurements were made from board a moving ship in four seas characterized by various water properties: in Gdansk Bay of the Baltic Sea, in the north-eastern part of the Black Sea, in the western part of the Aral Sea, in the Kara Sea including the Ob Bay. The normalized sea radiance coefficient spectra for the four seas are shown in Fig. 1.

The obtained sea radiance coefficient spectra were compared to the classification of the shelf sea waters developed for different water types and their peculiarities were explained. Comparing the types of the obtained spectra to the modeling results one can conclude that the Baltic Sea has the high content of dissolved organic matter, the Black Sea has abnormally high scattering, the Aral Sea water shows significant adsorption by some pigments though it is extremely saline and the Kara Sea differs greatly from the areas where it is similar to the open ocean waters to the areas of the river mouths with high content of dissolved organic and suspended matter.

Then the original calibration method based on the spectrum of pure sea water absorption was used to avoid the impact of different weather conditions on the explored spectra and the absorption spectra of sea water in the chosen areas of the four seas were calculated. Some examples of such conversion are shown for the Black Sea in Fig. 2. The absorption spectra allowed us to estimate the admixtures concentration and the efficiency of the suggested method in each case was discussed.

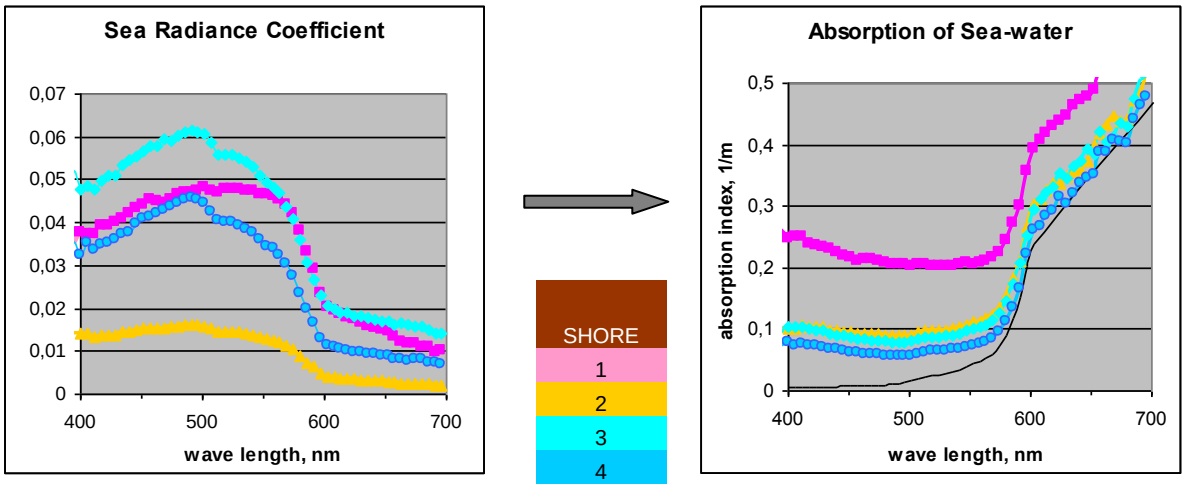


**Figure 2.** Sea radiance coefficient spectra measured in the Black Sea at windy weather and cloudiness. Absorption spectra calculated from them using the original calibration method. The colours of the curves indicate the distances from the shore where the measurements were done.

The suggested method of optical remote sensing from board a ship can be useful for sub-satellite measurements to obtain the coefficients for regional algorithms. It is also necessary for exploring the sea areas, which are too close to the coastal line or cannot be seen from satellites because of cloudiness.

# Extracting Spatial Information from Acoustic Doppler Velocity Measurements

P.J. Rusello

*Scientist, Nortek, Boston, MA, USA and Sandvika, Norway*

*e-mail pj@nortekusa.com*

**KEYWORDS**
Turbulence; coherent structures; Doppler velocity; boundary layers; singular value decomposition.

## EXTENDED ABSTRACT

### Introduction

Defining structure within a turbulent flow is a challenging but important task for fine scale processes such as sediment or larval transport. Optical methods which capture a 2D or 3D flow field, like Particle Image Velocimetry, are well suited to identification of flow structure, but are restricted to flows where optical access is not an issue.

Pulse coherent acoustic Doppler velocity profilers measure three velocity components and acoustic backscatter at a single frequency. Velocity measurements are low noise and at high spatial and temporal resolutions, making them well suited for turbulence studies in many environments. These datasets are similar to, but significantly richer than, an array of densely packed single point sensors like a hotwire rake. By using a variety of processing techniques, extracting additional information from the measurements reveals significantly more about the flow than one point statistics and mean profiles.

### Materials and methods

Taylor's Frozen Turbulence hypothesis is used to turn a rapidly sampled in time velocity profile into a velocity field in two dimensions. The along profile resolution is determined by the range cell size, while the temporal resolution times the local convective velocity determines resolution at each point in the profile. This field will typically be asymmetrically sampled on a grid with spacing on one axis determined by the profile cell size and on the other axis by the sample rate times convective velocity.

The velocity field is decomposed using the Singular Value Decomposition (SVD) (Strang, 2007). The SVD is a matrix factorization of the form:

$$A = U\Sigma V^T \quad (1)$$

where $A$ is the m x n velocity data stored in matrix form, $U$ and $V$ contain the eigenvectors of of $AA^T$ and $A^TA$ with sizes $m \times m$ and $n \times n$ respectively. $\Sigma$ is an $m \times n$ diagonal matrix with the singular values of $A$ along the diagonal.

A reduced order representation of the flow involving $k$ singular values (or modes) is obtained by

$$A_k = U_k\Sigma_k V_k^T \quad (2)$$

where the subscript $k$ indicates only the first $k$ singular values are used, i.e. columns 1-$k$ of $U$ and $V$ and rows and columns 1-$k$ of $\Sigma$. The first singular value contains the most information about the flow, the second the second most information, etc. By using a lower order (e.g. $k$ = 1) flow representation and decomposing the data matrix $A$, flow structure is revealed (Diamessis, 2010).

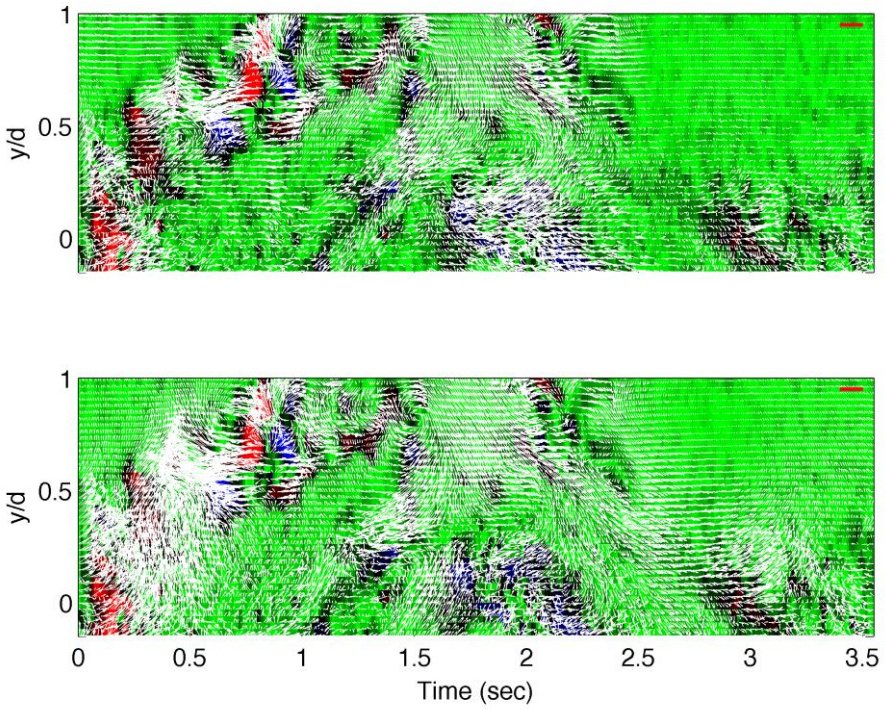


**Figure 1**. $u'$ and $v'$velocity vectors from (top) SVD decomposition overlaid on vorticity and (bottom) velocity vectors from phase decomposition overlaid on vorticity. Positive vorticity is shown in red, negative in blue.

## Results and discussion

Initial work focused on the turbulent cylinder wake. Length scales, location, and frequency of occurrence for vortices embedded within the wake were determined as a proof of concept for a flow with known regular vortex shedding. Results of the SVD decomposition were compared with a phase average decomposition of the flow field, exploiting the periodic nature of the cylinder wake for comparison (Figure 1). Both methods highlighted small scale structure within the wake, however, the phase average flow fields were typically fuzzier than the SVD fields because they represent an average of the flow, rather than an instantaneous snapshot.

Expanding on this work, two datasets in turbulent boundary layers were obtained. The first is from a laboratory open channel flow facility with measurements spanning 85% of the flow depth and a free stream velocity of 0.18 m/s, representing a smooth wall boundary layer. The second boundary layer dataset was obtained in a tidal creek at Good Harbor Beach, Gloucester, MA. The creek bed is sand with ripples forming during the periods of highest flow (mid-tide). SVD decomposition is used to identify near bed flow structure, while acoustic backscatter is used to determine if these flow structures are re-suspending sand grains.

**REFERENCES**

Strang, G. (2007), *Computational Science and Engineering*, Wellesley, MA. Wellesley-Cambridge Press.

Diamessis, P.J., R. Gurka, and A. Liberzon (2010), Spatial characterization of vortical structures and internal waves in a stratified turbulent wake using proper orthogonal decomposition, *Physics of Fluids*, **22**, 086601, http://dx.doi.org/10.1063/1.3478837.

# Large Eddy Simulation (LES) of wind-driven circulation in Lake Ledro

M. Santo[1]*, M. Toffolon[2] and V. Armenio[1]

[1] *Department of Engineering and Architecture, University of Trieste, Trieste, Italy*
[2] *Department of Civil, Environmental and Mechanical Engineering, University of Trento, Trento, Italy*

**Corresponding author, e-mail santomarco31@gmail.com*

**KEYWORDS**
Numerical Model; Turbulent Mixing; LES; Hydrodynamics; Lakes

## EXTENDED ABSTRACT

### Introduction

Lake Ledro (Trentino – Italy) is located 652 meters above the average sea level at 45.52° latitude N, with a surface of 2.1 $km^2$, a volume of $68 \cdot 10^6$ $m^3$ and a maximum depth of 48 m. It is used as a reservoir for hydropower production and, at the same time, it is one of the main touristic resources for the surrounding areas. In the recent years it has been affected by intense blooms of the harmful cyanobacterium *Planktotrix rubescens*. The algal vertical distribution depends on several factors like thermal stratification, light penetration, nutrients availability and water withdrawal. As a first step in the analysis of the influence of physical processes on the algal dynamics, we present a study of the wind-driven circulation in Lake Ledro (during summer stratification) by using a state-of-art high-definition model (LES-COAST), recently employed for the analysis of water mixing and renewal in coastal semi-closed areas (harbours).

### Numerical model

LES-COAST is a model suited to study closed or semi-closed areas and it is based on a Large Eddy Simulation (LES) turbulence closure model. It solves the three-dimensional, unsteady, filtered, non-hydrostatic, Boussinesq form of the Navier-Stokes equations. The large scales of the motion are resolved through a three-dimensional time dependent simulation, whereas the sub-grid scales (SGS) are parameterized through the Anisotropic Smagorinsky Model (ASM) described in Roman et al. (2010). The ASM requires two different eddy viscosities, one for the vertical direction and one for the horizontal direction, in order to deal with the characteristic anisotropy of the grid cells in water basins. A detailed description of the model together with the application to the study in a semi-closed bay is reported in Petronio et al. (2013). The application of the model to the study of mixing and water renewal in the Barcelona harbour is in Galea et al. (2014).

### Results and discussion

Figure 1 depicts Lake Ledro and the combination of grid topology and immersed boundaries used for discretization purposes. The frame of reference has the x-axis pointing east, the y-axis vertical pointing upward and the z-axis pointing northward and the grid has 64x32x64 points respectively. The horizontal grid spacing is on average 20 meters, whereas the grid spacing in the vertical is on average 1m.

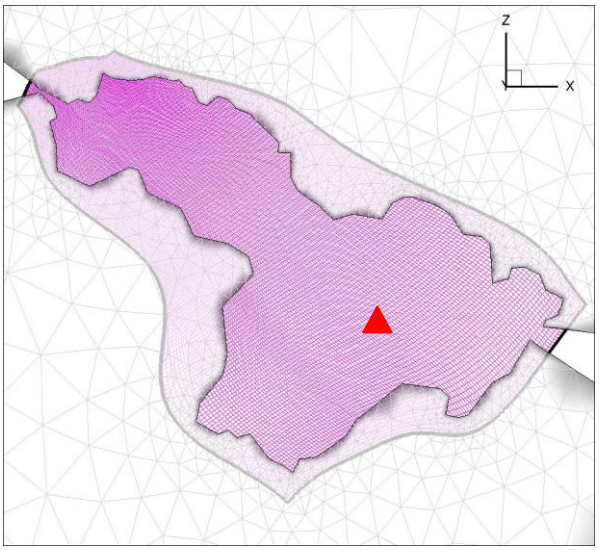


**Figure 1**. The immersed bodies used to model Lake Ledro are in gray with a gray triangular mesh; the pink grid is the discretization of the computational domain. The red triangle is the locations of the sampling point.

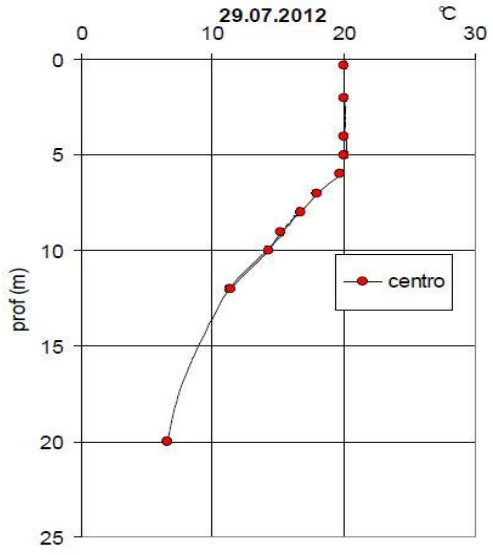


**Figure 2.** Measured temperatures at different depths on July 29 2012.

The initial temperature profile adopted is showed in Figure 2 and the wind velocity used for the simulation is 3m/s at 2.8m above the lake's surface with a direction of 315°, corresponding to one of the most frequent winds which blows in summer (Figure 3). All the data are sampled by the meteorological station located in the center of the lake (see Figure1).

The analysis will be carried out under statistical steady state conditions, thus considering a fully developed hydrodynamic field under the breeze condition here considered. At the workshop first and second order statistics will be shown. Specifically, we will show the mean three-dimensional velocity field, the spatial distribution of density anomaly turbulent kinetic energy and eddy diffusivities. The results will be also discussed in view of classical analytical theories.

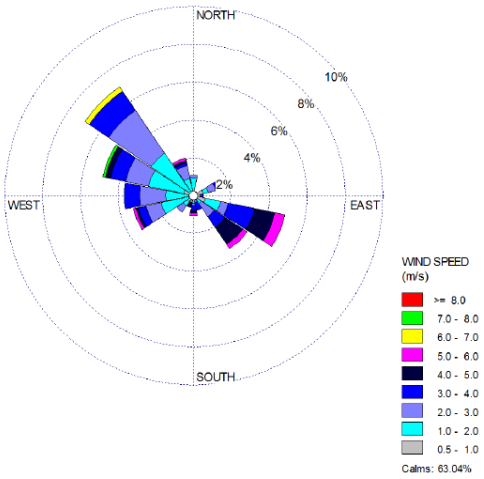


**Figure 3.** Wind rose for Lake Ledro, July 2012.

**Acknowledgments.** Wind and temperature data were measured by Fondazione Edmund Mach during the project "Quantificazione dei carichi di nutrienti ed analisi del trasporto nel lago di Ledro" funded by Provincia Autonoma di Trento.

**REFERENCES**

Roman, F., G. Stipcich, V. Armenio, R. Inghilesi, S. Corsini (2010), Large Eddy Simulation of mixing in coastal areas, *International Journal of Heat and Fluid flow*, **31**, 327-341.

Petronio, A., F. Roman, C. Nasello, V. Armenio (2013), Large eddy simulation model for wind-driven circulation I coastal areas, *Nonlin. Processes Geophys.*, **20**, 1095–1112.

Galea, A., M. Grifoll, F. Roman, M. Mestres, V. Armenio, A. Sanchez-Arcilla, and L. Z. Mangion (2014), Numerical simulation of water mixing and renewals in the Barcelona Harbour area: The winter season, *Environmental Fluid Mechanics*, accepted for publication, DOI: 10.1007/s10652-014-9351-6.

# Long term changes in thermal stratification in a deep lake: measurements from the last 45 years and predictions for the next 85 years

S. G. Schladow[1,2]*, G. B. Sahoo[1,2], A. L. Forrest[1,3], J. E. Reuter[1] and R. C. Coats[1]

[1] *Tahoe Environmental Research Center, University of California, Davis, CA, USA*
[2] *Dept. of Civil and Environmental Engineering, University of California, Davis, CA, USA*
[3] *Australian Maritime College, University of Tasmania, Launceston, TAS, Australia*

**Corresponding author, e-mail gschladow@ucdavis.edu*

**KEYWORDS**
Lakes; climate change; stratification; stability index.

## EXTENDED ABSTRACT

### Introduction

Lake Tahoe, CA-NV, is an iconic lake that has been studied for over 140 years (LeConte 1883). Continuous meteorological records exist for over 100 years, and since 1968 almost weekly profiles of the lake temperature in the upper 100m of this 501 m deep lake have been taken. Sahoo et al. (2011) documented the warming trends in the hydro-meteorological dataset (1950–2007) of the Tahoe basin showing that minimum and maximum air temperatures has increased at 0.04 and 0.02 ºC/year, respectively; timing of peak streams discharge resulting from snowmelt has shifted to earlier date at a rate of about 0.4 days/year; and the fraction of total annual precipitation falling as snow has decreased by 15-20 percent. As a result Lake Tahoe has become both warmer and more stable (Sahoo et al., 2011; Coats, 2010; Schneider et al., 2009; Stewart et al., 2005). Based on downscaled climatic projections, annual air temperature at Lake Tahoe is predicted to increase by additional 2 – 4.5 ºC, longwave radiation is predicted to increase by approximately 5 – 10 percent while wind speed is predicted to decline on the order of 7 – 10 percent by the year 2100 (Sahoo et al., 2013a).

We evaluate the long-term lake thermal data set (1968 – 2012) and the simulated lake thermal data set based on future climate trends for trends in lake thermal properties at Lake Tahoe. We utilize a simple stability index (SI) that quantifies the stratification intensity and duration.

### Materials and methods

Water temperature profiles have been regularly monitored at a site on the west shore at the 160 m isobath approximately every 10 days since 1968. A simplified stability index (SI), based on the summation of the potential energy of the upper 100 m is calculated. SI values greater than 600 kg/m$^2$ were taken to be the threshold of stratification to eliminate spurious diurnal stratification during periods of isothermy. Lake SI values are estimated using the interpolated daily temperature and conductivity profiles to estimate water column density.

For the lake stratification over the next century, Sahoo et al. (2013) estimated Lake Tahoe water temperature using the Dynamic Lake Model with Water Quality (DLM-WQ) (Sahoo et al., 2010) and spatially downscaled meteorology data (air temperature, precipitation, wind speed, longwave radiation, and solar radiation) during the 21st Century. The spatially statistically downscaled meteorology data were obtained from the coarse grid meteorological

output of the Geophysical Fluid Dynamics Laboratory Model (GFDL CM2.1) for the A2 and B1 emission scenarios (Dettinger, 2013).

## Results and discussion

The length (days) of lake stratification for the historical measurements (1968-2012) as well as the modeled GFDL A2 and B1 scenarios (2001-2098) are shown in Figure 1. The data illustrate that the general trend under the GFDL A2 scenario closely follow the historical trend. The best-fit regression line with very strong statistical correlation significance value ($p < 0.0001$) indicates the length of the stratification season may increase by 65 days in the entire 130-year, measured and modeled data set. The length of the stratification season for GFDL B1 scenario indicates that the stratification duration may increase by only 52 days in 130 years, which is proportionately lower than the historical record.

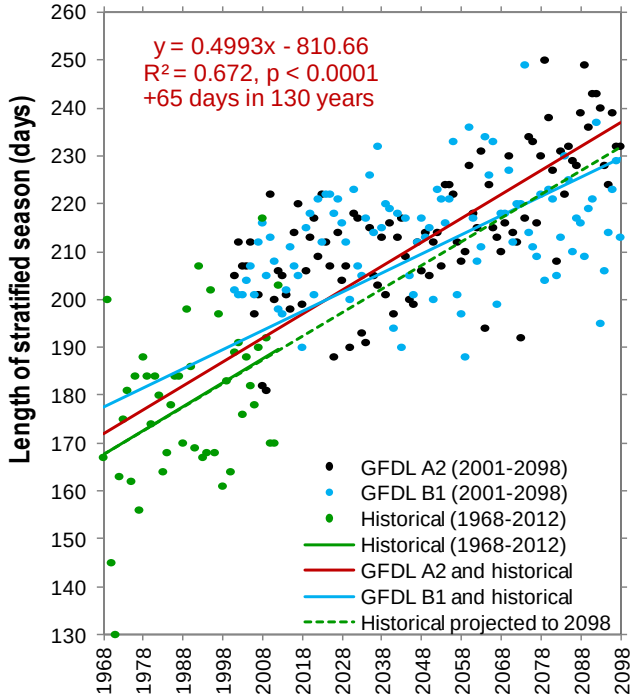


**Figure 1**. Length of stratification season for historical, GFDL A2 and GFDL B1 SRES scenarios. The solid lines show the best-fit regression trends. The broken green line represents the projected historical trend to 2098. The symbols "+" and "-" in red texts represent increasing and decreasing trend, respectively..

## REFERENCES

Coats, R. (2010), Climate change in the Tahoe basin: regional trends, impacts and drivers. *Climatic Change*, **102**, 435–466, doi:410.1007/s10584-10010-19828-10583.

Dettinger, M. (2013), Projections and downscaling of 21st century temperatures, precipitation, radiative fluxes and winds for the Southwestern US, with focus on Lake Tahoe. *Climatic Change*, **116**, 17–33.

LeConte, J. (Nov 1883), Physical Studies of Lake Tahoe.--I. *Overland Monthly and Out West Magazine* (1868-1935).

Sahoo, G.B., S.G. Schladow, and J.E. Reuter (2010), Effect of sediment and nutrient loading on Lake Tahoe (CA-NV) optical conditions and restoration opportunities using a newly developed lake clarity model. *Water Resources Research*, **46**.

Sahoo, G.B., S.G. Schladow, J.E. Reuter, R. Coats, M. Dettinger, J. Riverson, B. Wolfe, and M. Costa-Cabral (2013), The response of Lake Tahoe to climate change. *Climatic Change* **116**, 71–95, DOI 10.1007/s10584-012-0600-8.

Schneider, P., S.J. Hook, R.G. Radocinski, G.K. Corlett, G.C. Hulley, S.G. Schladow, and T.E. Steissberg (2009), Satellite observations indicate rapid warming trend for lakes in California and Nevada. *Geophysical Research Letters* **36**.

Stewart, I., D.R. Cayan, and M. Dettinger (2005), Changes toward earlier streamflow timing across western North America. *Journal of Climate* **18**, 1136–1155.

# Observation on Aeration Plumes in Homogeneous and Two-layer Stratified Water columns

B.S. Shiau[1]*,[2] and H.F. Lai[2]

[1] *Institute of Physics, Academia Sinica, Taipei, Taiwan,*
[2] *Department of Harbour and River Engineering, National Taiwan Ocean University, Keelung, Taiwan*

**Corresponding author, e-mail bsshiau@gate.sinica.edu.tw*

**KEYWORDS**
Aeration; bubble plume; two-layer stratified water column; air bubble intrusion

## EXTENDED ABSTRACT

### Introduction

The low concentrations of dissolved oxygen in water columns are often encountered for many rivers and breeding fishery farms in Taiwan, especially in the summer season. It is disadvantageous and harmful for river ecosystem and breeding fishery farms. As known it has many applications over years for the bubble plumes in oceanic, hydraulic, or environmental engineering. For example: bubble breakwaters, anti-freeze in harbor, bubble curtains for the oil slick on water surface, and de-stratification system that is to introduce aeration to inhibit eutrophication as improving water quality. To solve the problem of low concentrations of dissolved oxygen in water columns to improve the water quality, aeration will be an effective and economic method. The aeration devices placed at the river bed or breeding fishery farm bed form the bubble plumes. To understand the bubble plumes behavior under different air flow discharge rates and ambient water columns will be helpful for designing placement and control of the aeration devices in such cases.

### Experimental set-up

The experiments were conducted in the water tank of 60 cm by 60 cm with 50 cm in length. The air source was paced at the bottom center of the tank. A porous wood with a length of 5 cm and width of 0.5 cm was used bubble maker. This line source is to generate a two dimensional bubble plume. The flow rate of air was measured and controlled by employing the OMEGA FL-1443G flow meter. Water density was measured by using the KENEK MK-206 conductivity probe that was with a range of 300 ppm to 30000 ppm. The CCD (Charged Couple Detector, Oscar OS-40D, Light resolution of 0.02 Lux) was applied to grab the bubble plume images. The PVR image card of Digital Processing System Inc. was used to digitize the grabbed images. The resolution for each frame of image was 720 x 480 pixels. And the sampling rate for the image was 30 frames per second.

### Results and discussion

1. *The bubble plume in the homogeneous density of water column*

Observation of the averaged images of bubble plumes with the dimensionless discharging rate $M$=3.23x10$^{-6}$ in different densities (1.0000 g/cm$^3$, 1.0349 g/cm$^3$, 1.0555 g/cm$^3$) of the homogeneous water columns were shown in Figs.1. The image of bubble plume in fresh water (1.0000 g/cm$^3$,) shown in Fig. 1 had exhibited the similar bubble structure as that of Wilkinson (1979) who obtained in the homogeneous fresh water. The bubble plume reached

the water surface and spread laterally. Results show that increase of ambient water column density if favorable to growth of the bubble plume width. Such observational results are similar with results obtained by Sato and Sato (2001).

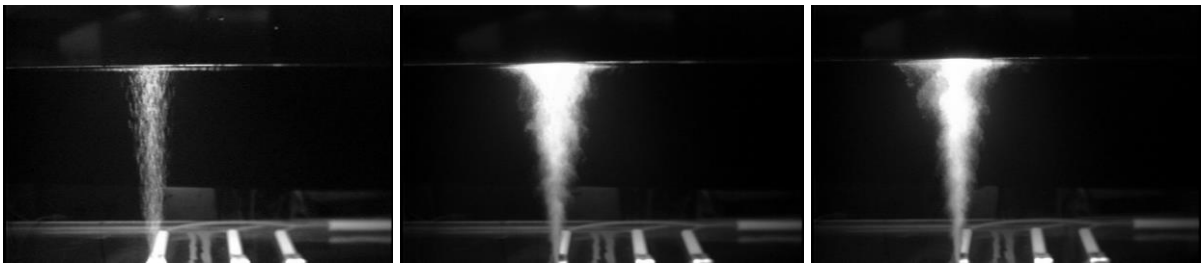

**Figure 1.** Averaged image of bubble plume in the homogeneous of water; Figure from left to right is with water column density 1.0000 g/cm$^3$ , 1.0349 g/cm$^3$, and 1.0555 g/cm$^3$, respectively.

## 2. *The bubble plume in the two-layer density stratification of water column*

The averaged images of bubble plume for dimensionless discharging rate $M$=3.23x10$^{-6}$ in different two-layer density stratifications ( $K_2 = \rho_{lower} - \rho_{upper} / \rho_{upper}$ , $K_2$=0.016, 0.034, 0.055) are shown in Fig. 2. The water depths of two layers are the same in three cases. From the images shown in these figures, an intrusion is clearly seen around the interface of the two different density layers. In the density interface region, the upper layer water strongly mixed with the lower layer water. And the bubble plume forms a mushroom shape around the two-layer interface. The density stratification in water, especially in the density interface, generally inhibits the bubble plume to go upward. And the inhibition causes the plume spread laterally around the local region of density interface. The lateral spread of the bubble plume forms the intrusion. The stronger the inhibition becomes, the wider the intrusion width is.

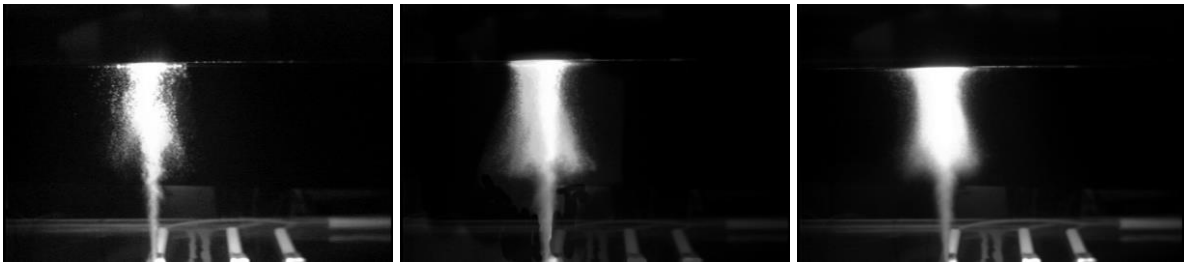

**Figure 2.** Averaged image of bubble plume in the two layer density stratifications for discharging rate $M$=3.23x10$^{-6}$. Figure from left to right is with density stratification $K_2$=0.016, $K_2$=0.034, and $K_2$=0.055, respectively.

## 3. *Interaction of two bubble plumes*

The images shown in Fig. 3 revealed the flow circulation region existed between two bubble plumes under the water surface for homogeneous and two-layer density stratification ambient water columns.

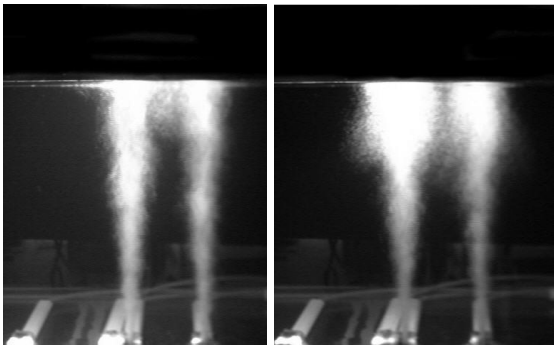

**Figure 3.** Averaged image of two bubble plume interaction for the width of bubble plume larger than the space of two sources. Left figure: in homogeneous water column. Right figure: in two-layer density stratification of water column.

**REFERENCES**

Sato, K. and T. Sato (2001), A study on bubble plume behavior in stratified water, *J. Marine Science and Technology*, **6**, 59-69.

Wilkinson, D.L. (1979), Two-dimension bubble plume, *J. Hydralic. Div., ASCE*, **105**(HY2), 139-154.

# Double Diffusion in Lake Kivu and Direct Numerical Simulations

T. Sommer[1,2]*, J.R. Carpenter[1,4] and A. Wüest[1,3]

[1] *Eawag, Surface Waters - Research and Management, Kastanienbaum, Switzerland*
[2] *Institute of Biogeochemistry and Pollutant Dynamics, ETH Zurich, Zurich, Switzerland*
[3] *Physics of Aquatic Systems Laboratory - Margaretha Kamprad Chair of Environmental Science and Limnology, ENAC, EPFL, Lausanne, Switzerland*
[4] *Institute for Coastal Research, Helmholtz Zentrum Geesthacht, Geesthacht, Germany*

**Corresponding author, e-mail tobias.sommer@eawag.ch*

**KEYWORDS**
Double diffusion, Lake Kivu, flux laws, interface, microstructure.

## EXTENDED ABSTRACT

### Introduction

The diffusive type of double diffusion occurs in oceans and lakes where both temperature and salinity increase with depth, creating staircase-like structures with nearly homogeneous mixed layers separated by thin high-gradient interfaces. Quantifying the vertical fluxes through such staircases is important, in particular in the Arctic Ocean, where double-diffusive heat transport contributes to the melting of the overlying ice. Direct Numerical Simulations (DNS) and microstructure measurements are two independent methods of predicting double-diffusive fluxes. By performing DNS under similar conditions as found in our measurements in Lake Kivu, we are able to compare results from both methods for the first time.

### Materials and methods

During two field campaigns to Lake Kivu (East Africa, surface area of 2300 $km^2$ , maximum depth of 485 m and volume of 550 $km^3$) (Descy et al. 2012) in 2010 and 2011, we measured 225 microstructure profiles of temperature and conductivity with a Vertical Microstructure Profiler manufactured by Rockland Scientific International. Double-diffusive staircases are found below ~100 m depth containing up to 300 interfaces and mixed layers. An algorithm was used to extract the temperature $T$ and salinity $S$ (both properties expressed in density units in the following) characteristics of 9,401 interfaces and adjacent mixed layers from the temperature and conductivity profiles (Sommer et al. 2013b).

For the DNS we simulate a two-dimensional (2-D) incompressible Boussinesq fluid assuming a linear equation of state (Winters et al. 2004). The domain size of the simulation is 66 cm (horizontal) x 33 cm (vertical) with an evenly grid spacing $\leq$ 0.64 mm. At simulation start an interface with two adjacent mixed layers is constructed by horizontally uniform hyperbolic tangent profiles with initial interface thicknesses $h_T = h_S = 3$ cm. Periodic boundary conditions are used on all boundaries. The interface and mixed layer structures of the DNS are evaluated in the same way as the ones measured in Lake Kivu.

### Results and discussion

A qualitative comparison between DNS and Lake Kivu profiles (Fig. 1) shows that the DNS successfully reproduces the double-diffusive structures observed in Lake Kivu. For example at $R_\rho = \Delta S/\Delta T \approx 2$ ($\Delta T$, $\Delta S$ in density units), $S$ interfaces are either extremely thin ($h_S$ = 4 mm and 2.3 mm in Figs 1d,j, respectively) or they contain very thin mixed regions (Figs.

1e,k), whereas for $R_\rho \approx 6$, interfaces are thicker and they are dominated by a diffusive core (green band in Fig. 1b) which contains linear gradients in $T$ and $S$.

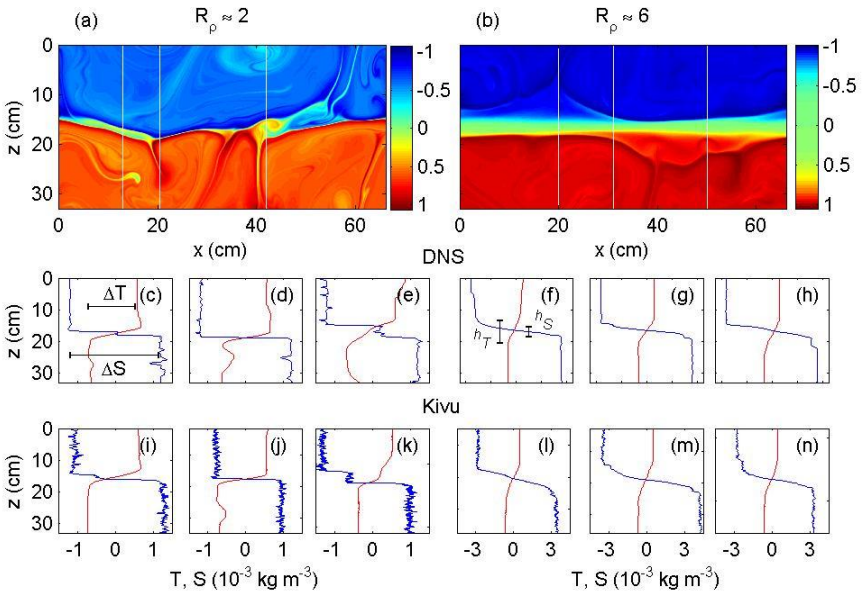


**Figure 1**. Comparison of DNS and Lake Kivu interfaces and mixed layers for $R_\rho \approx 2$ (left) and $R_\rho \approx 6$ (right). The colors in (a) and (b) (note the different scales) represent the density field (normalized with respect to the mean density and the maximum density difference) and the vertical lines indicate the positions of the $T$ (red) and $S$ (blue) profiles shown in (c) - (h) in the same order. Examples of matching Lake Kivu interfaces are shown in (i) to (n).

From our measurements of the interfacial gradients in both the DNS and Lake Kivu we estimate molecular heat fluxes through interfaces and compare their mean values to the mean total heat flux in the DNS for five simulations with $R_\rho = 2, 3, 4, 5, 6$. The agreement between total and molecular fluxes of the DNS is within 10% for $R_\rho \geq 3$ and we thus expect the total fluxes to be well represented by molecular fluxes through the interfaces. The deviations observed at $R_\rho \approx 2$ are probably caused by the 2-D limitation of the DNS and an increasingly turbulent interface. Molecular heat fluxes through interfaces in Lake Kivu agree within 38% to the DNS flux estimates for the entire range of $R_\rho$.

A popular heat flux parameterization by *Kelley* [1990] underestimates the total heat flux in the DNS by a factor of 1.3 to 2.2. However, a correction factor of 1.6, which was suggested by Sommer et al. (2013a) and is based on a modification in the Rayleigh to Nusselt number scaling, compensates for most of the observed difference.

Despite the limitations of the DNS (e.g. small domain size, 2-D) the small-scale interface structures measured in Lake Kivu were reproduced surprisingly well for $R_\rho \geq 3$. Whether the comparison also holds for double-diffusive staircases in the Arctic is an open question and should be addressed by extended simulations and detailed *in-situ* measurements in the future in order to obtain reliable estimates for the vertical heat transport in the Arctic Ocean.

**REFERENCES**

Descy, J.-P., F. Darchambeau, and M. Schmid, eds. (2012), *Lake Kivu: Limnology and Biogeochemistry of a Tropical Great Lake*. Aquatic Ecology Series 5, Springer Science+Business Media B.V., 190 pp.

Kelley, D. E. (1990), Fluxes through diffusive staircases: a new formulation. *J. Geophys. Res.*, **95**, 3365–3371.

Sommer, T., J. R. Carpenter, M. Schmid, R. G. Lueck, M. Schurter, and A. Wüest (2013a), Interface structure and flux laws in a natural double-diffusive layering. *J. Geophys. Res. Ocean.*, **118**, 6092–6106.

Sommer, T., J. R. Carpenter, M. Schmid, R. G. Lueck, and A. Wüest (2013b), Revisiting microstructure sensor responses with implications for double-diffusive fluxes. *J. Atmos. Ocean. Technol.*, **30**, 1907–1923.

Winters, K. B., J. A. MacKinnon, and B. Mills (2004), A spectral model for process studies of rotating, density-stratified flows. *J. Atmos. Ocean. Technol.*, **21**, 69–94.

# Towards the prediction of the starting point and expansion of phytoplankton blooms in shallow urban lakes

F. Soulignac[1]*, B. J. Lemaire[1,2], B. Vinçon-Leite[1], B. Tassin[1] and I. Tchiguirinskaia[1]

[1] *Laboratoire Eau Environnement Systèmes Urbains (LEESU)*
*Ecole des Ponts ParisTech (ENPC), Champs-sur-Marne, France*
[2] *AgroParisTech, Paris, France*

**Corresponding author, e-mail frederic.soulignac@leesu.enpc.fr*

**KEYWORDS**
Hydrodynamics; biogeochemistry; high frequency measurements; 3D modelling

## EXTENDED ABSTRACT

### Introduction

The eutrophication of shallow lakes in densely populated areas hinders their usages, including outdoor activities and bathing. The main disturbance is due to the proliferation of phytoplankton, especially of toxic species. Studies showed that hydrodynamics plays an important role in phytoplankton growth in shallow lakes (Pannard et al., 2011). Furthermore, measuring equipment improvements make it possible to measure current speed in such low energy environments, as well as chlorophyll-a fluorescence at high frequency. In parallel, 3D hydrodynamic and biogeochemical models have been developed. The coupling of these two types of models was successfully performed in large and deep lakes (*e.g.* Chanudet et al., 2012) but for shallow lakes, current velocity does not belong to the simulated variables compared with field data (Wu and Xu, 2011). Our objective is to calibrate a 3D hydrodynamic model and a biogeochemical model using high frequency data. This model will then be used in order to predict the location of the onset of phytoplankton proliferations and their expansion, and more precisely to disentangle the roles of nutrient resuspension due to wind and of the external nutrient loading by stormwater input.

### Materials and methods

Our study site is Lake Créteil, a sand-pit lake (40 ha, mean depth 4.5 m, maximum depth 5.5 m) situated 10 km south-east of Paris, France. Meteorological variables (solar radiation, wind speed and direction, air temperature, relative humidity, atmospheric pressure and precipitations), profiles of current velocity over 3 m, water temperature at five depths (0.5, 1.5, 2.5, 3.5 and 4.5 m) and chlorophyll-a fluorescence at two depths (1.5 and 2.5 m) have been measured in the deepest region of the lake. Water temperature and chlorophyll-a fluorescence have also been measured at two other locations, 150 m North and South of the central monitoring buoy, the former at three depths (1.5, 2.5 and 3.5 m) and the latter at 1.5 m depth. Data have all been recorded every 30 s since May 2012. Concentrations of nutrients (nitrate and phosphate) and vertical profiles of four families of phytoplankton (diatoms, green algae, cyanobacteria and cryptophyta) have been measured once a month since 2012. Between June 2013 and January 2014, the discharge from the stormwater inlet, the major inflow to the lake, was measured, as well as nutrient concentrations during six rainfall events of different intensities. The water level has been measured four times per day since 2012.

We present the first setup of the 3D hydrodynamic model Delft3D-FLOW (Deltares, 2013) and the water quality model DELWAQ (Deltares, 2014) applied to such a small lake. The domain was built using 1148 Cartesian grids of 20 m edgewise to mesh the surface of the lake and 18 vertical layers. The water temperature and the three components of water velocity were simulated. The Manning formulation was used to compute the bottom shear stress. Reynolds stresses were modelled using the k-ε turbulence model. The available high frequency meteorological data were used to force the model. Calibration coefficients were determined by a trial and error process as in Chanudet et al. (2012) and were consistent with literature values. Diatoms, green algae, ammonium, nitrate, phosphate and silicate were then modelled in coupled biogeochemical simulations.

## Results and discussion

The 3D hydrodynamic model was calibrated and verified during two one-month periods presenting each a sequence of thermal stratification, mixing and cooling. The vertical profiles of current velocity and water temperature are well reproduced by the model (RMSE = 0.007 $m.s^{-1}$ and 0.2 °C, see Fig. 1.A and 1.B). The variation of the water level, total net radiation, onset and end of thermal stratification, horizontal heterogeneities of water temperature (up to 2 °C) and the internal waves (periods of around 17 h) are also well simulated. The biogeochemical model DELWAQ was also calibrated. First results showed that the model reproduces well the fluorescence peaks (RMSE = 3.2 $\mu g.L^{-1}$, see Fig. 1.C).

In Lake Creteil, peaks of chlorophyll-a greater than tens of $\mu g.L^{-1}$ often took place during the first days of thermal stratification periods when maximal horizontal heterogeneities of water temperature were observed. Results of hydrodynamic simulations also show that high bottom shear stress occurs in the North-West of the lake. The internal nutrient loading caused by sediment resuspension will be compared to the external loading by the storm-water inlet and we will use the model to identify the areas of warmer temperature and higher nutrient concentration where phytoplankton blooms are expected to start.

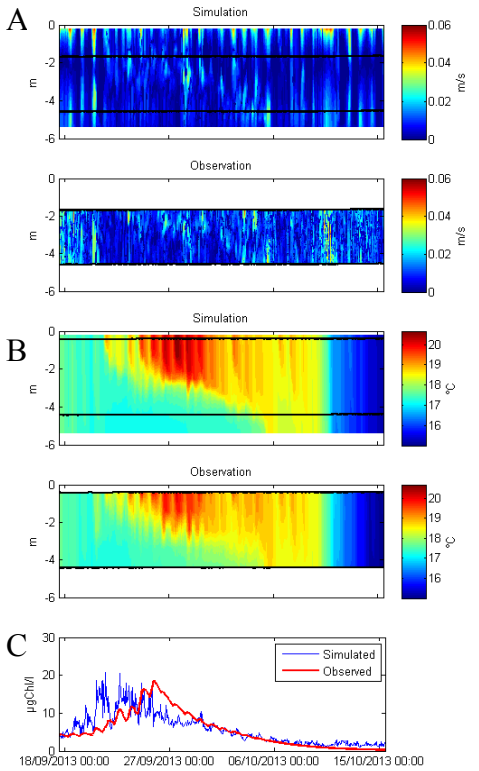


**Figure 1**. Comparison between simulated and observed profiles of current velocity (A), water temperature (B) and chlorophyll-a fluorescence at -1.5 m (C) at the central monitoring buoy. The horizontal lines indicate the limits of the measuring range along the vertical.

**Acknowledgements**. Experimental and modelling activities are supported by KIC-Climate 'Blue Green Dream' and R2DS (Ile de France) 'PLUMMME' projects.

## REFERENCES

Chanudet, V., V. Fabre, T. van der Kaaij (2012), Application of a three-dimensional hydrodynamic model to the Nam Theun 2 Reservoir (Lao PDR), *Journal of Great Lakes Research, 38(2), 260-269*

Deltares (2013), Delft3D-FLOW user manual

Deltares (2014), DELWAQ user manual

Pannard, A, B. E. Beisner, D. F. Bird, J. Braun, D. Planas and M. Bormans (2011), Recurrent internal waves in a small lake: Potential ecological consequences for metalimnetic phytoplankton populations, *Limnology and Oceanography, Fluids and Environements*, 1, 91-109.

Wu, G., Z. Xu (2011), Prediction of algal blooming using EFDC model: Case study in the Daoxiang Lake, *Ecological Modelling, 222(6), 1245-1252*

# Forecasts of global temperatures from statistical methods and global circulation models

A. Stips*, D. Macias and E. Garcia-Gorriz

*European Commission, Joint Research Center, Institute for Environment and Sustainability, Water Research Unit, Via E. Fermi, 2749, TP272, I-21027, Ispra, Italy.*

**Corresponding author, e-mail adolf.stips@jrc.ec.europa.eu*

**KEYWORDS**
Climate change; forecasting; anthropogenic forcing; multidecadal climate variability.

## EXTENDED ABSTRACT

### Introduction

During the past five decades, global air temperatures have been warming at a rather high rate (IPCC-2013) resulting in scientific and social concern. This warming trend is observed in field and model data and affects both air temperatures over land and over the ocean. However, the warming rate changes with time and this has led to question the causes underlying the observed trends. Here, we will analyze recent measured and modeled data on global mean surface air temperature anomalies (GMTA) covering the last 160 years using spectral techniques. The results from this analysis will then be used for statistical forecasting.

### Materials and methods

Data analysis and forecasts should be founded on a method that is both objective and non-parametric, in order not to depend a priori on the choice of the included or excluded processes. Singular spectrum analysis (SSA) is a methodology specifically designed to extract information from noisy time series and is analogous to apply an extended empirical orthogonal function analysis to successive lags of a univariate time series. The particular SSA used here was the *Rssa* package of the statistical software **R**, available from the Comprehensive R Archive Network (CRAN, http://cran.r-project.org/). SSA allows the decomposition of the time series into a sequence of elementary patterns of dynamics that are classified as either trends (ST) or oscillatory patterns (MDV). Bootstrapping basically means to take repeated (we choose 10000) random subsamples (bootstrap samples) from the sample time series, to perform the SSA on these subsamples and to compute their mean and variance.

Mean surface air temperature anomalies were obtained from the HadCRUT4 dataset available at http://www.cru.uea.ac.uk/cru/data/temperature/ (data downloaded on 01/2014), From the over 50 models that contributed to the CMIP5 modeling exercise, we extracted only models that fully cover at least the period from 1850 to 2100 and have an ensemble average derived from at least 3 repeated runs. All model data were downloaded on November 27, 2013, from the KNMI Climate Explorer (http://climexp.knmi.nl/). We focus here on the data from the EC-EARTH model, belonging to the most skilled models.

### Results and discussion

The spectral analysis of the HADCRUT4 data shows two major signals (Fig. 1, Left), a strong secular trend (ST) and a clear multidecadal sinusoidal oscillation (MDV) that seems to resemble the Atlantic Multidecadal Oscillation (AMO).

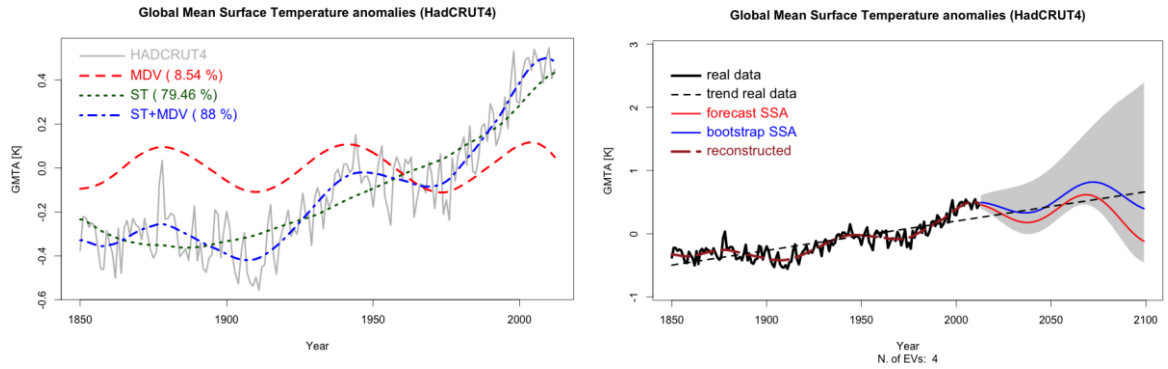


**Figure 1**. Left: Singular Spectrum Analysis of the HADCRUT4 time series. Right: Forecasted global surface temperatures from 2013 until 2100 based on the obtained two major climate signals.

The observed acceleration of the warming during the period from 1970 to 2000 appears to be caused by a superimposition of anthropogenic-induced warming (~60%) with the positive phase of a multidecadal oscillation (~40%). The recent slowdown (hiatus) of this tendency is likely due to a shift in the MDV phase. We forecast future global temperatures based only on the 2 identified main signals (4 eigenvectors). In these 87-year forecasts (Fig. 1, Right) periods of cooling alternate with periods of enhanced warming. The bootstrap method results in a forecasted temperature anomaly of +0.39 $^{o}$C [-0.47 - +2.46] in 2100.

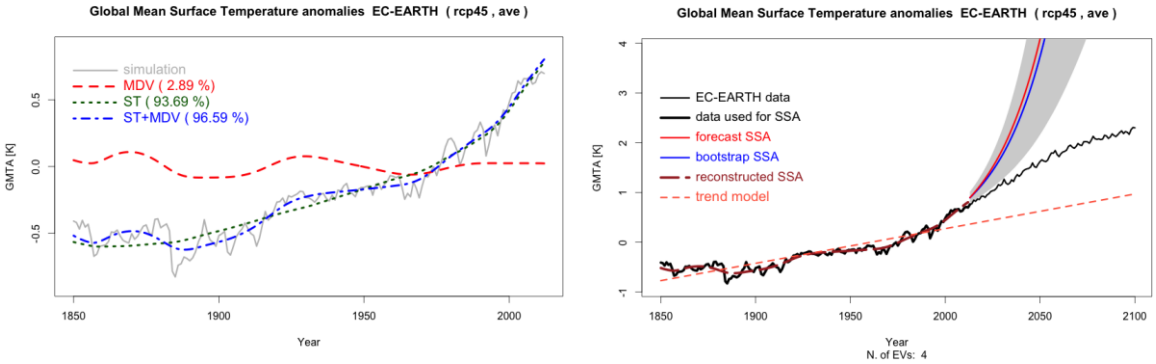


**Figure 2**. Left: Singular Spectrum Analysis of the EC-EARTH historical time series. Right: Forecasted global surface temperatures from 2013 until 2100 based on the obtained two major climate signals.

Most current generation global circulation models (CMIP5) capture the trend component but do not reproduce the MDV (Fig. 2, Left) and are missing the actual temperature hiatus. Using the same methodology, based on the first 4 eigenvectors, for temperature forecasting continues the strong trend component without the MDV and therefore results in exaggerated warming until 2100 for all models. As an example, the forecast for the EC-EARTH model beginning in 2013 results in an unrealistic warming already in 2050 (Fig. 2, Right). Therefore, it is less likely that these models could correctly forecast the temperature evolution during the coming decades.

We propose, for more realistic forecasts, to use the climate dynamics that is inherent in the GMTA data to obtain statistical forecasts of surface temperatures until 2100. These forecasts, based on the analyzed secular trend and the multidecadal oscillations are indeed capable of reproducing the actual hiatus and generally result, in comparison to CMIP5 forecasts, in much lower temperature increases for 2100 of only about +0.5 $^{o}$C. Global mean air temperatures could be even decreasing for the next 2-3 decades. Henceforth, for a correct assessment of the anthropogenic-induced warming of the global air temperatures in the future natural multidecadal temperature oscillations should be taken into account.

# Deepwater renewal by downwelling in the South Basin of Lake Baikal from 2000 to 2013

C. Tsimitri[1,2], N. M. Budnev[3], B. Rockel[4], A. Wüest[1,5] and M. Schmid[1]*

[1] *Surface Waters – Research and Management, Eawag, Kastanienbaum, Switzerland*
[2] *Institute of Biogeochemistry and Pollutant Dynamics, Dept. of Environmental Sciences, ETH Zurich, Switzerland*
[3] *Applied Physics Institute, Irkutsk State University, Irkutsk, Russia*
[4] *Institute of Coastal Research, Helmholtz-Zentrum, Geesthacht, Germany*
[5] *Physics of Aquatic Systems Laboratory, Margaretha Kamprad Chair, EPFL-ENAC-IIE_APHYS, Lausanne, Switzerland*

**Corresponding author, e-mail martin.schmid@eawag.ch*

**KEYWORDS**
Lake Baikal; deepwater renewal; downwelling; thermobaric instability.

## EXTENDED ABSTRACT

### Introduction

In the deepest layers of the South Basin of Lake Baikal (maximum depth 1461 m), sudden drops of temperature of up to a few tenths of a degree in the deepest layers of the basin have been regularly observed. These result from intrusions of cold water masses stemming from the surface layers of the lake. These intrusions are relevant for supplying oxygen to the deepest layers of the water column. One of these events that occurred in 2007 was analysed by *Schmid et al.* (2008) who concluded that the deepwater renewal had been caused by wind-driven coastal downwelling due to Ekman transport towards the steep northern shore of the South Basin. If surface water that is slightly colder than the deepwater of the lake is pushed down sufficiently deep, its density exceeds that of the surrounding water and it can subsequently plunge down to the deepest reaches of the basin. The typical volumes of these downwelling events have been estimated to 30 – 60 $km^3$ based on heat balance calculations. Our initial hypothesis for the study is that all observed sudden drops of temperature were caused by the same mechanism as described for the 2007 event.

### Materials and methods

We evaluated 13 years of temperature and current data obtained from moorings installed in the South Basin of Lake Baikal. The wind field over the lake was derived from a regional climate model and used to calculate Ekman transport towards the northern shore of the South Basin.

### Results and discussion

Between March 2000 and March 2013 altogether 13 cold intrusions were observed in the deepwater of the South Basin of Lake Baikal. The analysis shows three different types of events: (i) six winter events triggered by wind-driven coastal downwelling taking place at the vicinity of the monitoring site just before the complete ice cover of the lake, including the event analysed by *Schmid et al.* (2008); (ii) three events observed while the lake was ice covered which were most probably triggered by the same mechanism as the winter events, at an area of the South Basin different to the monitoring site; (iii) four spring events observed

just after the ice break-up which show no correlation with the wind conditions over the lake and whose causes remain unclear. The three different types of events are marked in Figure 1.

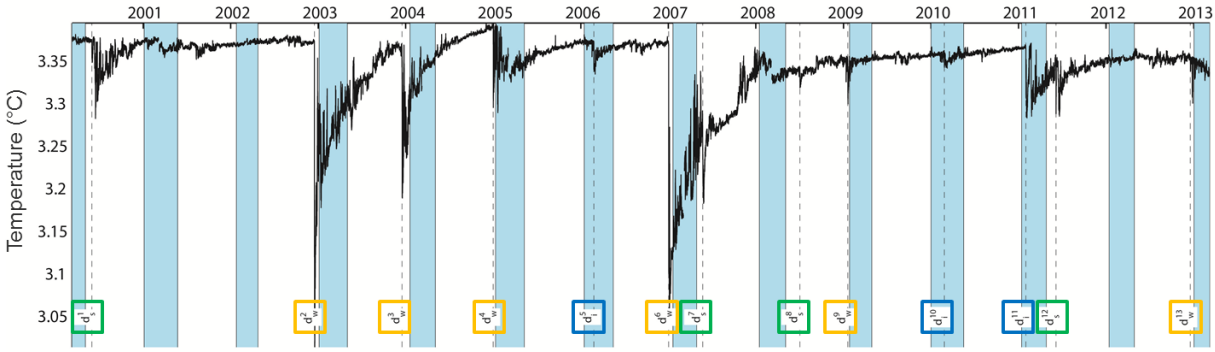


**Figure 1**. Time series of temperature observed at the bottom of the mooring installed in the South Basin of Lake Baikal, at a depth of 1360 m. The vertical lines indicate the 13 observed cold intrusion events. The winter events are marked with orange boxes, the under-ice events with blue boxes, and the spring events with green boxes. The shaded blue areas mark the dates of ice-cover at the monitoring station.

By calculating the Ekman transport for the period before the onset of ice cover for all years, we were able to differentiate between the years with and without coastal downwelling events. The analysis showed that downwelling events were usually observed following periods of a few continuous days of strong Ekman transport, whereas in years with a similar but less concentrated cumulative Ekman transport, no intrusions occurred. This is exemplified in Figure 2 for the years 2001 and 2002. We thus can predict whether downwelling is taking place by analysing the wind pattern over the lake during the time when water surface temperatures are favourable to induce a downwelling event.

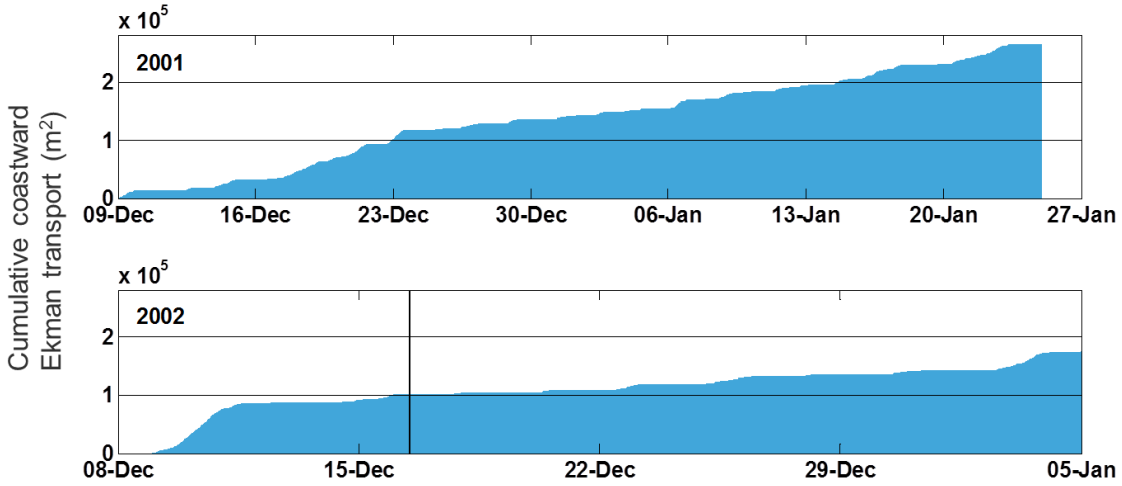


**Figure 2**. Cumulative Ekman transport calculated for the period when lake surface temperatures were favourable for downwelling before ice cover in the years 2001 and 2002. The vertical line indicates the downwelling event observed in December 2002.

**REFERENCE**

Schmid, M., N.M. Budnev, N.G. Granin, M. Schurter, M. Sturm, and A. Wüest (2008), Lake Baikal deepwater renewal mystery solved, *Geophysical Research Letters*, **35**, L09605.

# Degeneration of internal Kelvin wave in a continuous two-layer stratification using DNS

H. Ulloa[1]*, K. Winters[2,3], A. de la Fuente[1] and Y. Niño[1,4]

[1] *Department of Civil Engineering, Universidad de Chile, Chile*
[2] *Scripps Institution of Oceanography, University of California, CA, USA*
[3] *Mechanical and Aerospace Engineering, University of California, San Diego, USA.*
[4] *Advanced Mining Technology Center, Universidad de Chile, Chile*

**Corresponding author, e-mail: hulloa@ing.uchile.cl*

**KEYWORDS**
Internal Kelvin waves; stratified lakes; nonlinear degeneration; turbulent patches.

## EXTENDED ABSTRACT

### Introduction

Nonlinear processes that transfer energy from large scales to smaller scales cause the degeneration of large-scale internal gravity waves. These processes play an important role in the emergence of turbulence as well as in the transport of physical quantities through the fluid, such as tracers, mass, momentum, heat, etc. (Wüest & Lorke, 2003; Ivey et al., 2008)

Our goal is to explore the short-term evolution of the gravest internal Kelvin wave in terms of its initial available potential energy, in a rotating cylindrical basin with a continuous two-layer stratified fluid (see Fig. 1), via direct numerical simulations. First, we have used the density interface structure of the Kelvin wave, $\eta_i(t,\bar{x})$, derived by Csanady (1967), to obtain its linear 3D velocity and density fields in a continuous two-layer stratification. For this, we have introduced the length scale $\delta_i \geq 0$, which defines the thickness of a transition layer in the density interface. Then, a vertical diffusion process has been imposed on the density and velocity field to construct continuous and smooth fields in the vertical component of the Kelvin wave. In the case of Csanady (1967), this length scale is $\delta_i = 0$. Second, six (6) 3D direct numerical simulation, in a Boussinesq fluid, have been performed to compute the free evolution of the Kelvin wave, starting from a linear damped regime until a laminar-turbulent transition flow is achieved. The study is focused in the processes involved in the degeneration of the basin-scale internal waves, and their effects on the spatial-temporal distribution of the turbulence and the mixing regimes.

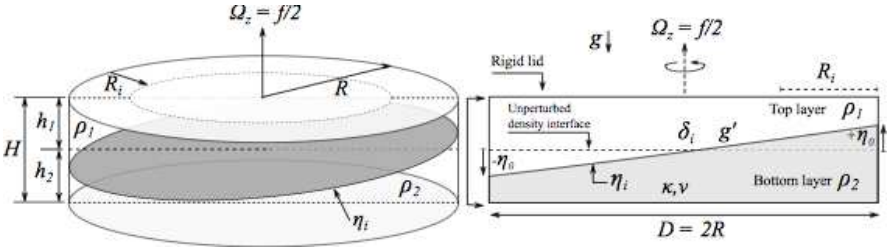


**Figure 1**. Schematic of conceptual model.

### Method

After the initial condition (defined by a gravest internal Kelvin wave), the flow motion is computed by the numerical solution of the momentum, continuity and mass transport equations in the Boussinesq sense, following a hyper viscosity/diffusivity approach on the momentum and mass transport equations, of order 3, using a spectral numerical model

(Winters and de la Fuente, 2012) based on the expansion of the dependent variables in even or odd Fourier series. The free-slip and no-flux boundary conditions are employed to solve the governing equations in the physical domain described in Fig. 1.

**Results and conclusions**

Fig. 2 exhibits a summary of the Kelvin wave evolution that has been classified into four dynamic regimes, called: damped linear (DLR), nonlinear (NLR), nonlinear/non-hydrostatic (NHR), and laminar-turbulent transition (TR). The first three regimes have been analysed in previous numerical and laboratory works; we have focused the analysis in the TR. The main characteristic of the TR is the degeneration of the Kelvin wave to solitary type waves and of the solitary waves to foci of turbulence and vertical mixing. In the TR we have identified two sources of turbulence and mixing in the density interface region: (1) interfacial instabilities associated to shear flows and (2) interfacial breaking related to the interaction of convective and shear flows over steep solitary waves.

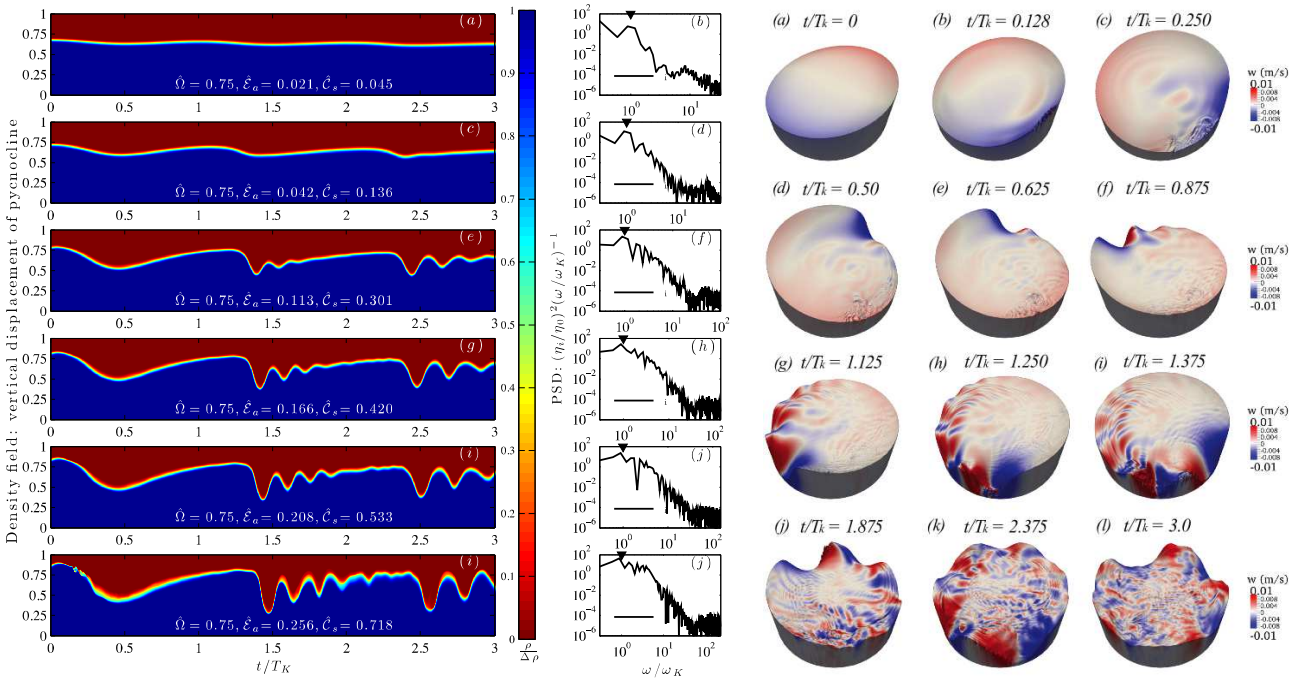


**Figure 2**. *Left Figure*. Left panels: time series of density field along the vertical profile where the maximum wave amplitude is achieved; right panels: power spectral density of vertical displacement of density interface. *Right Figure*. Evolution of the Kelvin wave in the TR: vertical velocity component at density interface.

The turbulent activity is predominantly located inside the internal Rossby ratio of deformation, $R_i$, and is enhanced when the pre-existent turbulent regions interplay with steep wave fronts. The bulk turbulence intensity parameter, $\langle I \rangle_V$, and the effective mass diffusivity, $K_h$, (Ivey et al., 2008) have been estimated to analyse the turbulent activity in each regime. The results show that turbulent patches that emerge from the collapse of shear and convective instabilities govern the bulk-mixing process.

**REFERENCES**

Csanady, G. T. (1967), Large-scale motion in the Great lake, *J. Geophys. Res.*, **72**, 4151-4162.

Ivey, G. N., K. B. Winters, and J. R. Koseff (2008), Density stratification, turbulence, but how much mixing?, *Annu. Rev. Fluid Mech.*, **40**, 169-184.

Winters, K. B., and A. de la Fuente (2012). Modeling rotating stratified flows at laboratory-scale using spectrally-based DNS, *Ocean Modelling*, **50**, 47-59.

Wüest, A, and A. Lorke (2003), Small-Scale Hydrodynamics in Lakes, *Annu. Rev. Fluid Mech.*, **35**, 373-412.

# The role of winter climate on the deep temperature evolution of a deep Italian lake

G. Valerio[1]*, M. Pilotti[1] and D. Copetti[2]

[1]*Department DICATAM, Università degli Studi di Brescia - Via Branze, 43, Brescia, Italy*
[2] *CNR IRSA, UOS Brugherio, Via del Mulino, 19, 20861 Brugherio (MB), Italy*

**Corresponding author, e-mail giulia.valerio@ing.unibs.it*

**KEYWORDS**
Lakes; deep temperature; modelling; mixing; winter climate.

## EXTENDED ABSTRACT

### Introduction

The annual temperature cycle in sufficiently deep lakes is divided into periods of thermal stratification, that keep lower layers isolated from the surface, and periods of isothermal conditions with deep mixing. In these lakes the vertical extent of circulation is a decisive factor for the evolution of water quality and biocenosis, because dissolved substances, such as oxygen or nutrients, get distributed over the entire water body mostly through mixing events. Accordingly, a comprehensive understanding of the way in which external forcings influence the extent of the mixing is of uppermost importance in deep oligomictic lakes, particularly if they are in a recovery state from eutrophication.

To explore the relationship between the indicators of winter climate and the mixing behaviour, several Authors have used a statistical approach (e.g. Salmaso, 2012). In order to overcome some of the limitations of these approaches, hydrodynamic modelling provides numerical instruments that can take into account the actual meteorological conditions and the specific responses of the lake under analysis (e.g. Valerio et al. 2014). Despite the acknowledged importance of convective mixing in deep lakes, only very few of these numerical applications (e.g. Straile et al. 2010) were developed to investigate its quantitative significance. Accordingly, in this paper we use a 3D model to investigate the role of winter climate on the deep temperature evolution in Lake Como, the deepest Italian lake.

### Materials and methods

Lake Como is a 425 m deep and 145 km$^2$ large lake, located at the southern edge of the Alps and composed by 3 branches. Starting from 2005, a long-term monitoring program was carried out to measure high-resolution hydrodynamic data. 3 floating stations were used to monitor the main thermal and mechanical forcings near the closures of each branch at a sampling period of 5 min (Morillo et al. 2009). Water temperature was measured between 0 and 165 m by the overall 57 sensors of 3 thermistor chains. Additionally, the continuous profiles of temperature, dissolved oxygen and conductivity, measured by ARPA Lombardia at the end of the winter at Argegno (about 400 m deep), are available for the period 2004-2011.

To explore the deep temperature dynamics observed in Lake Como, a 3D hydrodynamic model (Delft3D-FLOW) was used. The model solves the Reynolds-Averaged Navier-Stokes equations with the Boussinesque approximation, using a k-ε turbulence closure module and an advection–diffusion equation for the transport of heat and salinity. The lake's bathymetry was discretized on a curvilinear orthogonal grid in the horizontal direction with cell length in the range 200m<L<500m, imposing a time step of 2 min. In the vertical direction we used a a z-

coordinate non-uniform grid, with finer resolution close to the surface (1 m) and in the metalimnion (between 1 and 5 m), and coarser cells (10 m) under 50 m. Because of the observed differences among the measured wind speeds and directions, typical of these pre-alpine environments (Valerio et al., 2012), the model was forced by a spatially varying wind, each station being representative of each branch.

**Results and discussion**

After a sensitivity to the model parameters, the calibration was developed over the period 2007-2008, tuning the horizontal and background vertical eddy viscosity and diffusivity. The model succeeded in reproducing most of the predominant features of temperature dynamics observed around a depth of 160 m, which are dominated by "saw-tooth" structures (Livingstone, 1997), consisting of periods of gradual warming at an approximately rate of 0.15 °C/year, followed by abrupt reductions when the temperature approaches the one measured at the lake surface (see Fig.1). These cooling events reveal that in 2005, 2006, 2009, 2010 and 2011 the mixing depth exceeded 160 m. Reductions of the temperature under 350 m, instead, was observed only in March 2005 and 2006, where more than 8 mg/l was measured at the lake bottom. In the following years, the deeper temperature had increased at an average rate of 0.06 °C/year and the mixing depth ranged from about 100 m in 2007 to 300 m in 2010, according to the oxygen profiles.

Several numerical experiments were conducted to investigate the role of wind and energy fluxes on the extent of winter mixing and to test whether extreme events, such as the exceptionally shallow mixing in winter 2007-2008, was caused solely by a single winter meteorology or was the outcome of the climate of the previous years. This allowed to identify the meteorological parameters that exerted the strongest influence on the deep water dynamics, and to highlight the importance of the harshness of the previous winters. At the light of these findings, it was possible to provide an interpretation to the common features of the long-term circulation patterns observed in other deep prealpine lakes.

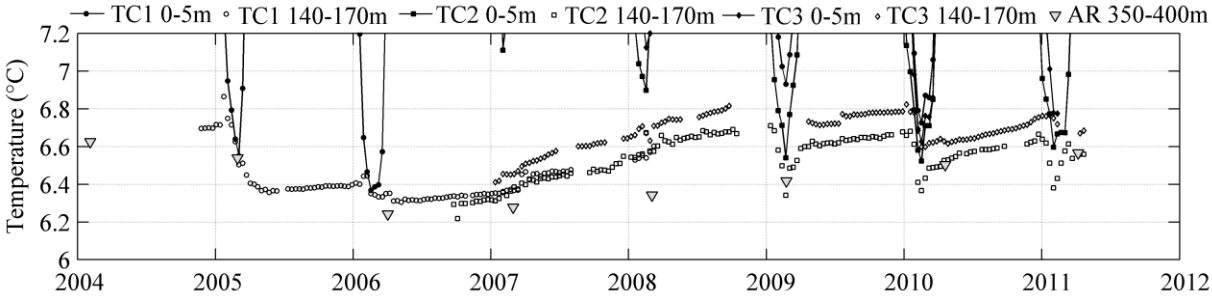


**Figure 1.** Time series of the 10-day averaged temperature, measured by the thermistor chains (TC) in the layers 0-5 m and 140-170 m. The triangles show the average temperature between 350 and 450 m at Argegno (AR).

**REFERENCES**

Livingstone, D. M. (1997), An example of the simultaneous occurrence of climate-driven 'sawtooth' deep-water warming/cooling episodes in several Swiss lakes. *Verh. Internat. Verein. Limnol.*, **26**, 822–826.

Morillo, S., J. Imberger, J. P. Antenucci, and D. Copetti (2009), Using impellers to distribute local nutrient loadings in a stratified lake, *Journal of Hydraulic Engineering*, **135**(7), 564-574.

Salmaso, N. (2012), Influence of atmospheric modes of variability on a deep lake south of the Alps, *Climate Research*, **51**, 125–133.

Straile, D., K. Onur, P. Frank, C.J. Marc, K. Reiner, R. Karsten, and R. Karl-Otto (2010), Effects of a Half a Millennium Winter on a Deep Lake – a Shape of Things to Come?, *Global Change Biology*, **16**, 2844–2856.

Valerio G., M. Pilotti, C. L. Marti, and J. Imberger (2012), The structure of basin scale internal waves in stratified lake in response to lake bathymetry and wind spatial and temporal distribution: Lake Iseo, Italy, *Limnol. Oceanogr.*, **57**, 772–786.

Valerio, G., M. Pilotti, S. Barontini, and B. Leoni (2014), Sensitivity of the multiannual thermal dynamics of a deep pre-alpine lake to climatic change, *Hydrological Processes*, in press, doi: 10.1002/hyp.10183.

# Mixing in stratified bottom boundary layers on the steep sloping walls of Monterey Submarine Canyon

D.J. Wain[1]*, M.C. Gregg[2], M.H. Alford[2], R.-C. Lien[2], R.A. Hall[3] and G.S. Carter[4]

[1] *Department of Architecture and Civil Engineering, University of Bath, UK*
[2] *Ocean Physics Department, Applied Physics Laboratory, University of Washington, Seattle, WA, USA*
[3] *School of Environmental Sciences, University of East Anglia, Norwich, UK*
[4] *Department of Oceanography, University of Hawaii at Manoa, USA*

**Corresponding author, e-mail d.j.wain@bath.ac.uk*

**KEYWORDS**
Internal waves, bottom boundary layers, complex topography, shelf processes, turbulence.

## EXTENDED ABSTRACT

### Introduction

Submarine canyons comprise nearly 20% of the western continental slope of North America (Hickey 1995). The internal tide interacts with their complex topography, leading to several processes that create turbulent mixing. Here, spatially intense measurements of elevated mixing along the bottom and sidewalls of upper Monterey Submarine Canyon (MSC) are presented.

### Materials and methods

Measurements were made in Monterey Bay with SWIMS3, a depth-cycling towed body that measures conductivity, temperature, and depth, and which also has two gimballed acoustic Doppler current profilers, one upward looking and one downward looking, to measure profiles of the water velocity. The measurements were focused on the upper canyon, with particular emphasis on the Gooseneck Meander, a 90-degree bend in the canyon thalweg approximately 15-km from the head of the canyon (Figure 1). During the experiments, 16 transects (10 cross-canyon) were measured over two spring tides and one neap tide, with each transect being occupied for 25 hours, resulting in 6-20 sections at each transect.

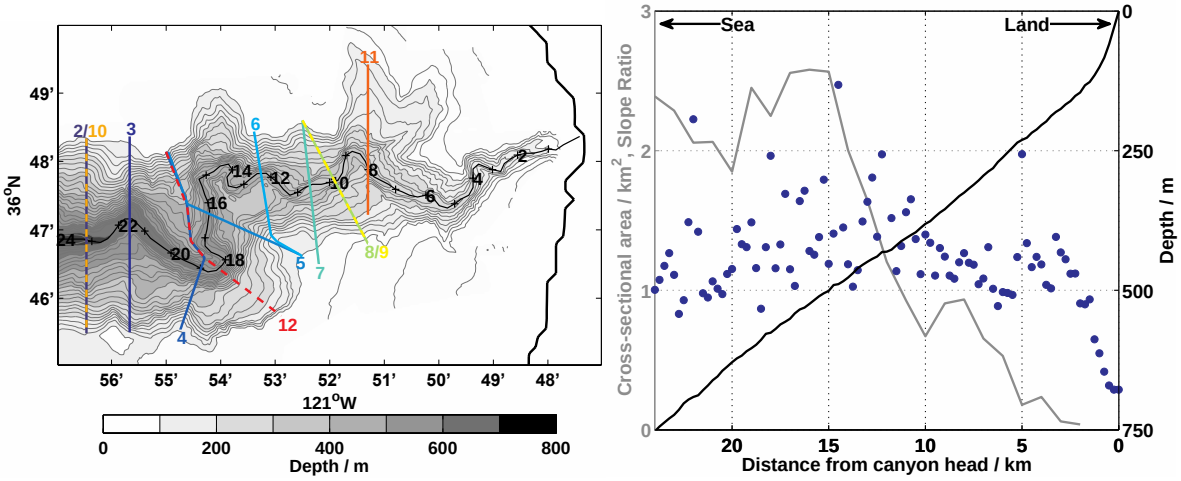


**Figure 1**. (left) Bathymetry of upper Monterey Canyon with 50-m contour lines below 100 m. The thalweg is marked by a + every kilometer from the coastline. The SWIMS3 transects are denoted by the thick colored lines and marked with the color-coded group number. (right) Thalweg depth (black line), cross-sectional area (gray line), and ratio between internal tide slope and topographic slope (blue dots) as a function of distance along the thalweg. A slope ratio of 1 indicates criticality, while above 1 is subcritical and below 1 is supercritical.

The dissipation rate of turbulent kinetic energy ε was computed from Thorpe scales measured from the SWIMS3 CTD package. The vertical eddy diffusivity K was computed using the Osborn model, $K = \Gamma\varepsilon/N^2$, with $\Gamma$ = 0.2. Elevated mixing was defined as $K > 10^{-4}$ $m^2/s$; the thickness of the mixing layer was defined as the height above bottom where K drops below this value.

**Results and discussion**

For all transects, the mixing (Figure 2) followed the spatial patterns of the turbulent dissipation rate (see Wain et al. 2013). These turbulent layers were not well mixed, but remained stratified, as observed by Kunze et al. 2012. The thickness of the turbulent layer along the canyon walls and the magnitude of mixing depended on the tidal forcing. Group 2 (measured during spring tide) had a stratified turbulent boundary layer over 150 m at its thickest, which was three times thicker than Group 10, measured at the same place during neap tide (not shown).

Groups 3 and 4, which are associated with the Gooseneck Meander and a smaller bend, show elevated mixing high above the bed, perhaps due to scattering of internal waves off of the topography. Groups 5-7 show intense mixing on the bottom of the canyon, but also a layer of elevated mixing along the canyon sidewalls. The structure of this layer in this upper region of the canyon was relatively similar between these three sections. These stratified turbulent boundary layers were observed all the way up to the shelf in all transects.

**REFERENCES**

Hickey, B. M. (1995), Coastal submarine canyons, in *Topographic Effects in the Ocean: Proc. Aha Hulikoa Hawaiian winter workshop*, pp. 95–110, Office of Naval Research.

Kunze, E., C. MacKay, E. E. McPhee-Shaw, K. Morrice, J. B. Girton, and S. Terker (2012), Turbulent mixing and exchange with interior waters on sloping boundaries, *J. Phys. Oceanogr*. doi:10.1175/JPO-D-11-075.1.

Wain, D. J., M. C. Gregg, M. H. Alford, R.-C. Lien, R. A. Hall, and G. S. Carter (2013), Propagation and dissipation of the internal tide in upper Monterey Canyon, *J. Geophys. Res. Oceans*, **118**, 4855–4877, doi: 10.1002jgrc20368.

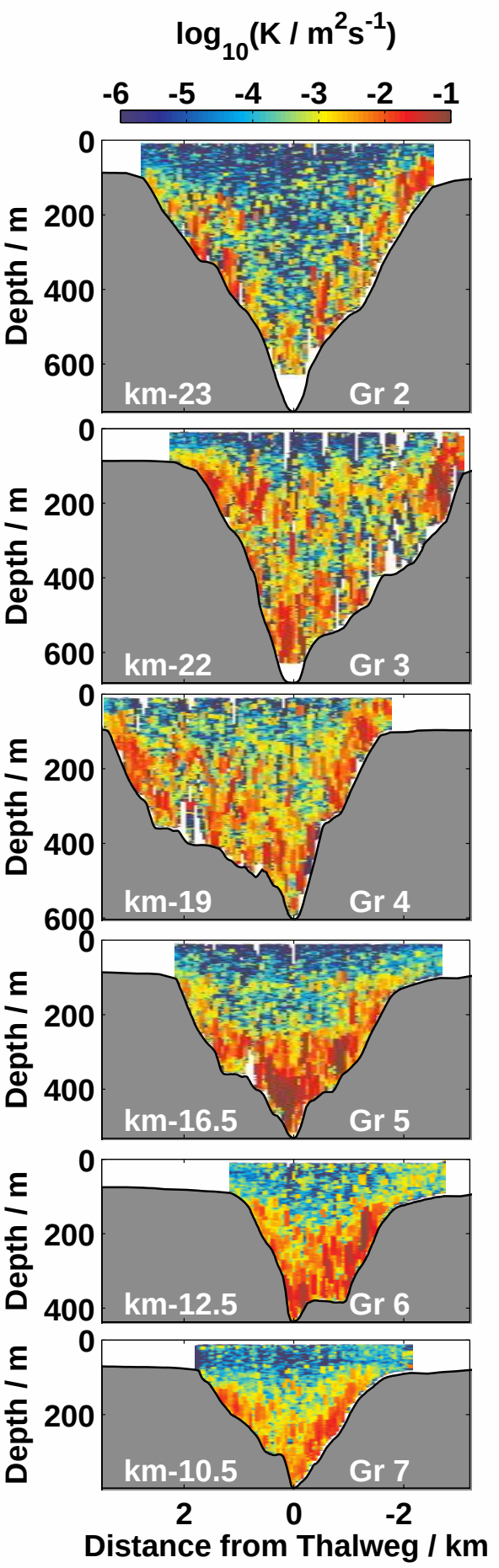


**Figure 2:** Transect averages of vertical eddy diffusivity during spring tide.

# Modeling spring bloom in Lake Michigan using an unstructured-grid coupled physical-biological model

J. Wang[1]*, L. Luo[2], H. Hu[3] and X. Bai[3]

[1] *NOAA Great Lakes Environmental Research Laboratory, Ann Arbor, Michigan, USA*
[2] *State Key Laboratory of Tropical Oceanography, South China Sea Institute of Oceanology, Chinese Academy of Science, Guangzhou, China*
[3] *Cooperative Institute for Limnology and Ecosystems Research, University of Michigan, Ann Arbor, Michigan, USA*

**Corresponding author, e-mail jia.wang@noaa.gov*

**KEYWORDS**
Great lakes; coupled physical-biological model; water quality; NPZD model; tributary loading.

## EXTENDED ABSTRACT

### Introduction

A 3-D coupled physical-biological model is used to simulate the ecosystem characteristics in Lake Michigan. The physical model is the unstructured grid, Finite-Volume Coastal Ocean Model (FVCOM) driven by the observed hourly meteorological forcing and river loaded nutrients in 1998. The biological model is a NPZD model, including phosphorus as the nutrient, which is the limiting element in Lake Michigan, phytoplankton, zooplankton and detritus. The model is calibrated by the satellite and in situ data. The main phenomena in the spring of 1998 are captured. During March to May, a circle-like phytoplankton bloom appears in South Lake Michigan, which looks like 'doughnut'. The formation and mechanisms of spring bloom were simulated. It is confirmed that the phytoplankton bloom along the coast is caused by the river-loaded nutrient in addition to rapid increasing temperature and light intensity in spring. Without the river loaded nutrient, the coastal bloom cannot be reproduced. River-loaded nutrient input was proven to be important Lake Michigan ecosystem, which is linked to regional climate change.

### Materials and methods

*Physical model*

A three-dimensional coupled physical-biological model of Lake Michigan is used to calculate the ecosystem process in Lake Michigan. The model is based on an Unstructured Grid, Finite-Volume Coastal Ocean Model (FVCOM) developed by Chen et al (2006). FVCOM has the following features: 1) unstructured triangular mesh in the horizontal to represent the complex geometry; 2) σ-coordinate in the vertical to represent the irregular bottom topography; 3) free surface; 4) energy conserving due to the finite volume strategy; 5) Mellor and Yamada level 2.5 turbulent closure scheme for vertical mixing and 6) Smagorinsky turbulent closure scheme for horizontal mixing.

In the physical model, we implement the wind-wave mixing parameterization newly developed by Hu et al (2010) to accurately simulate the mixed layer depth.

$$K_{mw} = \frac{2\upsilon^2}{g}\delta\beta^3 W^3 e^{\frac{gz}{\beta^2 W^2}}, \quad (1)$$

where $K_{mw}$ is the wave-induced mixing coefficient; β is the wave age (0<β<1 for growing wave, and β=1 for mature wave), δ is the wave steepness ($\delta = 2\alpha/\lambda$, α is the amplitude and λ

is the wavelength), W is the wind speed, z < 0 is the depth, n= 0.4 is the von Kármán constant, and g is acceleration of gravity. In this study, a mature but not breaking wave is assumed as β=1.0, δ=0.02. Heat diffusion coefficient $K_{hw}$ is assumed equal to $K_{mw}$ here.

Then the total mixing coefficients are

$$K_m' = K_m + K_{mw}, \qquad K_h' = K_h + K_{hw}, \tag{2}$$

where $K_m$ and $K_h$ are calculated by the level 2.5 closure turbulence model.

*Biological model*

The biological model implemented in FVCOM is a Flexible Biological Module. To simplify the biological process we choose four compartments, including phosphorus as the nutrient, which is the limiting element in Lake Michigan, phytoplankton, zooplankton and detritus, to establish a NPZD model in Lake Michigan (Luo et al. 2012). The concentration of chlorophyll is derived from the phytoplankton as a ratio of chlorophyll to carbon in phytoplankton. The biological model is run simultaneously with the physical model.

## Results and discussion

We conducted model simulations with and with no tributary loadings (Fig. 1) under the same atmospheric forcing in spring 1998. The observed surface chl-a had strong bloom along the coast (see Fig. 1, left). The model simulation with tributary loading can reproduce this feature with strong bloom along the coast (Fig. 1, middle) due to the facts: 1) river loading provides sufficient nutrient for phytoplankton bloom, and 2) shallower water temperature was higher due to absorbing more solar radiation. When this tributary loading was cut off, there was no coastal bloom (Fig. 1, right). This striking comparison indicates the importance of nutrient loading along Lake Michigan, which cannot be negligible.

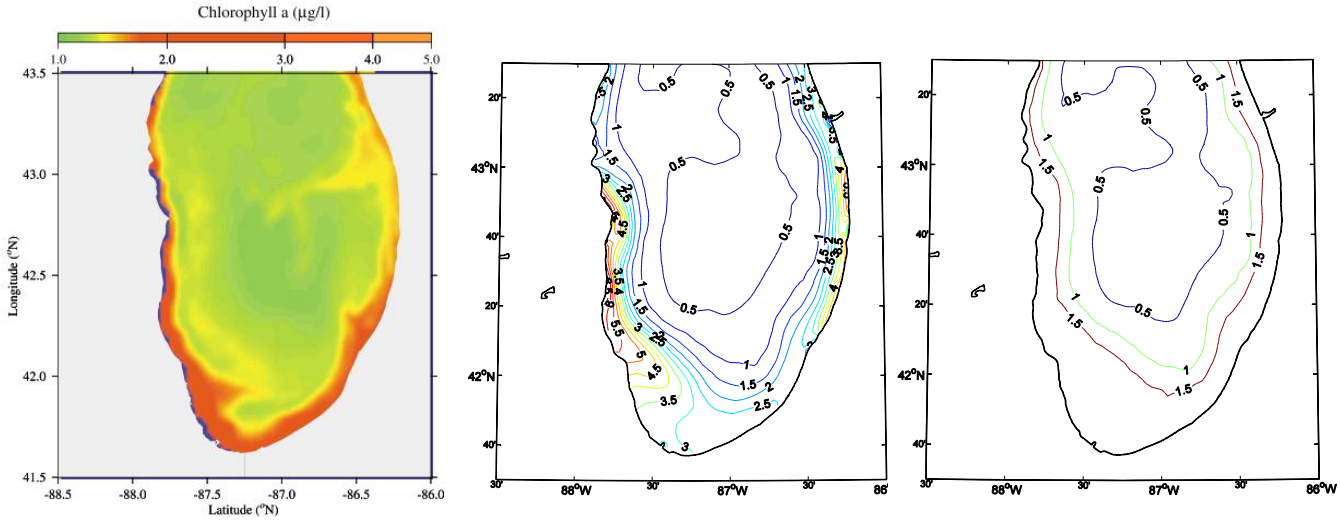


**Figure 1**. Left: satellite-measured Chl-a in south Lake Michigan on March 25, 1998; Middle: Model-simulated Chl-a with tributary loading, and Right: Model-simulated Chl-a with no tributary loading.

## REFERENCES

Chen, C., R.C. Beardsley, G. Cowles (2006), An Unstructured-Grid, Finite-Volume Coastal Ocean Model (FVCOM) System. *Oceanography*, **19**(1), 78-89.

Hu, H., and J. Wang (2010), Modeling effects of tidal and wave mixing on circulation and thermohaline structures in the Bering Sea: Process studies, *J. Geophys. Res*., **115**, C01006, doi:10.1029/2008JC005175.

Luo, L., J. Wang, D.J. Schwab, H. Vanderploeg, G. Leshkevich, X. Bai, H. Hu, and D. Wang (2012), Simulating the 1998 spring bloom in Lake Michigan using a coupled physical-biological Model, *J. Geophys. Res.*,**117**, doi:10.1029/2012JC008216.

# Double-diffusive convection in lakes – Nyos, Kivu and Powell Lake compared

A. Wüest[1,2,*], T. Sommer[1], J.R. Carpenter[3], M. Schmid[1], B. Scheifele[4] and R. Pawlowicz[4]

[1] *Eawag, Surface Waters - Research and Management, Kastanienbaum, Switzerland*
[2] *Physics of Aquatic Systems Laboratory - Margaretha Kamprad Chair, EPFL-ENAC-IIE-APHYS, Lausanne, Switzerland*
[3] *Institute for Coastal Research, Helmholtz Zentrum Geesthacht, Geesthacht, Germany*
[4] *Department of Earth, Ocean, and Atmospheric Sciences, University of British Columbia, Vancouver, Canada*

**Corresponding author, e-mail alfred.wueest@eawag.ch*

**KEYWORDS**
Lakes, meromixis, density (flux) ratio, microstructure, staircase, DNS modelling, interfaces, flux laws.

## EXTENDED ABSTRACT

### Introduction

The three lakes Nyos, Kivu and Powell Lake have in common that they are permanently stratified due to increasing salinity and gas contents with depth. Although all three freshwater bodies have a different history, which led to individual stratification structures, the temperature increase with depth favours double-diffusive convection in all three lakes (Figure 1). In Kivu and Nyos, deep subaquatic springs stratify the water column by releasing salt and $CO_2$ at great depth. In Powell Lake, it is the ancient ocean water, which is still present in the lowest ~1/3 of the deep-water with salinities of up to almost half of the original sea water value (Scheifele et al 2014). Gas has accumulated in the isolated deep-water by the decomposition of organic matter over the 10,000 years since the last ice-age, when the lake was formed from a fjord.

Although the details of the evolution of the water constituents and the subsequent vertical stratification are different, all three lakes are permanently stratified with temperature and salinity increasing with depth (Figure 2), and all three lakes have developed prominent staircases, with density ratios in the favourable range of 2 to 6.

### Materials and methods

The vertical structure of temperature and salinity were measure with different instruments. In Lake Nyos we lowered a Seabird SBE-17 very slowly by hand and resolved the interfaces by ~3 cm (Schmid et al. 2004). In Powell Lake, CTD profiles were collected using a Seabird SBE-25, equipped with an SBE-3F temperature sensor and a SBE-4 conductivity sensor sampling at 8 Hz. The CTD was lowered at ~11 cm/s which allowed to resolve the interface down to ~1.4 cm (Scheifele et al 2014). At the same time microstructure casts were collected using a Rockland Scientific International vertical microstructure profiler (VMP). The VMP samples at 512 Hz and freefalls at 0.38 m/s yielding digital vertical resolution of 0.75 mm. After senor response corrections, the salinity and temperature can be resolved to scales of ~1 mm and ~1 cm, respectively. The largest data set was acquired with the VMP for Lake Kivu. For details see Sommer et al. (2013a).

### Results and discussion

Given these three sets of small-scale microstructure data, we hope to be able to find some general relationships between the vertical fluxes and the thicknesses of the interfaces and the

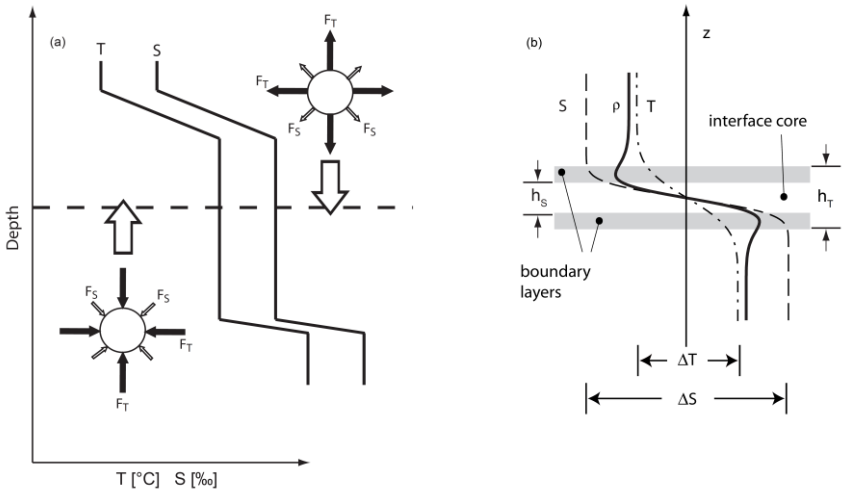


**Figure 1**. Left: Due to the ~100-times faster diffusion of heat (large arrows) relative to salt (small arrows), the fluxes at the interfaces are dominated by the heat and the convective plumes are driven by the buoyancy from temperature, which is slightly (typically 10 to 15%) reduced by the negative buoyancy of salt. Right: As a result of the large difference in molecular diffusivities, temperature interfaces grow thicker than salinity interfaces and therefore two unstable boundary layers form directly adjacent to the interface. These gravitational instabilities cause convection in both homogenous layers and maintain them well-mixed. Redrawn from Carpenter *et al*. (2012a).

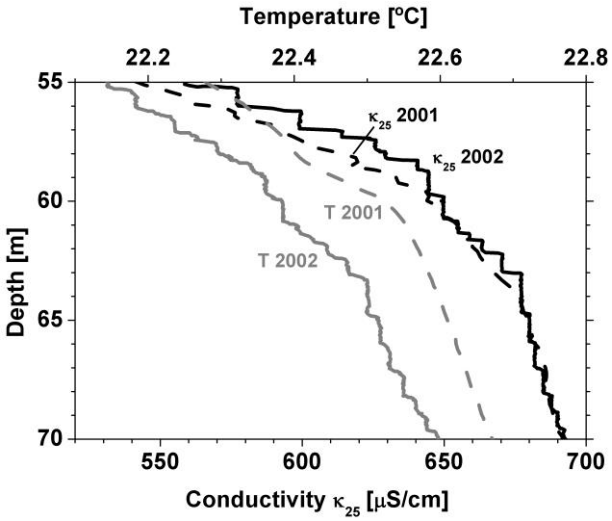


**Figure 2**. Conductivity and temperature observed in Lake Nyos in 55 to 70 m depth on 3 Nov 2001 (thin lines) and 8 Dec 2002 (thick lines). Besides the formation of the double-diffusive staircase (19 well-mixed layers shown) the heat loss (increased vertical heat fluxes) is well visible. Salinity (conductivity) is hardly affected by the double-diffusive fluxes.

mixed layers in relation to the boundary conditions, such as the water column stability, the density ratio or the heat flux from the deep-water. However, it turns out that this is not an obvious exercise. On the one hand it seems that the mixed layer thickness is not correlated to the density ratio and not to the vertical heat flux (Sommer et al 2013b). On the other hand, it appears the interface thickness, which can very well be reproduced by *Direct Numerical Simulations* (see presentation by Sommer) is not particularly sensitive to the boundary conditions. Although, the vertical structures of the staircase-like layering are distinctively different, the physical dimensions of the high-gradient interface and mixed layer thicknesses as well as the steps of salinity and temperature between the homogeneous mixed layers are astonishingly similar and even close to the staircase properties in the Arctic Ocean. Typical thicknesses of the interfaces and the mixed layers are 10 cm and 70 cm, respectively, in all three systems, despite the different heat fluxes and different density ratios. The goal of the presentation is to compare the findings in the three systems and to discuss a first attempt to categorize the double-diffusive signatures of the three lakes.

**REFERENCES**

Scheifele B., R. Pawlowicz, T. Sommer, and A. Wüest (2015). Double diffusion in saline Powell Lake, British Columbia. *J. Physical. Oceanography*. submitted.

Schmid M, A. Lorke, C. Dinkel, G. Tanyileke, and A. Wüest (2004). Double-diffusive convection in Lake Nyos, Cameroon. *Deep Sea Research I*, **51:** 1097-1111

Sommer, T., J.R. Carpenter, M. Schmid, R.G. Lueck, and A. Wüest (2013a). Revisiting microstructure sensor responses with implications for double-diffusive fluxes. *Journal of Atmospheric and Oceanic Technology* **30**(8): 1907–1923.

Sommer, T., J.R. Carpenter, M. Schmid, R. G. Lueck, M. Schurter, and A. Wüest (2013b), Interface structure and flux laws in a natural double-diffusive layering, *J. Geophys. Res. Oceans*, **118**(11), 6092-6106.

# The oxygen regime of a shallow lake in winter: Anaerobic conditions in bottom layers and wide-range variability in bulk of a water column

G. Zdorovennova[1]*, N. Palshin[1], R. Zdorovennov[1], S. Golosov[1, 2], G. Gavrilenko[1] and A. Terzhevik[1]

[1] *Northern Water Problems Institute, Russian Academy of Sciences, Petrozavodsk, Russia*
[2] *Institute of Limnology, Russian Academy of Sciences, Saint-Petersburg, Russia*

**Corresponding author, e-mail zdorovennova@gmail.com*

**KEYWORDS**
Ice-covered lake; dissolved oxygen; anaerobic conditions.

## EXTENDED ABSTRACT

### Introduction

The main causes of anaerobic conditions of shallow lakes during ice-covered period are: (1) absence of gas exchange with the atmosphere, and (2) the suppression of photosynthesis. The rate of dissolved oxygen reduction is determined by the intensity of its diffusion in sediments and bacterial consumption in water column (Boylen and Brock, 1973; Mathias and Barica, 1980). Density circulation, seiches, and internal waves can have a significant impact on rate of oxygen reduction (Baehr and DeGrandpre, 2002). The purpose of our investigation was to study the time scales of dissolved oxygen variability in a shallow lake during winter.

### Materials and methods

The oxygen regime of Lake Vendyurskoe (Karelia, Russia, 62°10N, 33°10'E, Fig. 1) was studied based on six consecutive years of observations (2007-2013). Lake Vendyurskoe is a mesotrophic polymictic small shallow lake of glacial origin (surface area 10.4 km$^2$, volume $54.8 \cdot 10^6$ m$^3$, maximal and average depths 13.4 and 5.3 m, respectively). Year-round measurements of dissolved oxygen with logger chains (DO-1050, RBR Ltd., Canada) were conducted at 2-3 locations (Fig 1), with a sampling interval of one minute; the space interval between loggers was 0.25-1.5 m.

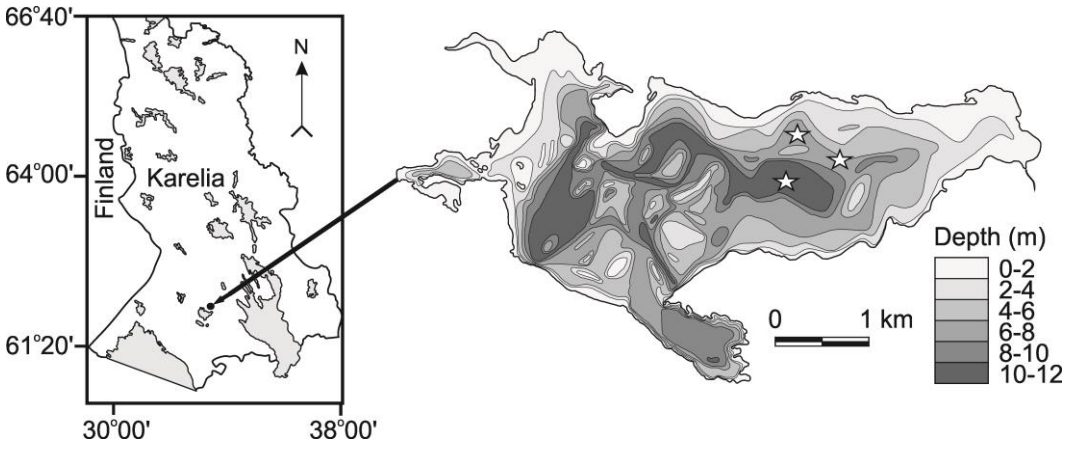


**Figure 1**. Lake Vendyurskoe map with the location of the measurement site (white srats).

## Results and discussion

Anaerobic conditions (dissolved oxygen content of less than 2 mg $l^{-1}$) appear in the bottom layers in the central basin of the lake in 1-2 months after freezing. The thickness of the anaerobic zone may exceed one meter by the end of winter (Fig 2, A).

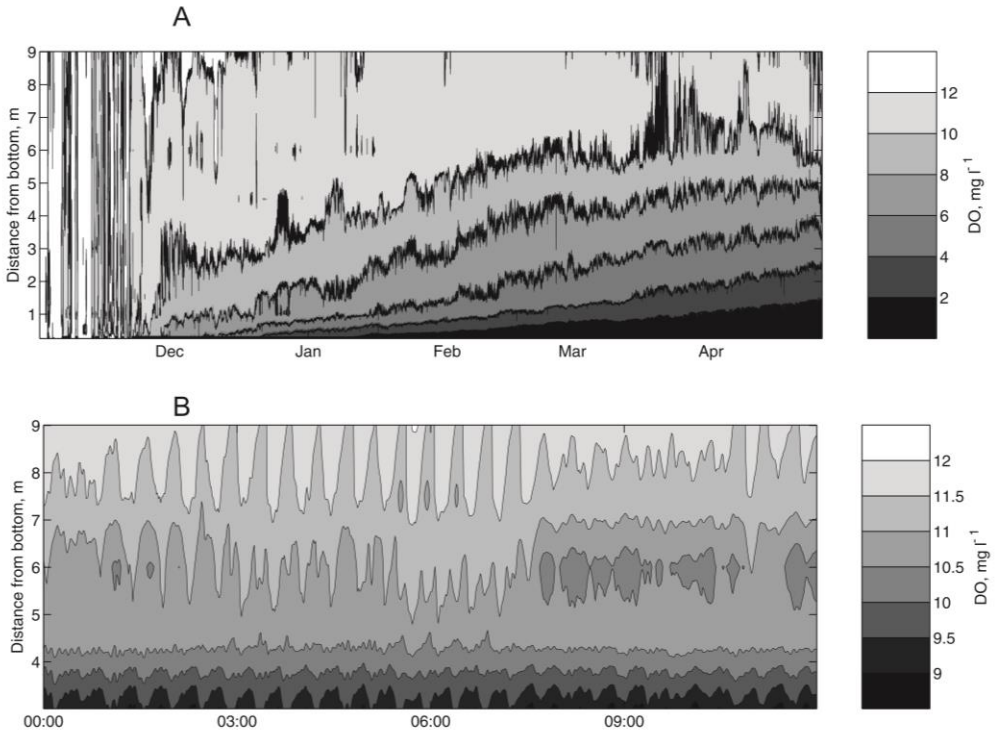


**Figure 2**. Dissolved oxygen in Lake Vendyurskoe (central part of the lake, depth 11.3 m): A - during 1 Nov 2010-24 April 2011, B – 16 Jan 2011 from 00h00min to 11h59 min.

On the background of the seasonal reduction of dissolved oxygen, a wide range of its variations is found, differing in amplitude, period, duration and the depths of events. The most notable fluctuations can be divided into three groups: (1) oscillations with a period of 6-30 minutes and amplitude of 0.1-1.2 mg $l^{-1}$ (Fig 2, B); (2) fluctuations lasting from several hours to several days with amplitude of 1-1.5 mg $l^{-1}$; and (3) the sharp increase in dissolved oxygen content of 2-4 mg $l^{-1}$ in 5-15 minutes, and further decrease to the previous values lasting for a few hours. Oscillations of the first and second types were observed in the surface layers of the water column, while the last-mentioned was registered only in the bottom layer of the central deep basin. Intensification of the first two types of oscillations occurred in a number of cases against sharp changes in atmospheric pressure, usually accompanied by strong wind. A complete disappearance of oscillations (type 1 & 2) in calm conditions and their appearance after the amplification of wind allows us to suppose that they are generated due to the impact of wind on the ice cover.

**Acknowledgments.** The present study was supported by the Russian Academy of Science, The Russian Fund of Basic Research (project 13-05-00338).

**REFERENCES**

Baehr, M. M., and M. D. DeGrandpre (2002), Under-ice $CO_2$ and $O_2$ variability in a freshwater lake. *Biogeochemistry*, **61**, 95–113.

Boylen, C, and T. Brock (1973), Bacterial decomposition processes in Lake Wingra sediments during winter. *Limnol. Oceanogr*., **18**(4), 628–634.

Mathias, J, and J. Barica (1980), Factors controlling oxygen depletion in ice-covered lakes. *Can. J. Fish. Aquat. Sci.*, **37**, 185–194.

# List of participants

Edoardo Bertone, *Griffith University, Australia*
edoardo.bertone@griffithuni.edu.au

Bertram Boehrer, *Helmholtz Centre for Environmental Research - UFZ, Germany*
Bertram.Boehrer@ufz.de

Damien Bouffard, *EPFL, Switzerland*
damien.bouffard@epfl.ch

Luca Carniello, *University of Padova, Italy*
luca.carniello@dicea.unipd.it

Xavier Casamitjana, *University of Girona, Spain*
xavier.casamitjana@udg.edu

Giuseppe Ciraolo, *University of Palermo, Italy*
giuseppe.ciraolo@unipa.it

Simone Cosoli, *OGS, Trieste, Italy*
scosoli@ogs.trieste.it

Remo Cossu, *Australian Maritime Collgege / Utas, Australia*
remo.cossu@utas.edu.au

Elena Debolskaya, *Institute for Water Problems of the Russian Academy of Science, Russian Federation*, e_debolskaya@yahoo.com

Christof Engelhardt, *IGB, Germany*
engelhardt@igb-berlin.de

Alexander Forrest, *Australian Maritime College, Australia*
alex.forrest@amc.edu.au

Galina Gavrilenko, *NWPI, Russian Federation*
south.sun.cr@gmail.com

Kelly Graves, *University of British Columbia, Canada*
kellygraves@civil.ubc.ca

Ben Hodges, *University of Texas, United States*
hodges@utexas.edu

Boris Katsnelson, *University of Haifa, Israel*
bkatsnels@univ.haifa.ac.il

Georgiy Kirillin, *Institute of Freshwater Ecology, Berlin, Germany*
kirillin@igb-berlin.de

Jovana Kokic, *Uppsala University, Sweden*
jovana.kokic@ebc.uu.se

Bernard Laval, *University of British Columbia, Canada*
blaval@apsc.ubc.ca

Gregory Lawrence, *University of British Columbia, Canada*
lawrence@civil.ubc.ca

Bruno Lemaire, *AgroParisTech, France*
bruno.lemaire@agroparistech.fr

John Lenters, *LimnoTech, United States*
jlenters@limno.com

Madis-Jaak Lilover, *Marine Systems Institute, Estonia*
madis-jaak.lilover@msi.ttu.ee

Andreas Lorke, *University of Koblenz-Landau, Landau, Germany*
lorke@uni-landau.de

Ilia Ostrovsky, *Israel Oceanographic and Limnological Research (IOLR), Israel*
ostrovsky@ocean.org.il

Sebastiano Piccolroaz, *University of Trento, Italy*
s.piccolroaz@unitn.it

Marco Pilotti, *University of Brescia, Italy*
marco.pilotti@ing.unibs.it

Eva Podgrajsek, *Uppsala University, Sweden*
eva.podgrajsek@geo.uu.se

Giuliano Rizzi, *CISMA, Trento, Italy*
giuliano.rizzi@cisma.it

Vera Rostovtseva, *P. P. Shirshov Institute of Oceanology RAS, Russian Federation*
vvrostovtseva@bk.ru

Peter Rusello, *Nortek, United States*
pj@nortekusa.com

Nico Salmaso, *Fondazione E. Mach, Trento, Italy*
nico.salmaso@fmach.it

Marco Santo, *University of Trieste, Italy*
santomarco31@gmail.com

Jose Rodolfo Scarati Martins, *University of Sao Paulo, Brazil*
scarati@usp.br

S. Geoffrey Schladow, *University of California, Davis, United States*
gschladow@ucdavis.edu

Martin Schmid, *Eawag, Switzerland*
martin.schmid@eawag.ch

Dongdong Shao, *Beijing Normal University, China*
ddshao@bnu.edu.cn

Bao-Shi Shiau, *Academia Sinica, Institute of Physics, Taiwan*
bsshiau@gate.sinica.edu.tw

Stefano Simoncelli, *University of Bath, United Kingdom*
netcelli@gmail.com

Tobias Sommer, *Eawag, Switzerland*
tobias.sommer@eawag.ch

Frédéric Soulignac, *LEESU/ Ecole des Ponts ParisTech, France*
frederic.soulignac@leesu.enpc.fr

Adolf Stips, *European Commission, Italy*
adolf.stips@jrc.ec.europa.eu

Marco Toffolon, *University of Trento, Italy*
marco.toffolon@unitn.it

Hugo Ulloa, *Universidad de Chile, Chile*
hulloa@ing.uchile.cl

Giulia Valerio, *University of Brescia, Italy*
giulia.valerio@ing.unibs.it

Danielle Wain, *University of Bath, United Kingdom*
d.j.wain@bath.ac.uk

Jia Wang, *NOAA Great Lakes Environmental Research Laboratory, United States*
jia.wang@noaa.gov

Alfred Wüest, *Eawag & EPFL, Switzerland*
alfred.wueest@eawag.ch

# Sponsors

Instrument Service S.r.l.

Via L. Von Comini 8, 39100 Bolzano, Italy

http://www.instrumentservice.eu/

Hortus S.r.l.

Via S. Caboto 8/B, 20025 Legnano (Milano), Italy

http://www.hortus.it/

Watec.it – YSI

Via del Follatoio 12, 34147 Trieste, Italy

http://www.watec.it/

UNIVERSITY OF TRENTO - Italy
Department of Civil, Environmental
and Mechanical Engineering

# PHYSICAL PROCESSES IN NATURAL WATERS
# PPNW2014

The focus of the PPNW workshops is the physics of inland and coastal water bodies and their interactions with the physical and biogeochemical processes that control water quality, ecosystem function, and the services such systems provide. The workshops traditionally cover a broad spectrum of scientific topics. Besides general topics, the Trento workshop pays special attention to the coupling of physical and ecological processes and water quality in alpine and peri-alpine lakes.

PPNW is an open workshop, actively seeking to expand contacts with neighbouring fields such as physical oceanography, the atmospheric sciences, and engineering. With 40 to 60 participants and a small number of invited speakers, the PPNW meetings are characterized by their active workshop atmosphere and a comfortable time frame for presentations and discussion.

ISBN 978-88-8443-551-4